Thermal Conductivity of Mine Backfill

Farzaan Abbasy

Thesis in the Department of Civil, Building and Environmental Engineering

Presented in partial fulfillment of the requirements for the degree of Master of Applies Science (Civil Engineering) at Concordia University

Montreal, Canada

August 2009

Your file Votre référence
ISBN: 978-0-494-63157-7
Our file Notre référence
ISBN: 978-0-494-63157-7

Thermal Conductivity of Mine Backfill

Farzaan Abbasy

Energy conservation is a national strategy for every country. To avoid shortage of energy and high prices, the green sustainable energy resources have become the center of attention. Mining as a prominent industry in Canada consumes a huge amount of energy, so any reduction in energy consumption would result in higher production and profit. In 2005, Hassani of McGill University proposed the use of mine stopes as the heat exchange area for the production of low temperature geothermal energy, since the extraction of ore/ rocks and the backfilling is a part of normal mining operation, then the very low cost associated with the implementation of such system, will make it very viable for mining industry. This work is in collaboration with energy research team of professor Hassani of McGill University (EMERG). This is a part of an overall research program on low temperature geothermal energy from mines. The research was focused primarily on investigating and obtaining a range values for thermal conductivity of different mine backfills, as well as the effect of some of the associated physical parameters. More than 800 samples and 2000 measurements were done on different backfills with different physical properties. This preliminary investigation indicates that pulp density, binder consumption, curing time, and sodium silicate content have negligible to slight influence on the thermal conductivity of backfill. However parameters such as saturation, and to a lesser extent porosity and the thermal conductivity of the inert material, have more significant influence.

- ✓ I would like to thank Prof. Hassani and Prof. Nokken for their extreme help and support during this project. Without their help finishing this work would be impossible.
- ✓ Mr. Ali Ghoreishi of EMERG for his unfailingly help, guidance and cooperation in this research.
- ✓ Prof. Jean Cote from Laval University for his useful help and good training.
- ✓ Prof. Yavari and Prof. Madani from Polytechnic of Tehran, for their valuable encouragements and guidance.
- ✓ My colleagues in Geomechanic lab of McGill University for helping me in preparing the samples.

Dedicated to my

MOTHER, FATHER, BROTHER and SISTER

For their extreme

Love, devotion, support, dedication,

Encouragements, kindness and hope

They have given to me at all time.

Table of Contents

List of Figures

List of Tables

Nomenclature

Area	A	m^2
Binder content	BC	%
Bulk density	BD	%
Confining pressure	c_p	Mpa
Current	I	A
Degree of saturation	S	%
Diameter	d	m
Exponential integral	Ei	Dimensionless
Fluid thermal conductivity	K_f	$^{W}/_{m°C}$, $^{W}/_{m\,°K}$
Grinding time	GT	hr
Heat	Q	J
Heat flux	q	$^{W}/_{m^2}$
Height	h	m
Length	l	m
Moisture content	W	%

Normalized thermal conductivity	K_r	%
Porosity	n	%
Pressure	P	Mpa
Pulp density	PD	%
Radius	r	m
Resistance	R	Ω
Solid particles thermal conductivity	K_s	$^{W}/_{m°C}$, $^{W}/_{m\,°K}$
Specific heat capacity	C_p	$^{J}/_{Kg°C}$
Temperature	T	°C , $°K$
Thermal conductivity	K	$^{W}/_{m°C}$, $^{W}/_{m\,°K}$
Thermal diffusivity	D	$^{mm^2}/_{s}$
Time	t	s
Uniaxial compressive strength	UCS	$^{MN}/_{m^2}$
Voltage drop	V	v
Volume fraction of unfrozen water	θ	%
Volumetric heat capacity	C	$^{MJ}/_{m^3°C}$

Chapter 1: Introduction

1.1 Introduction

The need for energy has been an essential issue in the lives of people. This need has been increasing with time as the number of people has been growing and energy resources especially fossil fuels have been decreasing. Such decline and further future shortage has and will increase the price of energy. That is why the time has come to more intensely evaluate alternative energy resources which could be long lasting, self sustaining and economically viable. Among many forms of energy alternatives, one of the promising options is geothermal energy considering the huge amount of energy that exists deep in the ground. Geothermal energy is the kind of energy which could be recovered from the inside layers of the earth (shallow or deep) according to heat transfer principle: "When a temperature gradient exists in a body, experience has shown that there is an energy transfer from the high-temperature region to the low-temperature region. The energy is transferred by conduction and the heat transfer rate per unit area is proportional to the normal temperature gradient" (Holman, 1963).

Mining is one of the most prominent industries in Canada (approximately 8.7% of the GDP (Encyclopedia of nations)) which at the same time is one of the most energy consuming industries. The increasing price of energy threatens the effort toward justifying the exploitation of low grade ores or going deeper for the mineral resources. In recent years, more attention has been given to the application of green sustainable energy

in the mining industry. The low temperature geothermal energy has good potential to help the mining industry. This is mainly for two reasons:

- Firstly providing a sustainable alternative energy resource which is also environmental friendly
- Secondly, the opportunity of gaining some profit even after closing down the mine.

The history of geothermal energy application goes back to tens of thousands of years ago. A long time before modern western civilization, indigenous people used hot water from hot springs for cooking, cleaning and bathing. According to archeological evidence, probably the first geothermal energy use in North America dates back to 10,000 years ago when Paleo-Indians used hot springs for cooking (US Department of Energy). The ancient Romans used geothermally heated water in their bathhouses for centuries. They also used the water to treat illnesses and heat homes (Ostridge, 1998).

Modern application of geothermal energy could be characterized by introducing structured commercial and industrial aspects to development of electricity production and geothermal heat pumps in 1800s. The first commercial use of geothermal energy in United States happened in 1830 (US Department of Energy). In 1892, the first district heating in the world occurred in Boise, Idaho in which eventually 200 homes and 40 downtown businesses were served. In early 1900s, the first geothermal power plant emerged, where in Larderello fields, Italy, steam was successfully used to generate electricity in 1904 (Clean energy Idea).

The first geothermal power plant in United States appeared in 1922, which produced 250 KW to light the streets and buildings in the area (US Department of Energy). During the 1960's, the first large scale industrial geothermal power plant was built in the USA that produced 11 Megawatts of power (US Department of Energy). From early in 1970's, many organizations, agencies, and governing bodies were set up to further research and development in geothermal energy that laid the foundation for actualization of more advanced types of geothermal energy applications and sites.

Today, there are more than sixty important geothermal power plants operating in the United States as well as over twenty nations that generate geothermal power. California is now home to the world's largest producer of geothermal energy, Chevron Corporation, which has the capacity to provide power to more than seven million homes (Economy watch). The geothermal energy and its technological advancements are going to make this a more popular sustainable alternative energy resource.

There are three main categories of geothermal energy sources. The first is named direct usage. The water that is heated by the hot rocks beneath the Earth's surface can be pumped to buildings and used in heat exchanging systems. The second one is through using the steam that comes from superheated water. If the steam vents are under sufficient pressure, then they can be used to move turbines. The third category of geothermal energy is dry steam. An outside water source is applied to fractured rock that has been heated to very high temperatures, and then the steam that is created can be used to generate electricity. Direct geothermal heating is far more efficient than geothermal electricity generation and has less demanding temperature requirements, so it is viable over a large geographical range. The other classification for geothermal energy sources

includes low-temperature sources (low temperature can be classified into low-temperature and medium-temperature sources) and high-temperature sources. Low-temperature sources are the same as direct usage in which geothermal energy is used beneficially for residential, commercial and industrial heating/cooling by implementing a geothermal cycle. According to the article on Enviro$ense, using geothermal energy to heat homes could save between 20%-50% in total emissions, and reduce the load of utilities and appliances (many of which are refrigeration or heating units) on the electrical power grid by 75% (Ostridge, 1998). High-temperature sources are the same as the second and third categories which are mentioned above, mostly used to generate electricity. The University of Erlangen Geology Department says that geothermal plants can be on-line an average of 97% of the time. In contrast to nuclear (65% average on-line time) and coal (75% average on-line time), geothermal sources score quite high (Ostridge, 1998). Geothermal energy in the U.S. currently costs a very competitive $0.03-$0.08 per kilowatt hour (Ostridge, 1998).

To extract geothermal energy in direct usage for heating/cooling two main cycles exist; open loop cycle and closed loop cycle. If the geothermal heat is extracted by siphoning out hot/cold underground water as shown in Figure 1 the cycle is called open loop which includes 3 methods: open loop-direct, open loop-indirect and standing column. In contrast, if the heat is recovered by circulating liquid (mainly water) in an underground tube network (heat exchanger), as shown in Figure 2, the cycle is regarded as closed loop that includes horizontal, vertical and pond/lake cycles.

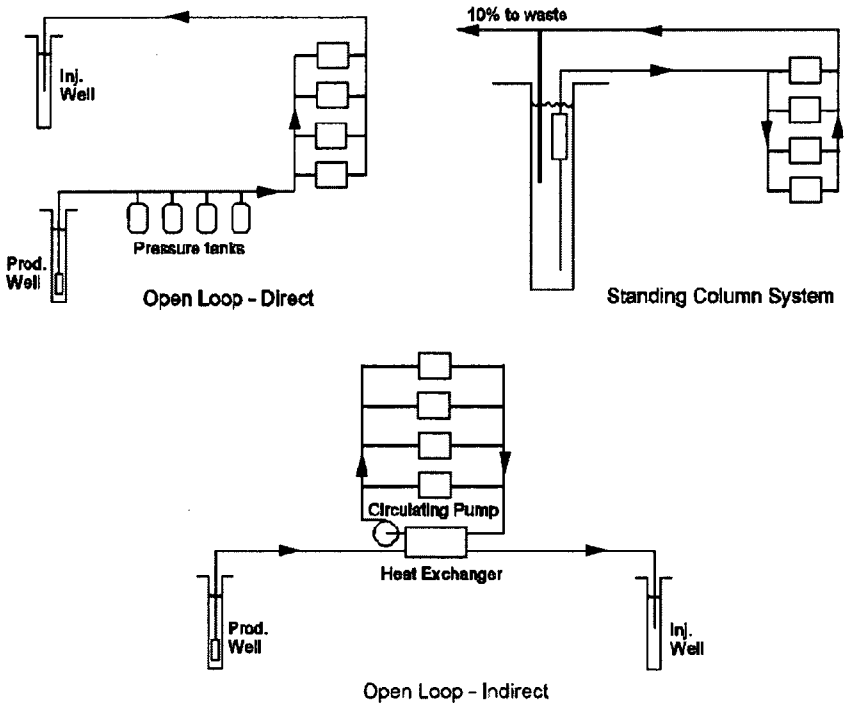

Figure 1- Open loop geothermal cycles (Rafferty, 2001)

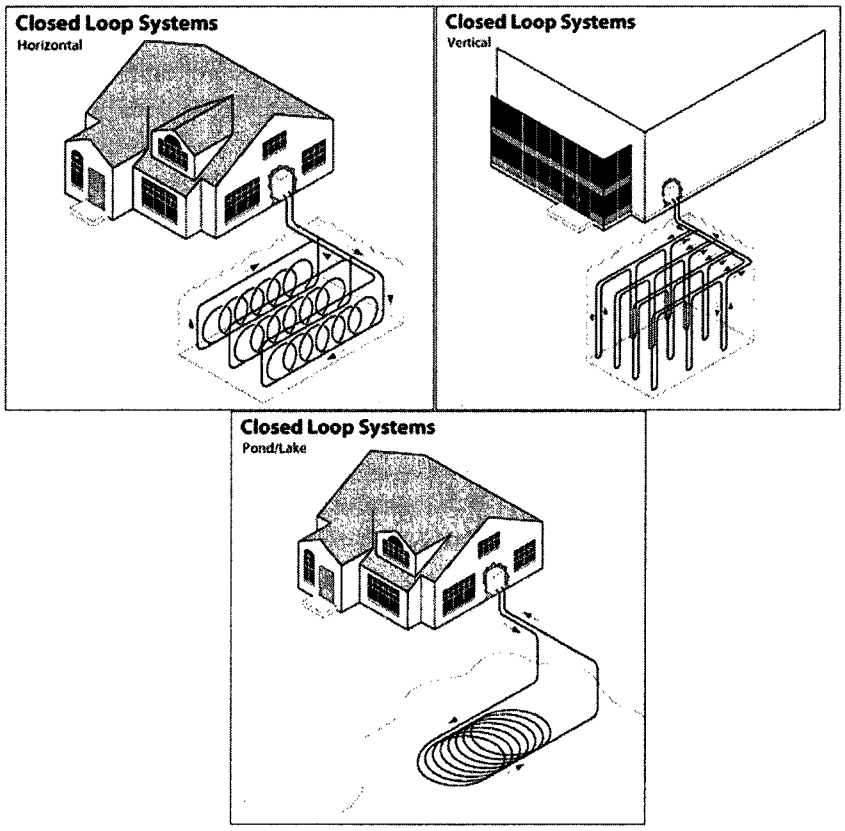

Figure 2- Closed loop geothermal cycles (US Department of Energy)

In 2005 Hassani (Hassani, 2005) of McGill University proposed the use of mine stope (patent pending) or mine tailing ponds as the heat exchange area for the production of low temperature geothermal energy. In line with this, the Earth Mine Energy Research Group (EMERG) was founded at McGill University by Hassani in 2005. It was suggested that cost of such systems will be low as the extracted area and backfilling is part of the normal ore extraction.

This unique idea requires understanding of rocks and the tailing/ backfill thermal properties and its influence on the efficiency of such systems.

Backfill is defined as material or the mixture of materials (mainly the rejects from mineral processing plant) used to fill openings excavated for ore extraction. This contributes to 100% extraction as no pillar containing ore is left behind. Furthermore, it provides working platform in certain mining methods (Cut and fill) as well as overall stability for mine working personnel. It is important to note that the more such mineral processing rejects is used as backfill in the underground mines, the less such materials are kept in the surface with its stability and environmental problem such as acid mine generation (Wilson, 1979; Hassani, 1992).

In underground mines with backfilling systems, the advantage of huge empty spaces which provide unique locations for implementing heat exchangers (tubes) as well as backfill which provides a good filling and support for these tubes, gives an excellent opportunity for low temperature geothermal system.

One of the most important issues in recoverable energy for geothermal systems is the thermal properties of the material around heat exchangers especially thermal

conductivity. So, in this case, the thermal conductivity of backfill could have a determining influence on the possibility and feasibility of such systems. Therefore, knowing thermal conductivity of backfill, its behavior and the factors which may affect it, would be of high importance.

This work is in collaboration with energy research team (EMERG) of Professor Hassani of the Department of Mining and Material Engineering of McGill University. This is a part of an overall research program on low temperature geothermal energy extraction from mines. There is very limited previous information and data available regarding this work; therefore, research was focused primarily on investigating and obtaining a range for thermal conductivity of different backfills. Furthermore, to evaluate the effect of factors that could influence the thermal conductivity of mine fill.

2.2 Outline of thesis

This research project has been presented in the form of the following chapters:

- Chapter 1; outlines briefly the background and the necessity of this research
- In Chapter 2; an overview of the thermal conductivity in rocks and soils, and the influencing factors as well as backfill characteristics and backfilling methods are discussed.
- In Chapter 3; the thermal conductivity measurement methods are explained,
- In Chapter 4; properties and characterization of materials which was used in this research are described,

- Chapter 5 ; deals with the experimental procedure and plan to carry out the tests including preparation, process, different categories of tests and the special devices which were used for the measurements,
- In Chapter 6; the results of the different tests are presented and analyses and discussion of the results are made.
- And finally in Chapter 7; Conclusions are made based on the results obtained and suggestions for potential future works are offered.

Chapter 2: Literature Review

2.1. Introduction

Energy saving has a vital contribution in any national energy strategy and its conservation for underdeveloped countries with inadequate resources is even more significant (Hassan, 1999) due to the increasing price of fossil fuel. This fact has led tendency toward using green sustainable energy at less expensive prices. In line with this need, an abundant resource is the energy from the earth which is mainly known as geothermal energy. Geothermal energy could be extracted from both shallow and deep in the ground considering the temperature difference of the surface from depth. This energy is based mostly on conduction heat transfer in that an energy transfer from the high temperature part to the low temperature part would exists in a body through conduction (Holman, 1963).

To reach deep into the ground, it requires drilling and excavation to a defined depth. There is a great deal of energy consumed in mining, so application of geothermal energy could have potential monetary and environmental benefit. Underground mined excavations (stopes) potentially are very suitable spaces for this objective, especially backfilled stopes (Hassani, 2005). In order to evaluate the amount of possible extractable energy and the design scheme of such a system, one of the most important factors is the thermal conductivity of material in which the system is implanted. Knowing the thermal conductivity is important because it is one of the main characteristics of geothermal energy transfer phenomenon. Holman (1963) defined thermal conductivity as the quantity of heat transmitted during a time through a thickness of material in a direction normal to

the surface of defined area due to temperature difference under steady state conditions and when the heat transfer is dependent only on the temperature gradient.

Archibald and Hassani (1998) in their short course and book noted that, "mine backfill is any material or combination of materials used to fill underground voids created by mining. The voids are filled either to dispose of mine or mill waste materials or to permit the use of mining methods for improved production and safety.

Backfill usage can be divided into either that of bulk backfill or that of exposable backfill (Grice, 1998). Bulk backfill consists of waste materials that are placed into a stope to provide waste disposal, confinement and resist rock wall closure or to provide a working floor. Exposable backfill consists of cemented backfill materials that are placed into a stope where the fill possesses sufficient strength to support its own weight when exposed as a vertical face or if it is undermined.

Most of the backfill used in underground mines is either hydraulic fill or rock fill. Hydraulic fill relies on water to transport silt or sand sized aggregates through boreholes and pipelines as a slurry or a paste. Rock fill, on the other hand, relies on mechanical methods, such as conveyors and mobile equipment, as well as a series of raises to transport rock sized aggregate to the stope.

As can be seen in Figure 3, a 20:1, 70% solids hydraulic fill is made up of crushed rock from surface quarries or underground development rock and the mill waste products, known as mill tailings. The solid aggregates can range from fine slimes to several centimeters in size. Chemicals (cement, pozzolans and other additives) added to backfill

to improve its physical characteristics, water added to transport the aggregates and air may make up the final backfill delivered to the stope".

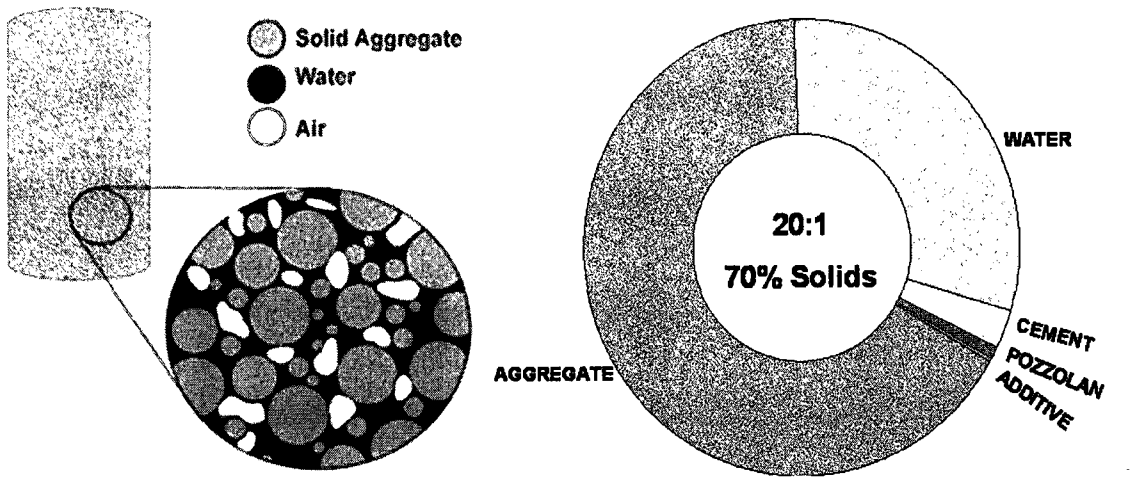

Figure 3- Relative make-up of hydraulic backfill (short course note Archibald and Hassani, 1998)

Backfill properties can vary considerably from mine to mine. The backfill used at a particular mine will depend greatly on any mining wastes produced and on any local natural resources available. Which aggregate is used depends on several design factors, including the availability of raw materials near the mine site, environmental concerns, the mining method used at the mine, other engineering requirements and production scheduling issues (Hassani and Archibald, 1998)

In the last two decades, considerable amount of research has been conducted around the world. These have been summarized in a "Mine Backfill handbook" by Hassani and Archibald (1998). Furthermore there has been series of mine fill conferences in the last twenty years reporting the latest development in mine fill technology .It is important to note that very little detailed research has been done on backfill thermal properties up to this time. Thermal properties; especially thermal conductivity of backfill may be

controlled by varying various constituent of the mixture to achieve the appropriate results for overall design. It is important to note that such research should also take in to account the primary objective of the mines fill which is its strength and the economics of the whole mine fill operation. Backfill has physical properties between soils and soft rocks with the behavior nearer to soils, so it could be classified as a cemented soil in assessment of thermal properties. With hydration occurring in the backfill after preparation and placement due to cementation as well as excess water drainage during that time, it is supposed that backfill will have variable thermal conductivity with the time, but after 28 days it could be considered that the backfill is cured and no further change is expected (Hassani, 1992). Also to shed light on the values of thermal conductivity of backfill and evaluating other conditions in underground excavations for geothermal energy extraction purposes, it is essential to know the thermal properties of different rocks and soils.

2.2. Thermal conductivity of rocks

In near surface rock formations, heat transfer mostly is dominated by conduction. Only at great depth, where temperature is above 1000 °C, heat convection and heat radiation dominate (Clauser and Huenges, 1995). For evaluating the potential of extractable geothermal energy, it is important to know the thermal properties of rocks, especially thermal conductivity. Furthermore, in order to calculate the required mine cooling load for the mine ventilation system one should know thermal properties of associated rock mass. In some very permeable rocks, heat convection due to saturant fluid can be effective but it is exempted regularly due to rock structure which caused negligible moisture movement. Thermal conductivity of rocks depends on its origin and make up, or one could say rock type (Clauser and Huenges, 1995). Although most igneous rocks have

isotropic heat transfer, sedimentary and metamorphic rocks are anisotropic; but, insitu examination is needed for determining the regime of heat transfer because of geological and tectonic processes as well as major discontinuities (Clauser and Huenges, 1995).

Thermal conductivity is principally calculated according to Fourier's law of heat conduction. Thermal conductivity of rocks can be measured in the laboratory on rock samples and insitu in boreholes, depending on the application of the resulting measurements using steady-state methods or unsteady-state (transient) methods. According to why it is needed to measure the thermal conductivity, it should be decided to carry out the measurements insitu or in the laboratory, since the results can be significantly different even if the insitu parameters also taking into account for laboratory tests due to the scale dependence (Clauser and Huenges, 1995) and this variability can be as much as a factor of 2 or 3, even within the same rock type (Abdulagatov, 2006). Also, in the case that there is no data available and no direct measurements can be done, one could estimate the thermal conductivity from some computational methods on the basis of other physical characteristics of the rock. Some of these models are based on well defined physical models while others are completely empirical. Thermal conductivity measurement as well as computational methods will be discussed in detail later in this chapter and the next chapter. Rocks have different thermal conductivities because of various mineral contents of different fractions as well as several physical and digenetic factors. Generally, the thermal conductivities of rocks depend on the following parameters (Clauser and Huenges, 1995):

- The mineral contents and constitution,

- The structural and textural features like mineral size; grain size distribution, mineral shape and the porosity as well as the presence of micro cracks
- The amount of pore fluid, and
- Test conditions

Clauser and Huenges (1995) classified rocks into four basic groups of similar thermal behavior and studied the effect of different parameters on each groups which consist of plutonic rocks, volcanic rocks, sedimentary rocks and metamorphic rocks. A brief result of his study presented in two following ternary diagrams.

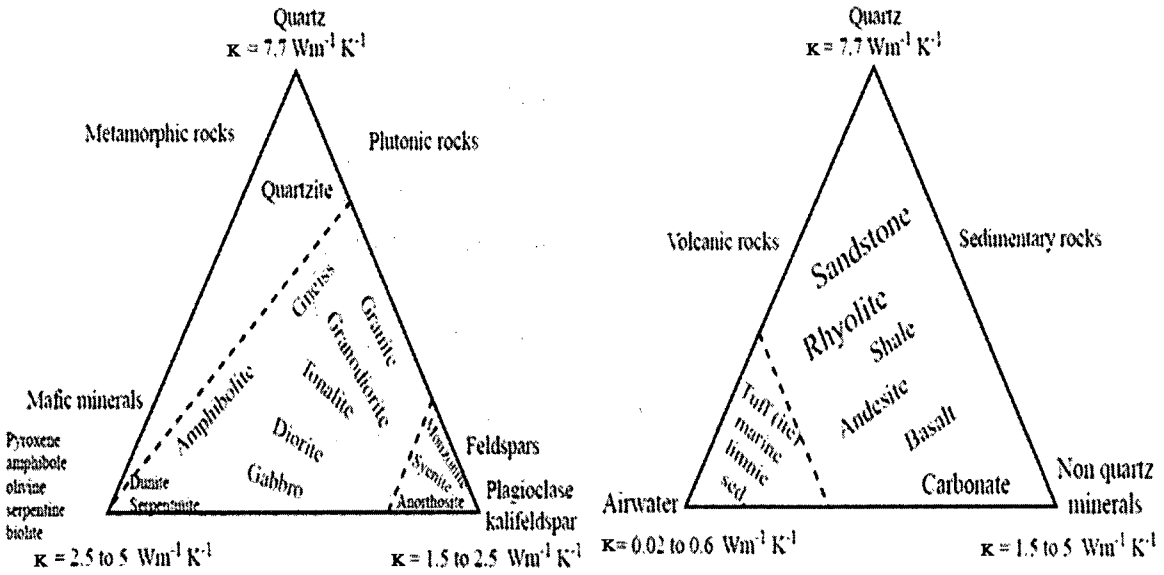

Figure4- Thermal conductivity relationship of rocks and basic rock-forming minerals (Clauser, 1995)

Here, different effective parameters and their influence on thermal conductivity of rocks are briefly explained, but it must be noted that any exceptions could be possible due to the nature and uncertainties that exist in the rocks.

2.2.1. Porosity

Porosity has an influential effect on thermal conductivity of rocks. As it is observed, thermal conductivity decreases significantly by increasing porosity. This is due to the low conductivity of void filling material that is generally can be air ($k = 0.024\ \frac{W}{m°C}$) or water ($k = 0.60\ \frac{W}{m°C}$) or the mixing of both which both have small thermal conductivity comparing to rock minerals content. For sedimentary and volcanic rocks porosity has a significant effect on thermal conductivity; but, in plutonic and metamorphic rocks it is observed that porosity displays lesser reduction on thermal conductivity of these types of rocks (Clauser and Huenges, 1995). Woodside and Messmer (1961) measured the thermal conductivity for six consolidated sandstones using air, water and heptanes as pore saturant for different porosities. In Figure 5, an example graph of the relation between thermal conductivity and porosity is shown. Since the replacement of very low thermal conductivity air with high thermal conductivity solids destroys solid particles contact, the decrease is bolder for less amount of porosity.

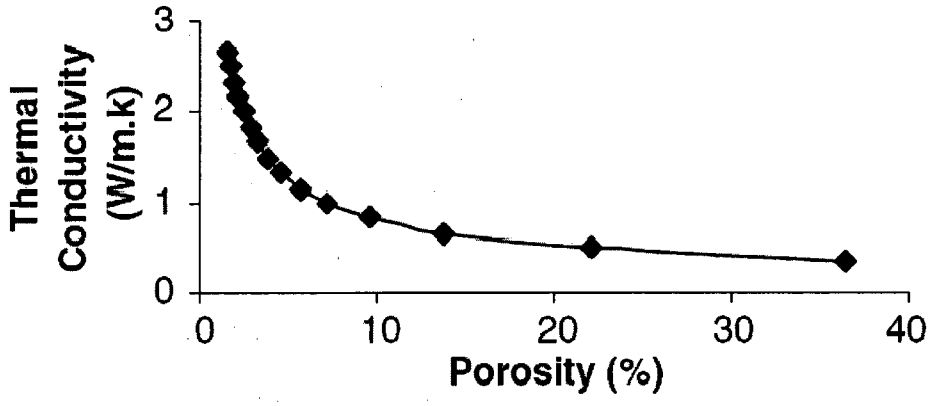

Figure 5- Thermal conductivity versus porosity (Singh et al., 2007)

2.2.2. Temperature

Thermal conductivity is also a function of temperature. In this case, lattice or phonon thermal conductivity has inverse relation with temperature. This would be explained mainly due to the thermal expansion during temperature rise and considering the differential expansions of rock's components, this may create a contact resistance as a consequence of thermal cracking (Clauser and Huenges, 1995). Closed cracks act as scattering centers for the heat carrying phonons (Seipold, 1998). This effect is more sensible in dry rocks compared to saturated rocks (Clauser and Huenges, 1995). For most rocks with crystalline structure, thermal conductivity decreases monotonically with increase in temperature until 700°C-1200°C and after this temperature, due to radiation, thermal conductivity which follows T^3-law, this trend reverses (Clauser and Huenges, 1988). In plutonic rocks, the decreasing trend is more pronounced for rocks that are poor in feldspar since in feldspar the temperature has an increasing effect on thermal conductivity, and in metamorphic rocks quartzite has significant impact since quartz thermal conductivity decreases dramatically (Clauser and Huenges, 1995). Figure 6 shows the effect of temperature on thermal conductivity of samples of sandstone and Pyroxine-granulites. The thermal conductivity of rocks decreases with temperature as porosity and the amorphous phase in rocks increase.

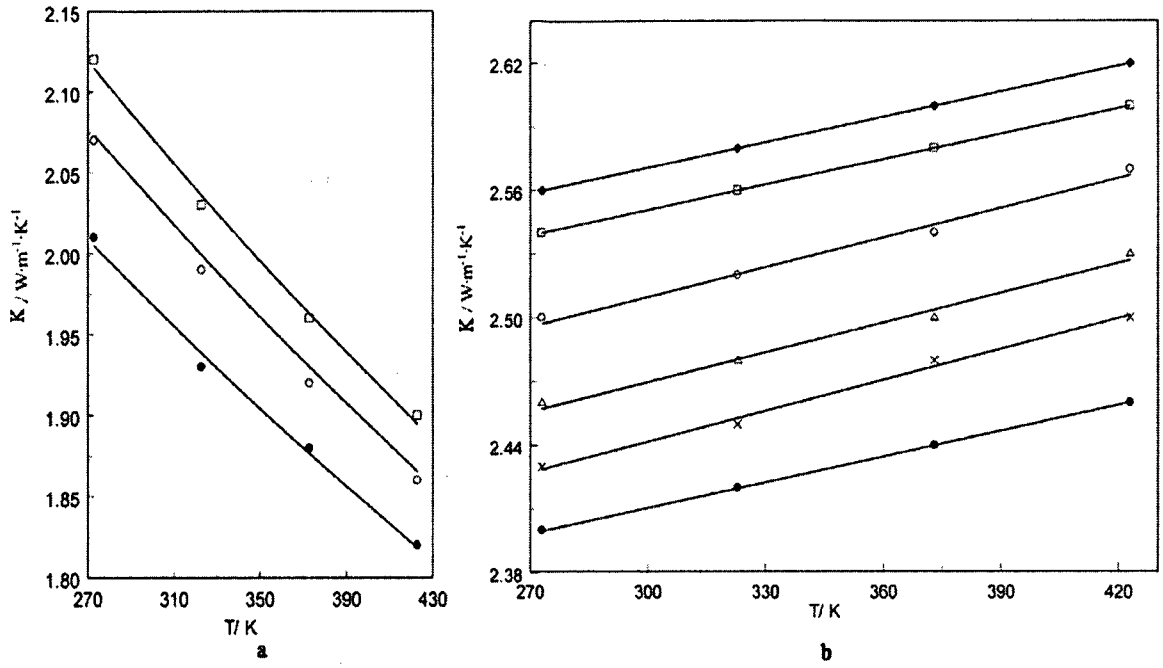

Figure 6- The effect of temperature at different pressures (● 0.1MPa,Δ 50MPa,O100MPa,× 150MPa,□ 200MPa,♦ 250 MPa, ■ 300MPa) on thermal conductivity of samples of sandstone (a) and amphibolites (b), (Abdulagatov, 2006)

Rocks with high feldspar content could show an increase in thermal conductivity with temperature because of plagioclase feldspar content which its thermal conductivity increases with temperature that compensates for the decrease in thermal conductivity. The greater the feldspar content, the smoother the decrease and in some cases thermal conductivity even increases with temperature (Cermak, 1982). Schatz (1972) measured the thermal conductivity of several important earth materials in the temperature range from 227 °C to 727°C. Seipold (1990, 1995, 1996, 1998, 2002) used a pulse method to study the thermal conductivity and thermal diffusivity of rocks at high temperature (up to 800°C) and high pressure (up to 1000 MPa) and offered specific relations to calculate thermal conductivity for each group of rock types.

2.2.3. Pressure

The pressure effect on thermal conductivity of rocks has some relation with the porosity. This effect is especially sensible when examined on laboratory samples. Upon removing samples from the field, cracks develop due to stress release and after the sample is brought to surface the cracks begin to close again with rising pressure in the lab when pressure is applied to the sample (Clauser and Huenges, 1995). This leads to a decrease in internal thermal resistance of the sample and if the pressure is high enough it can even reduce the intrinsic porosity, so first there are no significant changes in thermal conductivity but then a sharp increase was observed which stops at pressures between 15-70 MPa and afterward very smooth increases until the minimum porosity is reached (Clauser and Huenges, 1995), from this point on, a further pressure increase does not affect thermal conductivity significantly. These changes are more sensible for porous rocks in that the effect of pressure on thermal conductivity is different for distinct pressure range. Generally, the effect of pressure on thermal conductivity is smaller than the effect of temperature (Abdulagatov, 2006). Figure 7 shows the effect of pressure on thermal conductivity of samples of sandstone and amphibolites. Rock's thermal conductivity increases with pressure in the elastic region of deformation and its increasing trend becomes linear with a positive slope in the elasto-plastic region (Demirci, 2004).

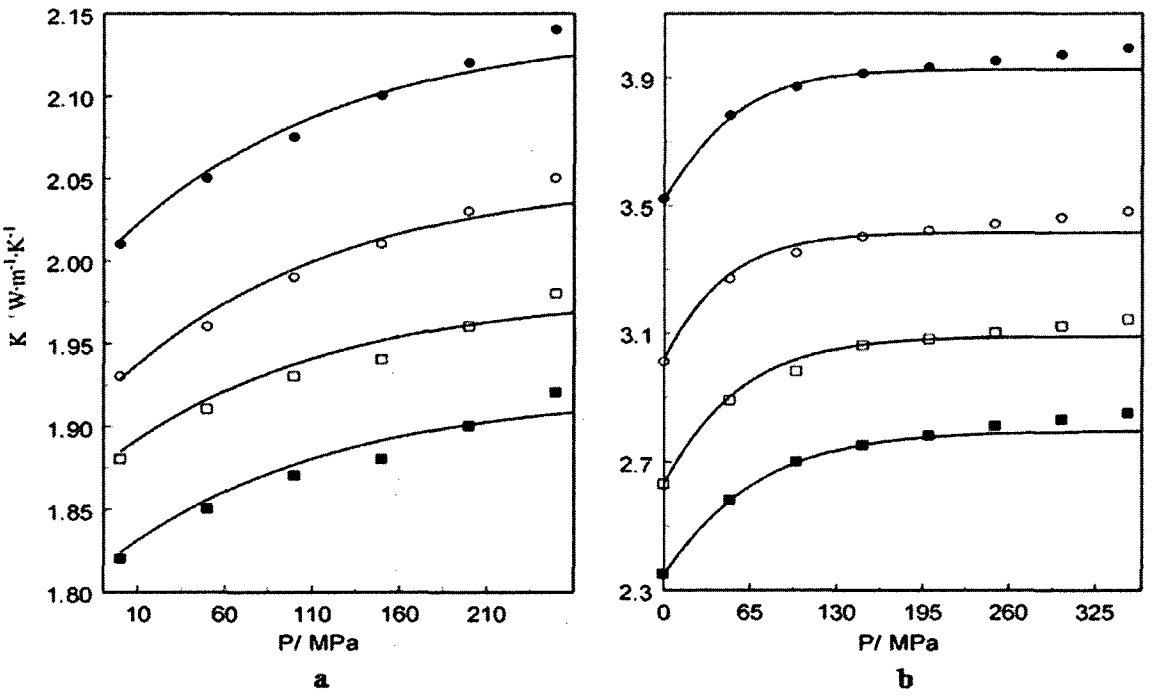

Figure 7-The effect of pressure at different temperatures (● 0°C, O 50°C ,□ 100°C, ■150°C) on thermal conductivity of samples of sandstone (a) and amphibolites (b), (Abdulagatov, 2006)

When pressure is applied to a rock sample, the stress –strain behavior indicates that in the elastic region high rate of deformation occurs initially with small stress, and then there is a linear portion prior to the plastic or initiation of micro fracture within the rock. In the last stage again high rate of deformation occurs with small increase of stress as it is easier for cracks to further deform. This directly relates to the finding of Demirci (2004) as pressure increases initially the pores start closing so the thermal conductivity also increases, this increase continues in the linear zone.

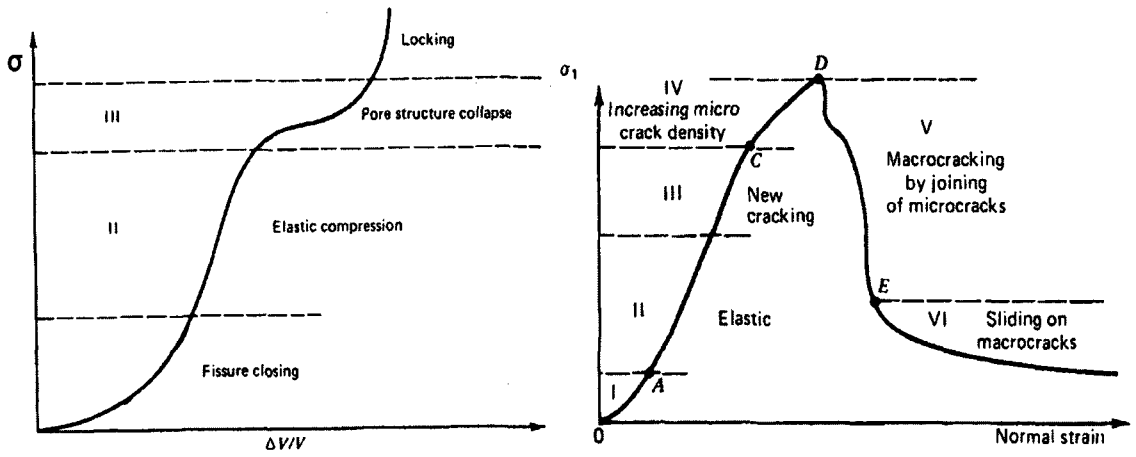

Figure 8 – Pressure (stress) deformation relation in rocks (Goodman, 1989)

Since deep in the ground, three dimensional field of stress exists; Demirci (2004) studied the effect of uniaxial and triaxial pressure and proposed a new form of Fourier's law considering these pressures. It was determined that the thermal conductivity of the rocks under triaxial stress (Equation 2) increases more, compared to thermal conductivity under uniaxial stress (Equation 1), according to the following equations but graphs behavior remains the same. Depending on the application conditions and results, the difference between these two could be neglected.

$$Q = -(k_0 + \lambda P^n)At\frac{d_T}{d_x} \quad \text{Equation 1}$$

$$Q = -(k_0 + \lambda_{cp} P^{n_{cp}})c_p^{\beta_{cp}} At\frac{d_T}{d_x} \quad \text{Equation 2}$$

Where Q is the heat flow to the rock surfaces, J; A is the area of the body whose heat is to be transferred, m^2; $\frac{d_T}{d_x}$ is the temperature gradient, $\frac{°C}{m}$; k is the thermal conductivity of the material, $^{W}/_{m°C}$; k_0 is the thermal conductivity of rock under normal condition; λ and n are the rock dependent constant parameters in uniaxial compression; P is the applied uniaxial pressure, MPa; λ_{cp}, n_{cp} and β_{cp} are the rocks dependent constant

parameters in triaxial compression, c_p is the confining pressure, MPa. Horai (1989) measured the thermal conductivity of 23 silicate rock samples at temperature from 27 °C to 427 °C and pressure of up to 1200MPa with an uncertainty of 4%-5% using a steady-state method and the results show that the thermal conductivity of all samples increases with increasing pressure. The increase is at its highest up to 200 MPa which could be resulted from the closure of microcracks in the samples.

2.2.4. Saturation

Thermal conductivity generally increases with increasing saturation, but the behavior and the trend depends on the kind of pore space. Porosity in porous rocks consists of bottlenecks and the bulk pore space which respectively contribute 10-20% and 80-90% of total porosity. In this kind of porous rocks, thermal conductivity increases to its near maximum with only of 10-20% increase in saturation and then a small increase could be expected until 100% of saturation (Clauser and Huenges, 1995). This is because that filling of intergranular bottlenecks can reduce contact resistance significantly by replacing low conductivity air by higher conductivity fluid (as water) and creating water bridges, the slight further increase is because of after having this water bridges, water replacement in bulk pores has a little effect on thermal conductivity (Reibelt, 1991).

If porosity is due to only the fractures, the pore space just consists of bottleneck and a linear increase with the saturation to 100% is expected (Clauser and Huenges, 1995). The saturation fluid could be effective as if the same rock gets saturated with different thermal conductivity fluids; the resultant thermal conductivities are higher for those whose saturation fluids have higher thermal conductivity (Reibelt, 1991). Woodside

and Messmer (1961) measured the thermal conductivity for six consolidated sandstones using air, water and heptanes as pore saturant. They found that higher pore satuarant thermal conductivity result in higher overall thermal conductivity and saturation with liquid instead of gas result in higher thermal conductivity at same saturant thermal conductivity. Thermal conductivity of dry and water-saturated low-porosity crystalline rocks (granitic samples) measured with a quick thermal conductivity meter at room temperature was reported by Scharli (1984). In Figure 9, a sample of the relation between saturation and thermal conductivity is shown.

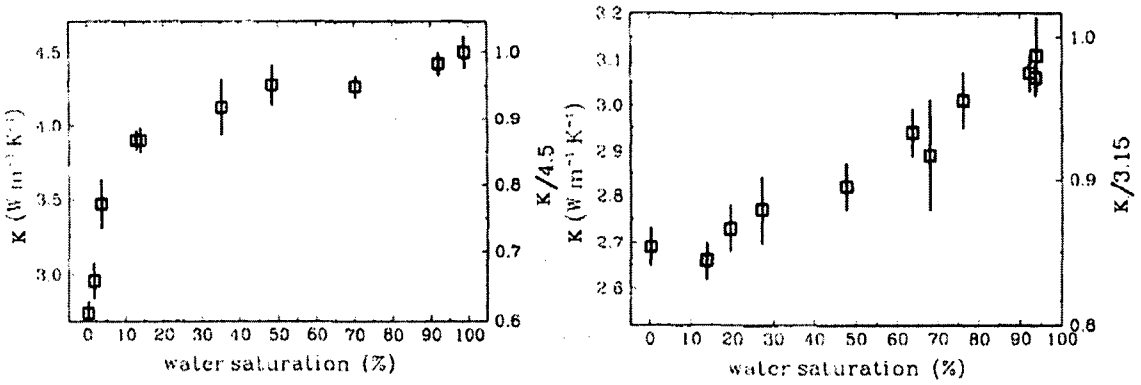

Figure 9-Variation of thermal conductivity with saturation: sandstone (right), granite (left) (Clauser and Huenges, 1995)

2.2.5. Mineral content

Mineral content also has an important effect on thermal conductivity of rocks. Rocks are very complicated and consist of minerals with various chemical elements. Therefore, the thermal conductivity of rocks strongly depends on the conductivity of its skeleton solid mineral components; rock-forming minerals and cementation substances; from which it is made (Clauser and Huenges, 1995). Rocks, made of minerals having high thermal conductivity, show high thermal conductivity and their thermal conductivity behavior is very dependent on the fraction of dominant mineral content. This behavior is

more recognizable in plutonic rocks as feldspar is the determining factor; plutonic rocks with higher amount of feldspar tend to have lower thermal conductivity than those being poor in feldspar and inversely in metamorphic rocks quartz makes the main contribution so that those being rich in quartz have higher thermal conductivity (Clauser and Huenges, 1995).

2.2.6. Density

There is not a specific work on relation between bulk density and thermal conductivity, but, generally due to the expected reduction in porosity and air-filled porosity with increasing of density it is expected that thermal conductivity increases with density. The increase in bulk density could stem from heavier mineral contents, considering that minerals with higher density generally have higher thermal conductivity. Ozkahraman (2004) and Singh et al. (2007) did some research on finding the relation between thermal conductivity with different parameters which one of them was bulk density. The result of Singh et al (2007) is shown in Figure 10.

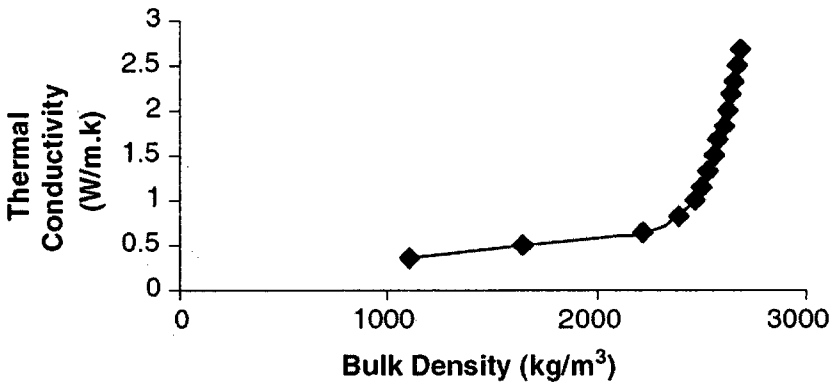

Figure 10- Thermal conductivity versus bulk density (Singh et al., 2007)

2.2.7. Anisotropy

Anisotropy in some cases has a significant effect which should be considered. In some rock types, it is important whether measurements are done parallel or perpendicular to the apparent direction of foliation. In some cases, like high thermal conductivity gneiss (3-4.3 $\frac{W}{m°C}$), a positive difference of 50% is observable when measurement is done parallel rather than perpendicular to the foliation (Clauser and Huenges, 1995). The anisotropy of thermal conductivity would not be affected by the pore space, fractures and the saturation; this is valid when the rock thermal conductivity is more than fluid thermal conductivity (Clauser and Huenges, 1995). Huenges (1990) reported thermal conductivity for 500 core samples with transient method and uncertainty of 5% considering anisotropy as one parameter and he found out that anisotropy in some cases could make important variation in measured thermal conductivity.

2.2.8. Thermal conductivity of minerals

In minerals, thermal conductivity is better measured since mineral crystal structure and chemical formula is better constrained (Clauser and Huenges, 1995). The two most problematic matters are purity and sample size in that lattice imperfections in crystals considerably reduce the thermal conductivity so correction of alien minerals is needed, and this point that samples of single crystal to meet the minimum sample size requirement in some methods is rare, also for monomineralic polycrystalline aggregate uncertainty due to the porosity could make unreliability in results (Horai, 1971). Horai & Simmons (1969) used a finely ground samples to measure the thermal conductivity of minerals and they achieved good results but they lost information on anisotropy.

Deminet & Pratt (1988), Birch (1954), Robertson (1988), Ratcliffe (1959), Clark (1966) and Dreyer (1974) did some measurements on some minerals and they determined most of minerals thermal conductivity. Knowing thermal conductivity of minerals is very advantageous especially when one wants to estimate thermal conductivity of rocks and soils using geometric mean method which will be discussed later on this chapter.

2.2.9. Thermal conductivity estimation

Estimation from mineral content and saturation fluid

One of the best and simplest physical models for estimating the thermal conductivity of rocks and soils is the geometric mean method. It is observed that generally thermal conductivity of rocks and soils can be estimated with acceptable accuracy from its mineral contents and saturation fluid according to mineral little variance in thermal conductivity than thermal conductivity of rocks and soils. But one should be cautious in using this method since it does not necessarily give accurate results for all cases. If k_i is the thermal conductivity of the i_{th} mineral or saturating fluid and x_i is the volume fraction of respective material, then thermal conductivity can be defined:

$$K = \prod {k_i}^{x_i} \quad , \quad \sum x_i = 1 \quad \text{Equation 3}$$

Well-log correlation

Using data from well-logs can give good estimation of thermal conductivity. It is possible to find relationships between thermal conductivity and data derived from well logs like porosity, density, p-wave velocity (Blackwell, 1989) and developing mixing model to the borehole scale or applying geometric mean as mixing model, but both couldn't consider

the effect of anisotropy since it needs direct measurement to be taken into account (Clauser and Huenges, 1995). A phonon conduction model applying temperature, acoustic velocity and bulk density measurements of well-log data was established by William & Anderson (1990) which gives results with 15% accuracy but is only limited to unfractured rocks.

Prediction methods are usually used to extrapolate laboratory measurements when direct measurements are not possible. The major difficulties in developing theoretical methods to anticipate thermal conductivity are the complexities of the geometries of the rock and soil structures (Abdulagatov, 2006). Even with a well-defined structure, the problem remains due to the existence of the interface resistance. Existing prediction methods are based on certain simplifications such as parallel cylinders, spheres dispersed in a conducting medium. Thus, a semi empirical approach is the best way to predict the thermal conductivity of a porous material. Walsh (1966) and Beck (1976) have established a correlation equation for the estimating thermal conductivity of geological porous materials by a three-phase geometric mean method in which the predictive results agreed with experiments within 22%. Anand (1971) studied the effects of various physical properties on the thermal conductivity of dry sandstone samples. Staicu (2001) developed a predictive analytical method as well as a numerical method for calculating the composite porous materials thermal conductivity. Zimmerman (1989) developed a model for calculating the thermal conductivity of low-porosity saturated rocks using porosity and pressure as the effective factors, which is an extension of Maxwell's model (1904).

Robertson (1988) introduced an empirical relation which considered combination effects of porosity, saturation and dominant mineral that gave better results for mafic and felsic rocks and sandstones. Ozkahraman (2004) made a relationship between P-wave velocity and thermal conductivity in which relatively accurate results for some kinds of rocks which are used for construction purposes were obtained. In Figure 11, the relation between P-wave velocity and thermal conductivity is shown.

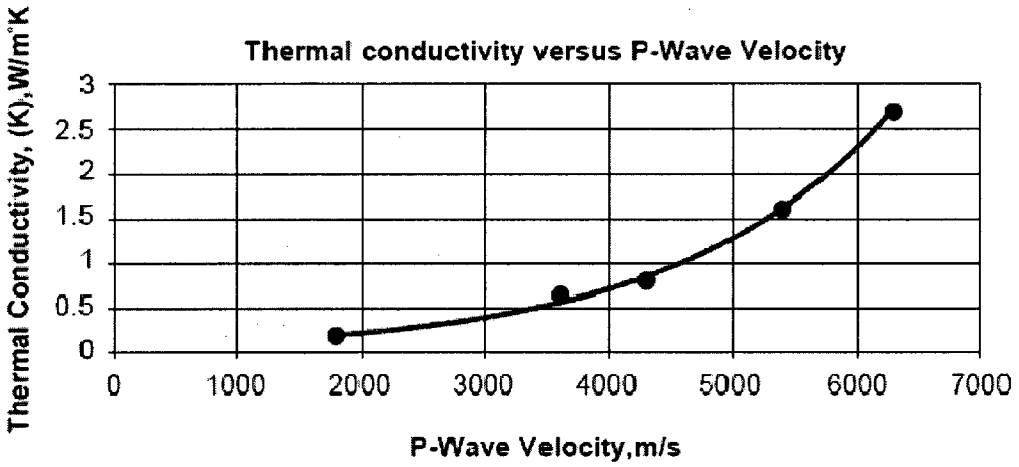

Figure 11- Thermal conductivity versus P-wave velocity (Ozkahraman, 2004)

The values of the thermal conductivity from thermal diffusivity measurements are defined as $k = \alpha\rho c_p$(α:thermal diffusivity, c_p:specific heat capacity, ρ:density). The theoretical and experimental problems of the laser flash technique in thermal diffusivity measurements have been discussed by Blumm (2002) and Blumm and Opfermann (2002). Xu (2004) calculated the lattice thermal conductivities from thermal diffusivity results using heat capacity and an equation of state for olivine, wadsleyite, and ringwoodite at temperatures up to 1100 °C and at pressures to $20^3 MPa$. Hofer (2002) reported thermal diffusivity data for quartz, orthoclase, and sanidine at elevated

temperatures and he found a non-linear decreasing trend of thermal diffusivity with temperature up to about 600°C.

Singh et al. (2007) presented a study which predicts the thermal conductivity of rocks by using 136 rock samples and Artificial Intelligence (AI) methods as Artificial Neural Network (ANN) and Adaptive Neuro Fuzzy Interference System (ANFIS). They used P-wave velocity, porosity, bulk density, uniaxial compressive strength of rocks as input parameters and compared six predictive models for the thermal conductivity of rocks. The drawback of this study is that they didn't consider saturation, as this factor is a significant parameter in thermal conductivity behavior. Among these predictive models, ANFIS was proved to be the best in results and captured a complete range, very accurately with average absolute percentage error of 0.03% as well as regression coefficient of 1, and Feed Forward Back Propagation neural network (FFBP) gave the best time performance with average absolute percentage error of 2.26%. P-wave velocity and thermal conductivity showed that has the best correlation coefficient among others. Figure 12 shows the results of six predictive models applied in this study. Also, some researchers established the relation between Uniaxial compressive strength as an essential parameter in geomechanical study of rocks and the thermal conductivity which shows the increase of thermal conductivity with this parameter. Also, in many cases this behavior has been observed but it cannot be considered for all kind of rocks. The results of Singh (2007) work for P-wave Velocity are shown in the Figure 13 below.

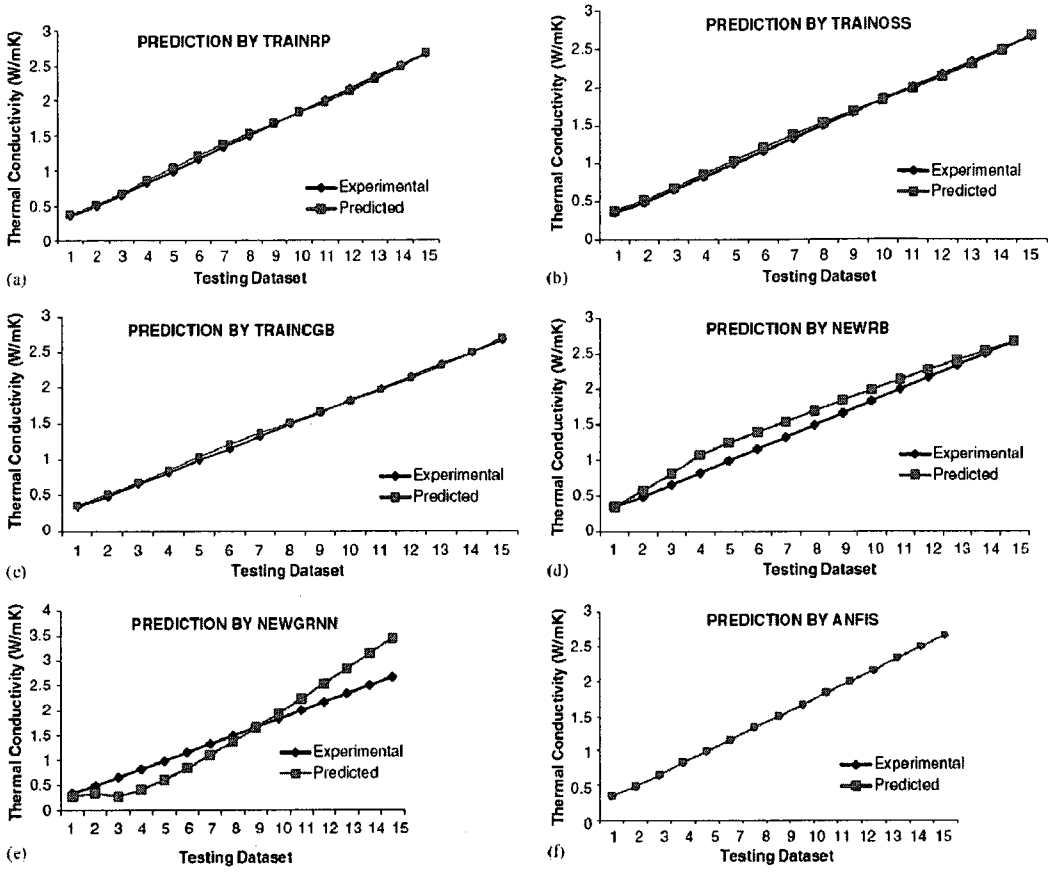

Figure 12- Comparison of experimental and predicted values for different networks (Singh et al., 2007)

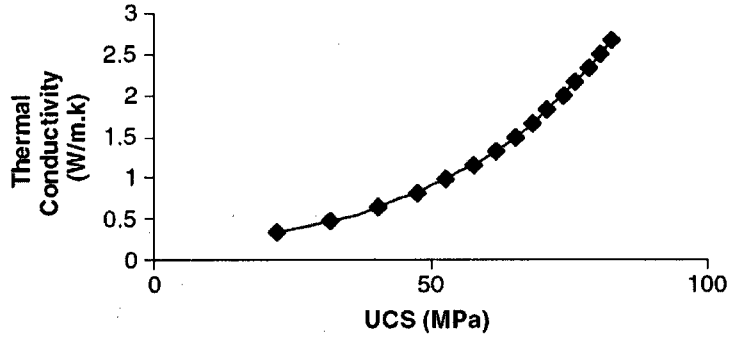

Figure 13- Thermal conductivity versus uniaxial compressive Strength (Singh et al., 2007)

2.3. Thermal conductivity of soils

Soil is a multiphase porous media. A dry or water saturated soil is a two-phase medium, composed of solid particles and air or liquid water, respectively. While a soil

partially saturated by water is a three phase medium with the liquid water distributed among the solid particles and replacing some air-filled pores by adsorption and capillarity (Buckman, 1975). In a partially saturated soil, heat transfer couples several mechanisms of thermally induced and potential-induced flow of water in liquid and vapor phases; if the temperature is below the freezing point, part of the water can be in the solid state and according to conditions in porous medium, it would form a four-phase medium (Gori, 2002).

Thermal conductivity of soils is an essential parameter in determining the heat transfer for different applications in the ground. For the design and operation of any kind of these installations, knowledge of the conductivity of those soils is required. Due to the importance of soil thermal conductivity, it was of interest to calculate its value on a physical basis. Soil thermal properties especially thermal conductivity is an important factor in the surface energy regime and resulting temperature distribution. Thermal conductivity of soils are different due to the variation of values of their basic components; for instance the thermal conductivity of solid particles generally varies from 1-5 $^{W}/_{m.\,°C}$, whereas values for water, ice and air (pore fluid) are $0.6^{W}/_{m.\,°C}$, $2.24^{W}/_{m.\,°C}$, and 0.024 $^{W}/_{m.\,°C}$, respectively (Côté and Konrad, 2005a). Among many factors that could have an influence on thermal conductivity of soils, the water content (degree of saturation), porosity, mineral composition, temperature and bulk density seem to have the most contribution. Also there could be difference between insitu results and lab results in the way that for lab samples usually a structured soil is disturbed and finely fragmented, then more gaps are introduced, therefore thermal conductivity may decrease significantly (Smith, 1942).

2.3.1. Porosity

Porosity has relation with distribution of grain sizes, shapes and packing condition of that kind of soil (Das, 2002). Heat conductivity in soils has a very close relation with contact points which is a function of porosity as a decrease in porosity leads to more contact points and therefore better conductivity. The importance of porosity is more observable in evaluating dry soils. Depending on the particle size range and distribution, soils with coarse particles generally can have less porosity than those with finer particles. Farouki (1986) describes the porosity effect this way: with a wide size range and a continuous grading of particles sizes, a less porous and denser mix could be obtained and therefore dry density and the number of contact points per unit volume are increased as well thermal conductivity. But conversely, open-graded soils show lower thermal conductivity due to increase in porosity. Also flat, angular particles may be fitted closer together and denser packing with less porosity could be reached, but in rounded-particle soils more porosity is expected generally. In Figure 14, the effect of porosity, n, on thermal conductivity for given moisture contents for two granular granite materials with $n = 0.18, n = 0.30$, respectively, is shown. For dry soils, grain size influence can be related to porosity with good accuracy (Farouki, 1986). Since with larger grain sizes the porosity decreased, higher thermal conductivity would be reached. This behavior is also observed for angular particles and rounded particles.

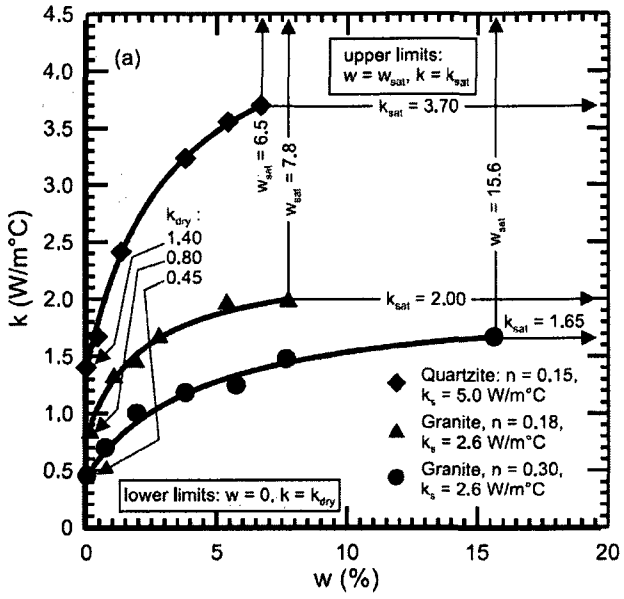

Figure 14- Thermal conductivity of granular pavement materials (Côté and Konrad, 2005b)

2.3.2. Structure effect

From the thermal characteristic view, the structure of solid matrix characterizes the contact resistance and continuity of the solid phase (Kaviany, 1995). In soils, the structure is generally associated with the effect of soil fabric(texture), soil composition and interparticle forces, which is influenced by size and shape of particles as well as the aggregation of particles (Mitchell, 1993). Considering thermal behavior, the structure of porous soils is divided in three categories: a) unbound rounded/sub-rounded particles, b) unbound angular/sub-angular particles and c) bound/cemented particles; which respectively the thermal contact and so that the conduction potential increases because of better contact and less porosity(Côté and Konrad, 2008). Hashin and Shtrikman (1962) proposed two bounds where the effective thermal conductivity of a two-phase material should locate, the upper bound applies to a continuous solid phase including uniformly dispersed fluid filled and the lower bound applies to a continuous fluid phase including uniformly dispersed solid spheres. These bounds are mathematically equivalent to the

Maxwell (1904) model. Considering the structure effect, the theoretical model developed by Fricke's (1924) which is further extended by De Vries (1963), gave fairly good estimation for the thermal conductivity of soils when fitted to data sets from Woodside and Messmer (1961). It was shown that the effect of structure is more influential when the k_f/k_s ratio is smaller, where k_f is Thermal conductivity of fluid and k_s is thermal conductivity of solid (Côté and Konrad, 2008).

Côté and Konrad (2005) developed a generalized relationship on the basis of degree of saturation where the dimensionless empirical parameter κ is associated with the structure of three-phase soils. Côté and Konrad (2008) developed a new semi empirical modeling approaches to assess the effect of structure on the effective thermal conductivity of two-phase porous geomaterials. They introduced κ_{2p} parameter, with presenting a simplified relationship between this parameter and k_f/k_s ratio, as well as empirical parameter β related to the structure of geomaterials, which is associated to structure effect that has the highest values for cemented/bounded particles corresponding to the highest thermal conductivity for the same solid particles. The results of their study demonstrated that the structure effect is considerable as the k_f/k_s ratio decreases and is not considerable when this ratio is lower than 0.066. They also found out that pore distribution and particle size have very minor effect on thermal conductivity for two-phase porous soils.

2.3.3. Saturation

Water in all its forms has important and very complex effects on the thermal properties of soils. The relative volume fractions occupied by the various constituents of a soil affect the value of its thermal conductivity. Thermal conductivity of soils generally

increases with saturation. Gemant (1950) explained this as the dry soils have a lower thermal conductivity because air which exists in pores and separates the grains of soils has a very small thermal conductivity; by addition of water to soil the air is replaced by water with higher thermal conductivity and therefore the conductivity increases. The effect of increasing water content depends on the type of soil, by means that, for some a rapid increase is observed and for some others it is mild, while for some it is slow. But, soils in general show a high rate of increase in thermal conductivity at low moisture contents the same as most rocks. Thermal conductivity of soils increases with water content due to bridges which established by pore liquid between particles. Experiments have shown that the thermal conductivity of a soil depends on whether the particular moisture content is achieved by drying or wetting (Farouki, 1966). Because of hysteresis effects, soils may show considerably different thermal properties at the same water content, depending on whether this saturation is reached by wetting or drying (Winterkorn, 1961). In fine-particle soils, more water is needed to reach to a certain thermal conductivity comparing to coarse-particle soils; This is because of less water is needed to establish water bridges in well-graded coarse-particle soils due to lower specific surface area (Farouki, 1986). It must be noted that the effect of microstructure, which represents the spatial distribution of the components relative to each other, on thermal conductivity variations at the same volume fractions should not be neglected (Farouki, 1986). In frozen soils, the presence of unfrozen water is the major factor in the thermal properties behavior of those under saturation condition (Farouki, 1986).

A water content which varies from point to point results in variable thermal conductivity that affects the temperature distribution in the soil and vice versa (Farouki, 1986). Ice has

a thermal conductivity four times of water and it is expected that frozen soils have higher thermal conductivity than those unfrozen. This is true for saturated and high moisture content soils while at low moisture contents the unfrozen soils slightly higher thermal conductivity is observed (Kersten, 1963), but the important influence of liquid water in connecting points, could contradict this fact. The thermal conductivity of frozen or freezing fine-grain soils are influenced by their unfrozen water (Farouki, 1986). McGaw (1968) supported this view that in frozen fine-grain soils, the unfrozen water plays an important part in improving thermal contacts while this effect could not be seen in frozen coarse-grained soils. Kersten (1949) explored the relationship between thermal conductivity and moisture content in a soil in some detail and presented some empirical equations showed that thermal conductivity is linearly related to logarithm of moisture content at a constant dry density. Johansen (1975)(Côté and Konrad,2005b) introduced the concept of the Kersten number (normalized thermal conductivity) using some of the data provided by Kersten (1949) for medium and fine sands as well as fine-grain soils as below, considering thermal conductivity in dry, partially and fully saturated states. But he didn't consider the migration of moisture's effect in calculation.

$$K_r = \frac{k - k_{dry}}{k_{sat} - k_{dry}} \qquad \text{Equation 4}$$

$$k_{sat} = k_i^{n-\theta} k_w^{\theta} k_s^{1-n} \qquad \text{Equation 5}$$

Where i, w, s represent ice, water and solid parts respectively; n is porosity, and θ is volume fraction of unfrozen water. Figure 15 shows the normalized thermal conductivities (K_r) behavior as a factor of degree of saturation (normalized water content) for 3 granular materials.

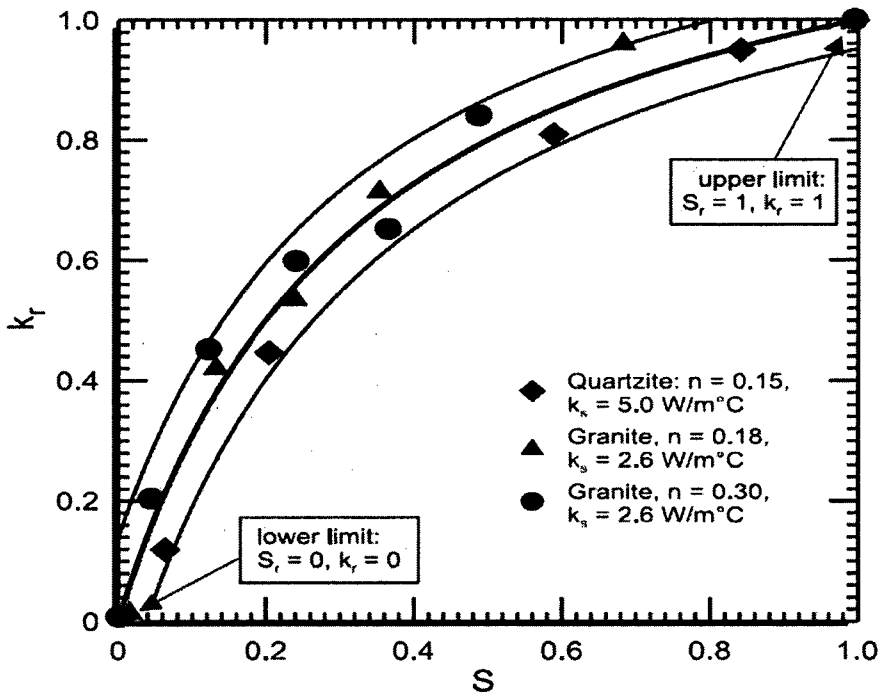

Figure 15- Normalized thermal conductivity as function of degree of saturation (Côté and Konrad, 2005b)

Johansen (1975) also proposed three empirical relationships for soils studied by Kersten (1949) on the basis of normalized thermal conductivity and the degree of saturation. Côté and Konrad (2005) introduced a generalized thermal conductivity model for soils and construction materials, which is an improvement of Johansen (1975) work considering degree of saturation and κ which is an empirical parameter used to account for the different soil types in the unfrozen and frozen states, as below:

$$k_r = \frac{\kappa S}{1+(\kappa-1)S} \qquad \text{Equation 6}$$

2.3.4. Density

Density has a proportional relation with porosity. An increase in the dry density of soil, with its associated decrease in porosity, results in an increase in the thermal conductivity, mostly due to having more solid material per unit soil volume that enables

less pore air or pore water per unit soil volume and better heat transfer which is occurs across the contacts. In general, experiments have shown that there is relatively a linear trend between the thermal conductivity of a soil or its logarithm on one hand and the dry density of that soil (Farouki, 1986). Kersten (1949) found that at constant moisture content, the logarithm of thermal conductivity increased linearly with the dry density. In Figure 16, the relation between dry density and thermal conductivity for sandy soils is shown. For the dry soil, an increase in dry density has an important effect on the thermal conductivity, as there is more solid material per unit soil volume (replacing poorly conducting air) and better thermal contacts, so thermal conductivity shows higher sensitivity to dry density and microstructure variations. It must be noted that in fully saturated condition an increase in dry density means that solid particles replaces the water and thermal conductivity increase occurs only if the thermal conductivity of solid particle would be higher than that of water which is mostly the case for the soils (Farouki, 1986).

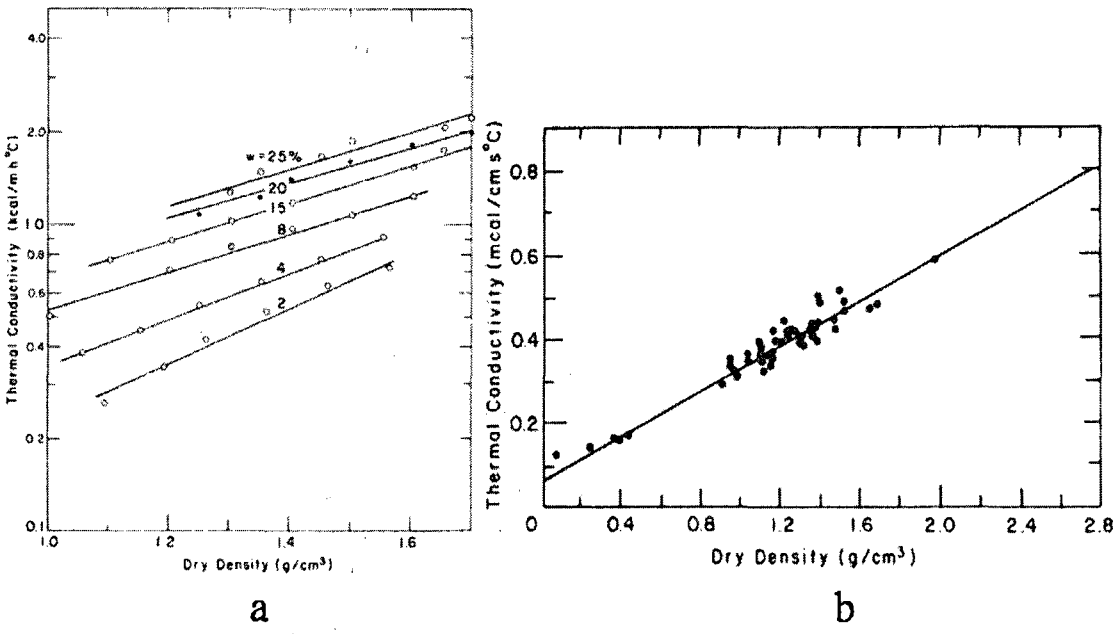

Figure 16 - Thermal conductivity of a) sandy soils, b) dry soils vs. dry density (Farouki, 1986)

2.3.5. Temperature

The magnitude of soil temperature affects the soil properties from different aspects like intrinsic properties of soil water, the amount of unfrozen water in frozen soils, the rate of water movement and other soil-water properties (Farouki, 1986). The effect of temperature is important since it influences the degree of binding, the energy state and the movement of the water (Farouki, 1986). Temperature gradients cause water movement directly. Temperature and particles size has a close relation as in coarse-grain soils almost all the water turns into the ice at 0°C, while in "fine-grain soils an appreciable amount of unfrozen water may remain at temperature as low as -40°C" which affect the thermal conductivity (Anderson & Tice, 1973; Farouki, 1986). "In a simple manner, it could be assumed that the increase in thermal conductivity through the freezing point to be abrupt for gravel but gradual for fine-grain and peat soils" (Figure 17) (Farouki, 1986).

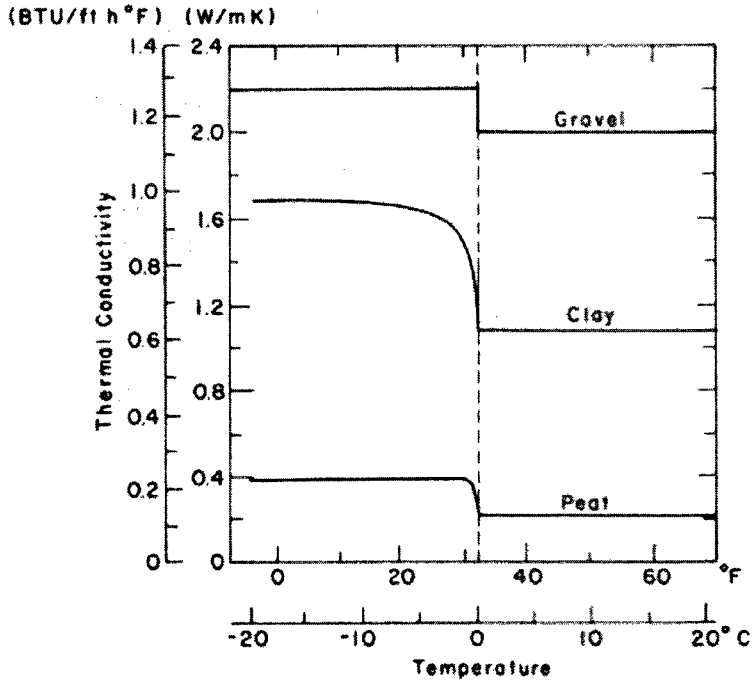

Figure 17-Thermal conductivity changes against temperature for different particle sizes (Farouki, 1986)

In negative temperatures, there is a sudden jump in the percentage of frozen water at a definite degree of saturation which is named critical degree of saturation (Lange and McKim, 1963). Bellow this point, the thermal conductivity of frozen soil decreases as the temperature is lowered, while above this point this effect is inversed by the large amount of ice formed and thermal conductivity increases with decreasing temperature (Farouki, 1986). In Figure 18, the thermal conductivity change for fine sand against negative temperature at different saturation from dry condition ($S_1 - S_6$:0.0, 0.382, 0.523, 0.725, 0.866, and 0.936) is shown. At temperatures above 0°C, it seems that thermal conductivity increases with temperature, especially for coarse-grained soils (Flynn and Watson, 1969). The increasing rates are different for various kinds of soil. In Figure 19, this change can be seen for Ottawa sand. Considering that thermal conductivity of soil solids and minerals decrease with increasing temperature, this behavior resulted from some interfacial effects leading to increased heat transfer and some surface bonding improvement (Flynn and Watson, 1969), the increase in thermal conductivity of water with temperature and/or the increase in moisture migration and hence in the effective thermal conductivity as the temperature increase. Van Rooyen and Winterkorn (1957) explained this as chemical, crystallographic and sintering changes were occurred, it led to a decrease in surface area per unit volume which together with the better condition in interfacial thermal conductivity, result in an increase in thermal conductivity. For saturated soils, thermal conductivity of liquid water and ice increases with temperature and the absolute value of temperature, respectively.

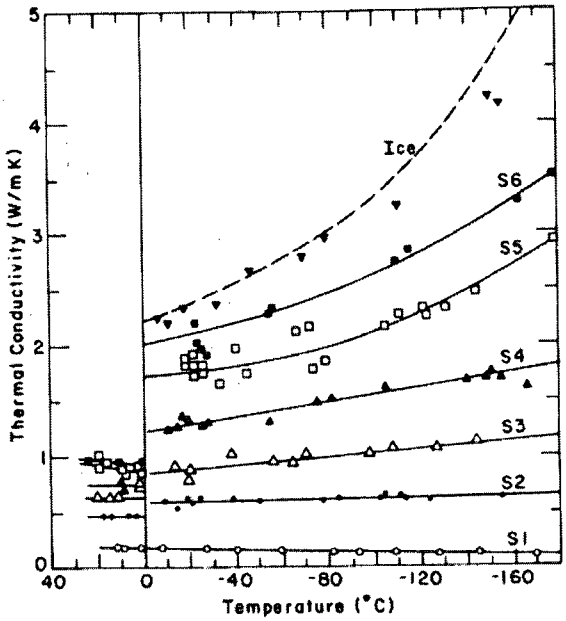

Figure 18-Thermal conductivity vs. temperature for a fine sand at different saturation (Farouki, 1986)

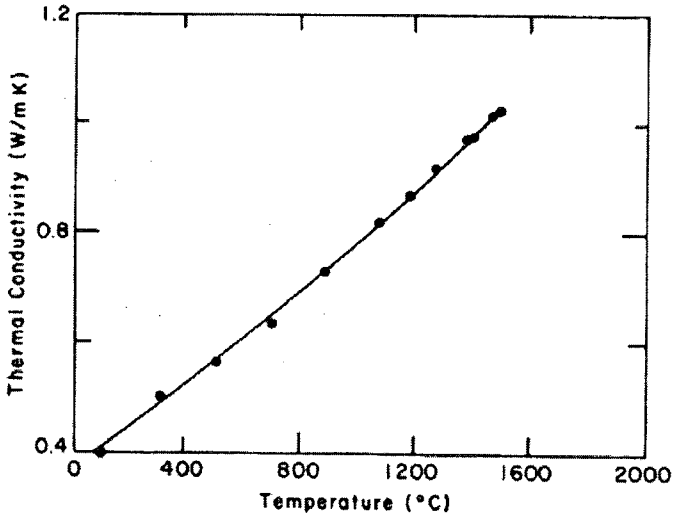

Figure 19- Thermal conductivity vs. temperature for Ottawa sand at high temperature (Flynn and Watson, 1969)

2.3.6. Mineral composition

Mineral composition has a similar effect on thermal conductivity as what was discussed for the rocks. Soils composed of high conductivity minerals at considerable amounts show high conductivity and behavior of thermal conductivity of such soils is

very dependent on fraction of dominant mineral content. The common mineral in soil with the highest thermal conductivity is quartz, so knowing the quartz fraction could be particularly effective in accurate evaluation of thermal properties; Johansen (1975) used this concept as part of his model for determining thermal conductivity of soils. To determine the effective thermal conductivity of solid soil particles composed of different conductivities the geometric mean value equation (Equation 3) is used as below:

$$k_s = \prod_{j=1}^{m} k_j^{x_j}$$

Where x represents the volume fractions and the subscripts j refers to the each component. The thermal conductivity of soils may have dependency on the direction of heat flow. anisotropic minerals which have different thermal conductivities due to direction of heat flow to the principal (optic) axis (parallel or perpendicular), may result in various thermal conductivities for a kind of soil that must be considered (Farouki, 1986). This effect would be intensified if water movement occurs due to a temperature gradient. Figure 20 shows the effect of anisotropy for quartz particles. Organic components have thermal conductivities about the one-tenth that of general mineral solids that should be considered. A range of 0.25-0.45 $^{W}/_{m.\,^{\circ}C}$ is introduced for these materials in the literature. The presence of peat and organic materials in a mineral soil reduces its thermal conductivity in both the frozen and unfrozen states and Kudryavstev (1974) deal with this matter in details.

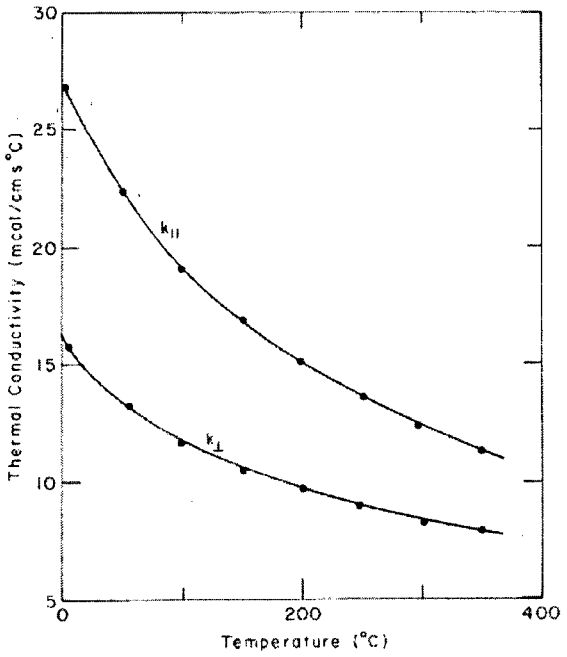

Figure 20-Anisotropy and temperature effect on thermal conductivity of quartz (Farouki, 1986)

2.3.7. Thermal conductivity estimation

The prediction of thermal conductivity of soils is very important in many heat and mass transfer phenomena related to ground, including waste disposal in unsaturated geologic media, geothermal energy extraction, drying problems in multiphase heat and mass transfer in porous and fractured media, enhanced oil recovery, radioactive waste storage, ground heat pumps and heat exchangers and many other ground applications which is dependent on a wide variety of properties related to soil which were explained early in this chapter (Gori, 2002).

In 1963, De Vries presented a model to calculate the thermal conductivity of soil according to the mineral composition, volume fractions and shape of soil particles in two-phase soils. He also dealt with the influence of moisture movement on thermal conductivity by the fact that temperature gradients cause moisture movement so that the

moisture tends to redistribute itself when the temperature field is changed. He specially studied quartz sand, Fairbanks sand, Healy clay and Fairbanks peat. Campbell et al. (1994) presented a modified version of the De Vries model which requires four parameters including texture, bulk density, moisture content and temperature as inputs that are fitted to measured thermal conductivity data.

Kersten (1949) developed an empirical model which only requires bulk density as an input parameter, but it was not appropriate for predicting thermal conductivity at low water content. Tarnawski (2000) developed the Kersten model that gives the Kersten function for computing the thermal conductivity of soils which depends on soil temperature and the degree of saturation. This new Kersten function enables the prediction of thermal conductivity of moist soils with the degree of saturation greater than 0.125 and within the temperature range of up to 90°C. Although for the temperature range of 70°C-90°C in soils with medium or high moisture content the results are not very accurate.

Johansen (1975) proposed the concept of normalized thermal conductivity and presented a simple empirical model which is based on the degree of saturation and soil mineral composition. For many soils this model gives accurate predictions. Côté and Konrad (2005a) made some improvement to Johansen's model and developed a model which introduced an empirical relationship between the normalized thermal conductivity and degree of saturation, but it does not give good results for low water content and very fine-texture soils. Gori (2002) developed a theoretical model; using water content, porosity, dry and solid particle density, used to simulate three-phase (unsaturated) porous soils which gives predictions in very good agreement with experimental results at the

temperatures of 30°Cand 50°C. This work was a developed model of his previous model for frozen soil.

Farouki (1986) briefly compared eleven estimation methods for thermal conductivity of soils. He concluded that Johansen (1975) method generally gives the best results for unfrozen or frozen coarse grain or fine grain soils at degree of saturation above 0.10. De Vries (1964) method is better for unfrozen coarse grain soils when saturation is between 0.10 and 0.20. Below degree of saturation of 0.10 the methods do not give good results. Kersten (1949) method gives good results for frozen fine grain soils at degree of saturation values less than 0.90, otherwise the predictions are not consistently appropriate and Johansen method is better. In particular the Kersten method should not be applied to coarse grains soils with either low or high quartz content. For saturated soils different methods could be used but Johansen method is the easiest one to use.

Usowicz (2006) presented a model for predicting the thermal conductivity of the silt loam by a regression equation based on easily measured quantities such as penetration resistance and water content or air-filled porosity. It was observed that using penetration resistance and air-filled porosity in the regression equations resulted in a substantial improvement in accuracy over using penetration resistance and water content. It shows that it is more strongly correlated with air-filled porosity than with volume fractions of water or solids. Also adding sand content could contribute to more accuracy in predictive thermal conductivity. In Figure 21, graphs resulted from this work are shown.

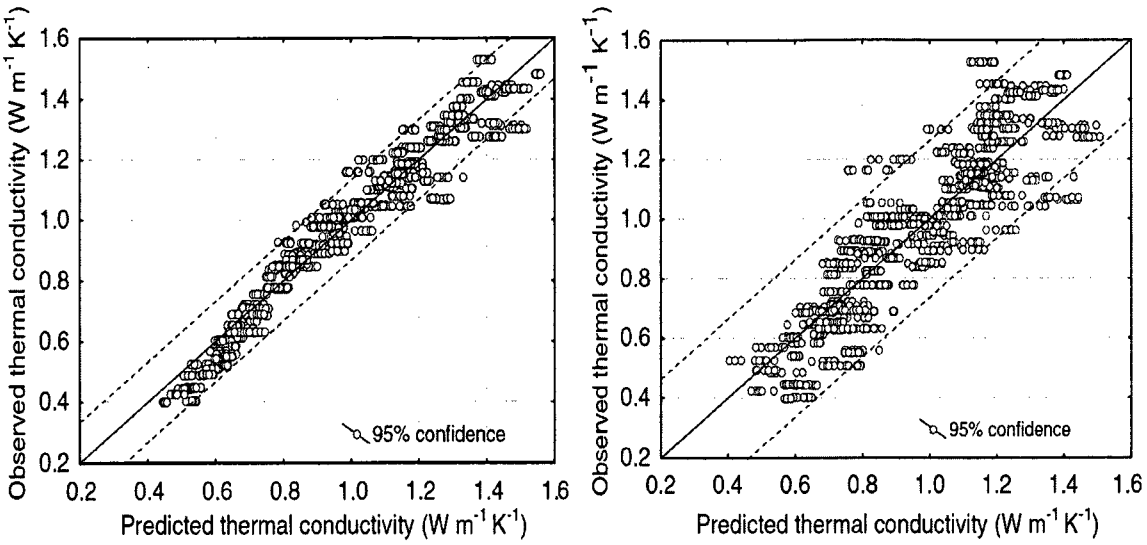

Figure 21- Predicted thermal conductivities vs. observed ones based on air-filled porosity (left) and soil water content (right) (Usowicz, 2006)

Côté and Konrad (2005b) introduced a method using their model to predict the thermal conductivity of soils for a wide range of soils with an acceptable accuracy. In their method normalized thermal conductivity of soils calculated, considering thermal conductivity of soil in dry and saturated states, as a function of porosity, degree of saturation, mineral content, particle size distribution and particle shape of unfrozen and frozen soils. Their proposed method could be seen in Figure 22.

Lu et al. (2007) developed an improved model from Côté and Konrad (2005b) which describes the relationship between thermal conductivity and volumetric water content of soils. With this model, soil thermal conductivity could be estimated using soil bulk density, sand (or quartz) fraction and water content. This model gives accurate results for a wide range of soils and shows sensitivity to the quartz fraction of coarse-texture soils. It has been observed that the coarse-texture soils and the soils which have the higher sand fraction, have higher thermal conductivity comparing to fine-texture soils and those with less sand fraction, as well.

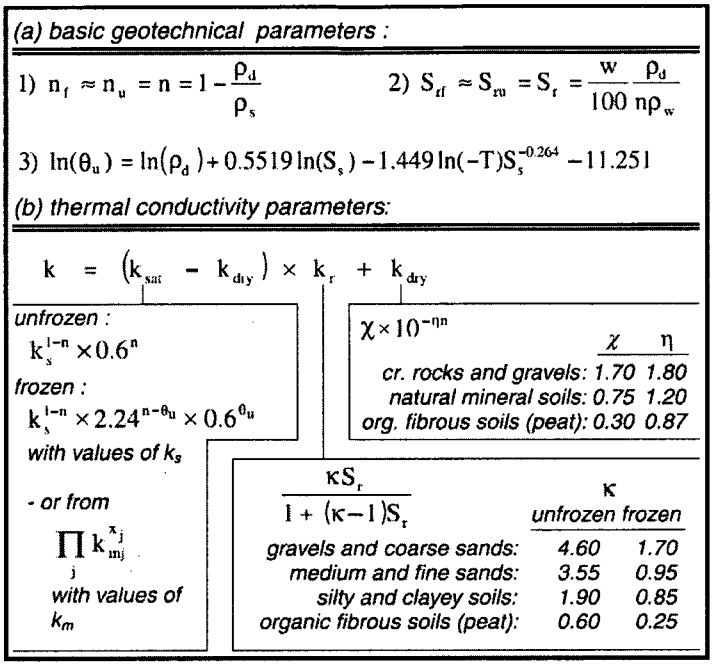

Figure 22- Method for calculating the thermal conductivity of unfrozen and frozen soils, cr: crushed, org: organic (Côté and Konrad, 2005b)

Côté and Konrad (2007) summarized five indirect methods to determine the thermal conductivity of soil solid particles, in which each method is more convenient depending on the kind of soil composition and its physical condition, and validated them for solid particle of Quebec marine clays, which includes:

1. Method 1 based on saturated soil thermal conductivity data,
2. Method 2 based on data sets of thermal conductivity of partially saturated samples and their respective degree of saturation,
3. Method 3 based on a single set of thermal conductivity of partially saturated sample and its respective degree of saturation,
4. Method 4 based on mineral content of soil using the well-known generalized geometric mean method,
5. Method 5 based on quartz fraction using a simplified geometric mean model.

In tables 1 and 2 below, thermal conductivity of some rocks and minerals are shown.

Table 1- Thermal conductivities of some minerals (Côté and Konrad, 2005b)

Mineral	ρ_s (g/cm³)	k (W/m°C)
1. Nesosilicates (single tetrahedron)		
Olivine		
Chrysolite	3.47	4.81
Fayalite	4.36	3.16
Forsterite	3.28	5.03
Hyalosiderite	3.77	3.45
Garnet		
Almandine	3.93	3.31
Andradite	3.75	3.09
Grossularite	3.49	5.48
Pyrope	3.75	3.18
Spessartite	3.99	3.40
2. Sorosilicates (double tetrahedron)		
Epidote		
Clinozoisite	3.36	2.40
Epidote	2.19	2.83
Zoisite	3.27	2.15
Idocrase	3.34	2.41
3. Cyclosilicates (rings of tetrahedrons)		
Beryl	2.7	3.99
Cordierite	2.59	2.72
Tourmaline	3.13	5.28
4. Inosilicates (chains of tetrahedrons)		
Amphibole (double chains)		
Actinolite	3.06	3.48
Grunerite	3.40	3.32
Hornblende	3.18	2.81
Tremolite	2.99	4.78
Pyroxene (single chains)		
Acmite	3.54	3.49
Augite	3.27	3.82
Bronzite	3.36	4.16
Diopside	3.33	4.93
Enstatite	3.27	4.47
Spodumene	3.16	5.65
5. Phyllosilicates (sheets)		
Chlorite	2.75	5.15
Mica		
Biotite	2.98	2.02
Glauconite	2.85	1.63
Lepidomelane	2.86	1.57
Muscovite	2.85	3.48
Phlogopite	2.85	2.13
Pyrophyllite	2.83	8.14
Serpentine		
Antigorite	2.66	2.95
Chrysotile	2.60	5.30
Lizardite	2.60	2.34
Talc	2.81	6.10
6. Tectosilicates (framework)		
Feldspar		
Celsian	3.09	1.44
Microline	2.56	2.49
Orthoclase	2.58	2.32
Sanidine	2.57	1.65
Feldspathoid		
Nepheline	2.62	1.73
Sodalite	2.33	2.51
Plagioclase		
Albite	2.63	1.96
Anorthite	2.77	1.68
Bytownite	2.72	1.56
Labradorite	2.70	1.53
Oligoclase	2.64	1.98
Silica		
Hyalite	2.08	1.21
Novaculite	2.66	7.21
Quartz	2.65	7.69
Vitreous silica	2.21	1.35
7. Carbonates		
Calcite	2.71	3.59
Dolomite	2.90	5.51
Siderite	3.81	3.01
8. Oxides		
Hematite	5.14	11.28
Ilmenite	4.55	2.38
Magnetite	5.15	5.10
Magnesiochromite	4.23	2.54
9. Hydroxides		
Brucite	2.39	8.44
Gibbsite	1.88	2.60
10. Sulphates		
Anhydrite	2.98	4.76
Barite	4.41	1.34
Gypse	2.30	1.26
Selenite	2.32	1.26
11. Halides		
Fluorite	3.10	9.51
Halite	2.10	6.11
12. Sulphides		
Chalcopyrite	4.09	8.20
Pyrite	5.1	19.21
Pyrrhotite	4.6	1.89
Sphalerite	4.00	12.73
13. Phosphates		
Amblygonite	3.03	4.99
Chlorapatite	3.15	1.39
Fluorapatite	3.22	1.37

Table 2- Average values of thermal conductivities of rocks computed from different sources (Côté and Konrad, 2005b)

Material	ρ_s (g/cm^3)	k_s (W/m°C)
Rocks		
Anorthosite	2.73	1.8
Basalt	2.90	1.7
Diabase	2.98	2.3
Dolostone	2.90	3.8
Gabbro	2.92	2.2
Gneiss	2.75	2.6
Granite	2.75	2.5
Limestone	2.70	2.5
Marble	2.80	3.2
Quartzite	2.65	5.0
Sandstone	2.80	3.0
Schist	2.65	1.5
Shale	2.65	2.0
Syenite	2.80	2.0
Trap rock	2.90	2.0
Soil and organic matter		
Coal	1.35	0.26
Peat	1.50	0.25
Silt and clay	2.75	2.90

2.4. Backfill

Mine backfilling defined as a process in which the cavities created by mining activities are filled with mostly waste materials and addition of other materials. The first recorded use of mine backfill in North America went back to 1864 at Shenandoah, Pennsylvania by the Philadelphia & Reading Coal & Iron Co (Hassani & Archibald, 1998). The involvement of Normal Portland cement as a strengthening agent led to introduction of binding concept in backfill industry (Hassani & Archibald, 1998). The increasing trend in cemented backfill along with the increasing price of Portland cement has caused considerable interest in the use of alternative materials to replace Portland cement. Recent works has focused on binder alternatives, the development and application of high density backfills which have improved backfill strength, cement consumption and water disposal while allowing for full tailings disposal requirements

underground (Hassani & Archibald, 1998). Binder addition, environmental aspects and resource conservation are the main aspects in developing the backfill technology in recent years.

2.4.1. Backfill purposes and properties

Backfill initial benefits could be mentioned as wall support and subsidence prevention which were the most important ones, and later followed by its application as working floors in mines, void filler and an economic method for disposing of tailings (Hassani & Archibald, 1998). As a whole, the reasons for backfilling consist of ground control, economics, environmental considerations, need for preparation of a working floor as in some underground mining methods and ore recovery increase (Hassani and Bois, 1992).

Backfill system concerns include backfill transportation, bulkheads, quality control, fill material preparation, placement, maintenance, labor and stope preparation (Hassani & Archibald, 1998). The basic mechanical properties that should be considered in backfill design from the mining view are compressive strength and permeability (slurry and paste backfill) (Hassani & Archibald, 1998). Compressive strength is considered after a 28-day period which could be less than 1 MPa in general, up to 5 MPa and sometimes even 7 MPa in delayed backfill with pillar recovery (Hassani & Archibald, 1998). Permeability is a very important property of backfill that affects the stope dewatering capability and not giving enough consideration could result in serious damages. A universally accepted percolation rate of 100 $^{mm}/_{h}$ in mining industry is considered for the slurry fill and in the case of placed slurry fill; slightly higher rate is preferred (Hassani & Archibald, 1998.

As mentioned before, after cement involvement in backfill technology, cemented backfill from different material compositions (classified tailings, or mixtures of rock, sand and binder) has been employed as a support, with growing popularity in recent 3 decades (Hassani & Archibald, 1998). Practical studies show that cement content in a backfill and its slurry (pulp) density are critical factors in backfill stability and its economy (Hassani & Archibald, 1998). Binder consumption is the most economic matter in backfill and its optimization has been an important point in backfill studies. When short curing time and high compressive strength is needed as in cyclic backfilling higher binder consumption is expected and for most other cases like delayed backfill less amount of binder is employed (Hassani & Archibald, 1998). Basically in backfill design, fill composition determination, pulp density (water requirement) and binder content are required to produce an acceptable mixture, having desired mechanical and physical properties, that is economic (Hassani & Archibald, 1998).

Backfill has the physical and mechanical properties like soils and rocks with more tendencies toward soils especially cemented soils. Among these properties are Water Content and Saturation (w, S_r), Void Ratio and Porosity (e, n), Bulk Density, Unit Weight and Specific Gravity (r, G, G_s), Particle Friction and Cohesion (f, C), Particle Shape, Size and Distribution, Permeability and Percolation Rate.

2.4.2. Fill materials

Fill materials which are most commonly used are classified into three categories as follows: inert material (which is the main part of the backfill), the binding agent and chemical additives (Hassani & Archibald, 1998). The inert materials commonly used are

mineral processing tailings, sand or gravel, waste rock and coarse slag. Binding agents such as Portland cement, ground blast furnace slag and fly ash are applied in backfill technology to improve the mechanical properties of the fill especially the strength (Hassani & Archibald, 1998). Chemical compositions of 4 kinds of binder are presented in Table 3. Chemical additives, if necessary, are mostly employed to improve the fill permeability, flowability of the slurry and the consolidation properties of the fill (Hassani & Archibald, 1998). Inert materials sometimes should be sized or deslimed to meet percolation rate and transportation requirements. More details about fill materials concentrating on those which employed in this work are explained in following chapters.

Table 3- Chemical composition of different binders (Neville, 1996)

	Portland cement	Blast furnace slag	Fly ash Class C	Fly ash Class F
CaO	65	45	25	3
SiO_2	20	33	37	58
Al_2O_3	4	10	16	20
Fe_2O_3	3	1	7	10
MgO	3	6	7	1

2.4.3. Backfill methods

The backfilling method depends on the mining method and can be divided into two general categories; these are cyclic and delayed backfilling (Hassani & Archibald, 1998). In delayed backfill, the fill must be capable of remaining as a free standing wall after getting exposed during pillar recovery (Hassani & Archibald, 1998). In cyclic backfilling, backfill in each cycle acts as a platform for mining personnel and equipment, and mining could occur below, beside or through the backfill, consequently these

conditions and requirements should be taken into account in design (i.e. under cut & fill or undermining) (Hassani & Archibald, 1998).

To define appropriate backfilling methods, the following criteria are proposed (Hassani & Archibald, 1998):

1. Backfill technology should be reliable and guarantee safety and continuity in mining operations,
2. Backfill capacity should be optimized based on technical and economic analysis and backfilling operation time should not exceed 20% to 25% of the overall mining operation period,
3. Fill preparation and the placement system should be simple and efficient,
4. Stope preparation should be minimized and fill facilities utilize efficiently,
5. The backfill operation must be economical.

2.4.3.1. Slurry (hydraulic) backfill

Slurry fill includes tailings, sand and/or rock materials which can be mixed with a binding agent and water. Preparation can take place on surface or underground and placement is typically at a pulp density of less than 70% by weight (Hassani & Archibald, 1998). Slurry fill technology has been widely used in underground mining. Recent optimization in the solids concentration resulted in substantial savings in cement consumption, a large proportion of operating costs.

Simplicity to install, full control of constituents in fill station, easiness in desliming technology for percolation rate, possibility of gravitational transportation and availability of inert materials are advantages of this method (Hassani & Archibald, 1998). Excess

water drainage, inadequate strength due to cement marbling, costly slime clean up after drainage, interruption of backfilling operation with other production activities and possibility of washing out are the problematic matters (Hassani & Archibald, 1998).

2.4.3.2. Paste fill

Paste fill is similar to toothpaste and characteristically has different flowability compared to slurry fill in that it has higher pulp density, between 75% and 85% by weight, which depends on the grain size distribution and the specific gravity of solids (Hassani & Archibald, 1998). Total tailings are utilized and sand or waste rock may also be used. It is possible to transport the material from surface and does not need in-situ dewatering. Cement may be added at sites of preparation or immediately prior to placement.

State-of-the-art fill technology is used in making Paste fill and it holds promising long-term potential in mining. Using paste fill could considerably reduce the cyclical nature of mining, improves ground conditions, increases production rate and highly reduces environmental costs (Hassani & Archibald, 1998). A comprehensive study on fill technology, dewatering and delivery mechanism is necessary to design a proper paste fill system. Improvements in drainage technology and processes continue to reduce the cost of paste fill application (Hassani & Archibald, 1998). For a long time flow behavior design and transportation have been important issues in paste fill.

Total tailing usage and consequently less surface disposal, less cement consumption comparing to slurry fill and very little or no dewatering in stope, are among advantages of paste fill (Hassani & Archibald, 1998). High pressure in pipelines due to displacement

pumps, superior dewatering, more sophisticated technology and control, are some of past fill disadvantages (Hassani & Archibald, 1998).

2.4.3.3. Rockfill

In rockfill, Waste rock from underground operations or surface quarry which was dumped into raises, is distributed by trucks or conveyors to the stopes. When cemented rockfill is needed, the cement in a slurry form can be added by a pipeline and mixed with the waste rock before placement or can be used to post-consolidate placed rockfill (Hassani & Archibald, 1998).

Rockfill has considerable advantages in mining, especially when development waste is used, since it is free of cost (Hassani & Archibald, 1998). Rockfill is a highly economic option for mines with a surface mine on site or nearby as a method of waste disposal (Hassani & Archibald, 1998). Considering the advantage of using waste rocks and high strength support that rockfill provided, it is unlikely to be totally replaced by other types of backfill (Hassani & Archibald, 1998).

Rockfill has the advantages such as waste disposal reduction, simple preparation, high strength especially when cement is applied and no stope dewatering (Hassani & Archibald, 1998). Crushing cost, achieving less tight filling due to segregation, additional cost to fill voids in rockfill, are issues that confine the application of rockfill (Hassani & Archibald, 1998).

In Table 4, a comparison between the properties of slurry fill, paste fill and rockfill is presented.

Table 4- Comparison between main backfilling methods (Hassani & Archibald, 1998)

Properties	Slurry Fill	Paste Fill	Rockfill
Placement State	60% to 75% solids (by weight)	75% to 85% solids (by weight)	Dry
Underground Transport System	Borehole/pipeline via gravity	Borehole/pipeline via gravity, can be pumped	Raise, mobile equipment, separate cement system
Binder Application	Cemented or uncemented	Cemented only	Cemented or uncemented
Water to Cement Ratio (w/c)	High w/c ratio, low binder strength	Low to high w/c ratio. Low to high binder strength	Low w/c ratio, high binder strength
Placement Rate	100 to 200 Tonne/hr	50 to 200 Tonne/hr	100 to 400 Tonne/hr
Segregation	Slurry settlement and segregation, low strength development	No segregation	Stockpile and placement segregation, reduced strength and stiffness
Stiffness	Low stiffness	Low or high stiffness	High stiffness if placed correctly
Tight Filling	Cannot tight fill	Easy to tight fill	Difficult to tight fill
Binder Quantity	Requires large quantity of binder	Usually lower quantity of binder required	Moderate binder quantities
Barricades	Expensive	Inexpensive	Not necessary
Water Runoff	Excessive water runoff	Negligible water runoff	No water runoff
Capital Costs	Low capital costs	High than for slurry fill	Moderate capital costs
Operating Costs	Low distribution costs; lowest cost for an uncemented fill	Lowest cost for a cemented fill	High operating costs

Chapter 3: Measurement Methods

3.1. Introduction

The measurement of thermal conductivity always involves the measurement of the heat flux and temperature difference in a body. The thermal conductivity can be determined based on measurements of temperature in response to heat input (Jackson, 1965) or by a heat-pulse probe (Campbell, 1991). The difficulty of the measurement is always associated with the heat flux measurement; where the measurement of the heat flux is done directly (for example, by measuring the electrical power going into the heater) then the measurement is called absolute; and where the flux measurement is done indirectly (by comparison), the method is called comparative (NSD, 2004).

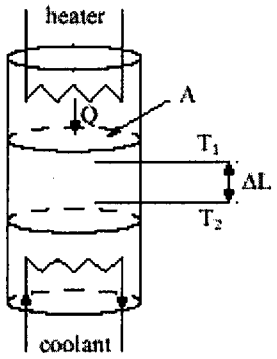

Figure 23- Schematic view for thermal conductivity measurement (NSD, 2004)

In general, the thermal conductivity can be calculated using Fourier's law as given below:

$$\frac{d_Q}{d_t} = -kA\frac{d_T}{d_x} \qquad \text{Equation 7}$$

Where $\frac{d_Q}{d_t}(W)$ is the rate of heat that is transferred in time; $A(m^2)$ is the area of the body which heat is transferred through; $\frac{d_T}{d_x}(\frac{m}{°C})$ is the temperature gradient along the heat direction and k is the thermal conductivity of the material ($W/m°C$).

In addition to these main methods, other secondary methods exist which can also result in thermal conductivity. In all cases, the entire heat flux must be uniaxial, that is, it has to flow through the specimen (and the references, in the comparative case). Thus, the heat losses or heat gains must be minimized in the radial direction. To some extent, this can be accomplished with placing insulation around the specimen, or, at higher temperatures, where such simple solutions become inefficient, with installation of a guard. If the guard is controlled to have the identical temperature gradient as the specimen, then the radial heat flow will be minimized with acceptable accuracy (NSD, 2004). The configuration of a given measurement system and of the specimen itself is influenced most prominently by the amount of the thermal conductivity. When the specimen conductivity is high, the heat flux is usually fairly high so that, heat losses from the large lateral surface area of the specimen are small; a long (like long cylindrical samples) specimen in the direction of flow helps create a reasonably high temperature gradient which can then be accurately measured (NSD, 2004). Conversely, when the specimen conductivity is low and the heat flux accordingly is low, only a relatively small thickness (for example, in the form of plates or disks) is required to generate a large, precisely measurable gradient. With this low specimen heat flux, lateral losses are matters; therefore a plate-type specimen itself tends to minimize these extra flows since the lateral surface area is small (NSD, 2004). As a matter of fact, in some cases the lateral surfaces of the specimen are surrounded by

pieces of the same sample material to provide self-guarding (NSD, 2004). Another independent parameter of fundamental attention is the amount of specimen conductivity relative to the surroundings. It is generally of interest that the specimen effective conductivity be as high as possible relative to that of the surrounding insulation. This generally becomes problematic as the temperature of the measurement system rises due to the increase in convection and radiation heat transfer from sample to the environment which doesn't allow negligibility of the measurement terrors from heat loss. With some measurement methods used at very high temperatures, the lateral heat loss is allowed to be high, but they are considered in quantitative measurement of conductivity (NSD, 2004).

The following section covers the principal methods of measuring thermal conductivity for temperatures up to 1500°C on solid materials showing a very wide range of conductivity. These techniques are divided in two main categories; Steady state and unsteady state methods

3.2. Steady state methods

In steady states methods, the sample of rock or soil being tested should be in steady state when the measurements are made. Reaching to such a condition sometimes takes a considerable time after the initial temperature difference has been applied. There are several ways to do a steady state measurement, among them; the following are the most important methods.

3.2.1. Axial flow method

Axial flow methods have been long introduced and have led to some of the most consistent, highest precision results reported in the literature (Anter Co., 2008). Key measurement issues focus mainly on reduction of radial heat losses in the axial heat flow developed through the specimen from the electrical heater mounted at one end (the power dissipation of this heater is used in calculating column heat flux) (NSD, 2004). These losses are minimal at low temperatures. As the specimen temperature goes above room temperature, control of heat losses becomes very difficult (NSD, 2004). Therefore a great deal of attention focuses on important experimental factors such as the ratio of effective specimen conductivity to lateral insulation conductivity (the higher, the better), and the quality of guarding (that is the match of the axial gradient in the specimen to that of the surrounding insulation) (NSD, 2004). In practice, only cylindrical symmetry heat transfer is applied. In addition to guarded and unguarded solution other categories separated as below (NSD, 2004):

a.) Absolute axial heat flow, which is mostly used in sub-ambient environments. Systems of this kind require very precise knowledge of the electrical power charging the heater. Consequently, the losses from the hot heater surfaces also play a major role.

Comparative cut bar (Divided-bar method) (ASTM E 1225 Test Method): This is maybe the most widely used method for axial thermal conductivity testing. In this method, the principle of the measurement is, passing the heat flux through a known specimen and an unknown specimen and comparing the thermal gradients of each, which will be inversely

proportional to their thermal conductivities. Mostly, the unknown is located between two known samples, "the references" (Figure 24).

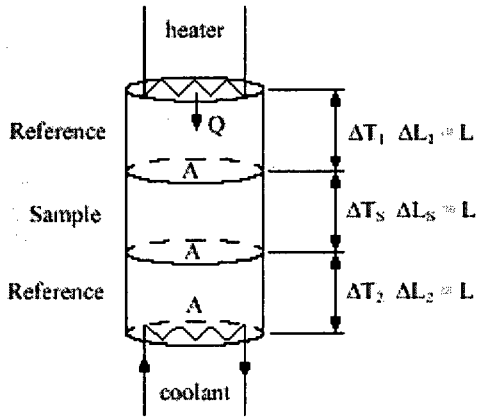

Figure 24- Divided bar set up (ASTM E1225)

From this, the thermal conductivity of the unknown specimen can be calculated as:

$$\frac{Q}{A} = k_s \frac{\Delta T_s}{L} = k_r \frac{\Delta T_1 + \Delta T_2}{2} \times \frac{1}{L} \qquad \text{Equation 8}$$

Where k_r the thermal conductivity of the references is, k_s is the thermal conductivity of unknown specimen and others as they are shown in Figure 24.

c.) Guarded or unguarded heat flow meter method (ASTM C 518, E 1530 Test Methods): Flux gauge is using in this method. The flux gauge is very similar, in its usage, to the references in the comparative cut bar method. Practically, the reference material has a very low thermal conductivity and, therefore, it can be very thin. Usually, a large number of thermocouple pairs are placed on both sides of the reference plate, connected differentially to give directly an electrical signal proportional to the differential temperature across it.

$$k_s = k_r \times \frac{\frac{\Delta T_1 + \Delta T_2}{2}}{\Delta T_s} \qquad \text{Equation 9}$$

The set up is placed into a protective cover for durability (NSD, 2004). This type of flux gauge is mostly used with devices testing very low thermal conductivity materials, such as highly porous soils and peat. In a similar procedure, flux gauges can be made from just about any material, thick or thin, depending on the material's thermal conductivity (NSD, 2004). Usual requirements for all flux gauges are that the material used for the measuring part should be stable, not influenced by the thermal cycling, and the gauge can be calibrated independently (NSD, 2004). A very large variety of steady state testing devices use this method.

3.2.2. Guarded hot plate method

According to ASTM C 177 Test Method, Guarded hot plate is a widespread and versatile method for measuring the thermal conductivity of solid materials. In fact, it is considered the most important steady state method for measuring thermal conductivity of rocks and soils. Although the samples are often rather large, this usually causes no difficulty. "A flat, electrically heated metering part engulfed on all peripheral sides by a guard heater section controlled through differential thermocouples, supplies the planar heat source given to the hot face of the specimens" (NSD, 2004). The most used measurement configuration is the conventional, symmetrically arranged guarded hot plate where two identical test samples are put above and below a flat-plate which surrounded by an outer guard heater (Figure 25).

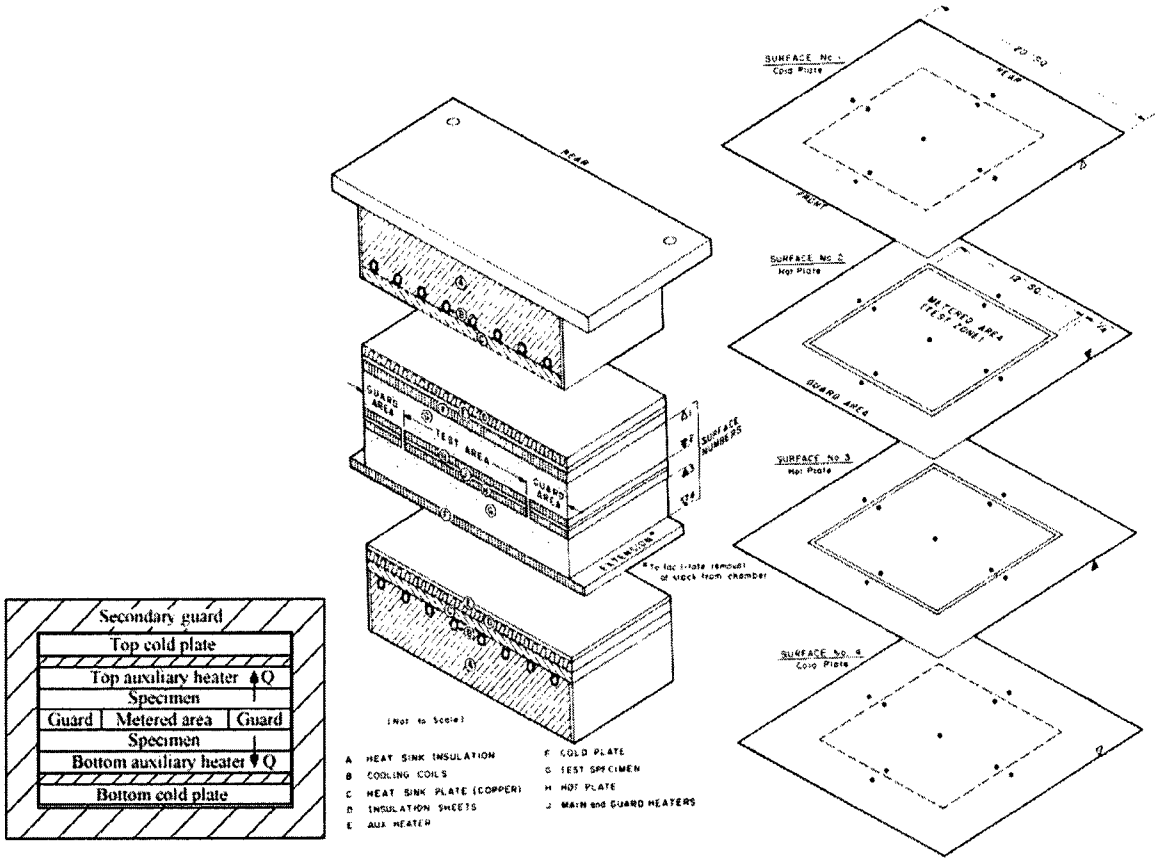

Figure 25- Guarded hot plate method set up (Farouki, 1986)

The guard doesn't allow horizontal heat losses. In the single sided configuration, the heat flow is passing through one sample and the rear of the main heater operates as a guard plate causing an adiabatic environment (NSD, 2004). This is an absolute method of measurement and its applicability needs (NSD, 2004): (a) providing steady-state conditions, and (b) the measurement of the one directional heat flux in the measurement area, the temperatures of the hot and cold surfaces, the thickness of the specimens and other parameters which may affect the one directional heat flux through the metered area of the specimen. Three different classes of measurement devices have been designed (NSD, 2004): device working around room temperatures, device working below room temperatures (down to about -180°C), and device working at high temperature (600°C or

above). A given device is most often best set for measurement in one of these temperature ranges.

Due to the considerable time needed to reach the steady state as well as relatively high temperature differential, appreciable moisture migration can be taken place. Woodside and Cliffe (1959) shown that thermal conductivity is greater when the heat flows upward than downward and this difference increases as the applied temperature differential increases.

3.2.3. Cylindrical configuration

Cylindrical arrangement for the steady state measurement has been used by different researchers. Kersten (1949) tested his soil samples in a cylindrical arrangement as shown in Figure 26. The main heater is in the center and is guarded by upper and lower heaters. The sample is placed in surrounding annular space. The heat flows radially outward across the specimen and towards the cooling chamber through which alcohol is circulated in determined temperature.

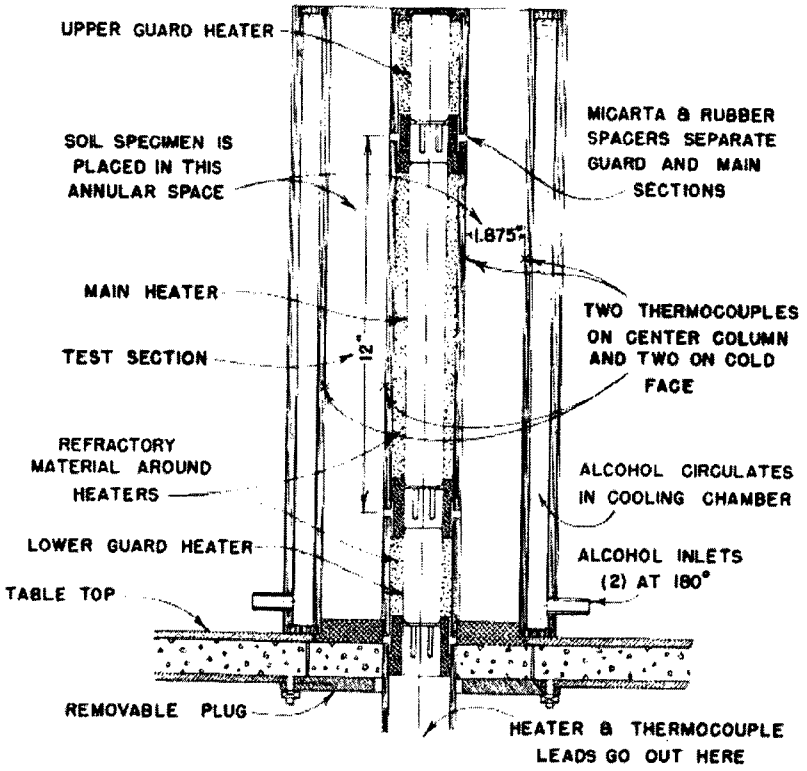

Figure 26- Cylindrical configuration method set up (Kersten, 1949)

3.2.4. Insitu sphere method

In this insitu method a spherical heater is used to measure the thermal conductivity. The sphere could be solid or hollow from copper or aluminum (Farouki, 1986). The outside diameter is $7.6cm$ or $10\ cm$ and it should be inserted into the soil or rock with the least disturbance possible. Because this is difficult especially in the case of rocks, a borer with the same diameter as the sphere should be used beforehand.

If the depth at which the measurement is taken is large comparing to the sphere radius, the thermal conductivity could be calculated after steady state has been reached as follows (Farouki, 1986):

$$k = \frac{Q}{4\pi r(T_1 - T_2)} \qquad \text{Equation 10}$$

Where r is the sphere radius, Q is the rate of heat flux, T_1 is the temperature of the heat sink and T_2 is the temperature of external surface of the sphere after a steady state condition has been reached.

3.3. Unsteady state (Transient) methods

With transient methods the temperature of the specimen varies with time. Unsteady state methods are more versatile than the steady state methods and can be easily performed in a considerably shorter time.

3.3.1. Hot wire method

According to ASTM C 1113 Test Method, Hot wire methods are most widely used to measure the thermal conductivity of solid materials such as insulating bricks and powder or fibrous materials. Since it is principally a transient radial flow technique, isotropic specimens are required. The technique has been used in a more limited way to measure thermal conductivity of liquids and plastics materials if they have relatively low thermal conductivity and convection is prevented.

3.3.2. Probe (needle) method

Relatively recent modification of long-established hot wire method is called the "probe" method (NSD, 2004). According to ASTM D5334, This method is particularly applicable where the specimen conductivity is measured by using hypodermic (hollow) needle probe inserted in the test specimen (NSD, 2004). Thus the method is conveniently applied to low-conductivity materials in soils or other semi-rigid materials (soft rocks), since short measurement time is needed. With some modification this method is also

applicable in hard rocks and material with pre-drilled hole(s). This method is a rapid and convenient technique for measuring the thermal conductivity in the laboratory or insitu. A probe device can be used to measure the thermal properties of soils or rocks in situ. The needle is inserted into the specimen and due to the thin structure should cause the least disturbance.

The probe contains a heater producing thermal energy at a constant rate and a temperature sensing element like thermocouple. The rate of rise in the temperature of the probe depends on the thermal conductivity of surrounding material and it is generally on the order of 1 or 2°C. "When a specific amount of current is passed through the heater for a short length of time, the temperature regime of the heater's surface takes on a characteristic form" (NSD, 2004). In the primary phase, the temperature will quickly increase, and as the heat soaking in begins, the increase rate becomes constant. When the thermal front gets to the exterior boundary of the sample, the increase will slow down or stop altogether due to losses into the surrounding environment (NSD, 2004). From the straight part of the rate curve (temperature vs. time) the thermal conductivity can be determined.

According to the tests have been carried out, the obtainable accuracy is at least equal to guarded hot plate and this advantage that no considerable moisture redistribution is occurred during the short period of test (NSD, 2004). The theory of the probe method is based on the theory of the line heat source placed in the semi-infinite, homogeneous and isotropic medium that is explained below.

3.3.3. Line heat source theory

The concept of this method is that the constant heat produced by a line source of heat be engulfed in an infinite volume of material produces a cylindrical temperature field (Carslaw and Jaeger, 1959). The temperature increase at any point within the material is (Carslaw and Jaeger, 1959):

$$T(t) = -\frac{Q}{4\pi k} Ei(-\frac{r^2}{4Dt}) \qquad \text{Equation 11}$$

Where r is the radial distance from the line source, Q is the heat power per unit length of probe, k is the thermal conductivity, D is the thermal diffusivity, t is the time from initiation of heating and Ei is the exponential integral as below (Anter Co., 2008):

$$-Ei(-x) = \int_x^{\infty} \frac{e^{-t}}{t} d_t \qquad \text{Equation 12}$$

At first ($t = 0$), the material is supposed to be at a uniform temperature $T(0) = 0$.

For small values of ($0 < r \ll 1$), the exponential integral can be approximately calculated as:

$$-Ei(-x) = -0.577216 - \ln(x) \qquad \text{Equation 13}$$

The temperature increase becomes (KD2 Pro Manual, 2006):

$$\Delta T(t) = -\frac{Q}{4\pi k}\left[-Ei\left(-\frac{r^2}{4Dt}\right) + \mathrm{Ei}\left(\frac{r^2}{4D(t-t_1)}\right)\right], t > t_1 \qquad \text{Equation 14}$$

This is the basic equation of the line heat source method. The temperature of the line heat source is recorded, and the thermal conductivity can be calculated from the slope of the plot of temperature rise vs. logarithmic of time (Anter Co., 2008):

$$k = \frac{Q}{4\pi}\left(\frac{d_T}{d_{\ln(t)}}\right)^{-1}$$ Equation 15

The experimental plot of T (t) vs. time is curved at the upper and lower boundaries with a linear part in between. The equation is only valid for points on this linear part. The lowest curved part of the graph shows the earliest possible time when the thermal conductivity can be measured (Anter Co., 2008). It is caused by the heat transfer between heater and tested materials. The upper curved part is resulted from the heat front getting to the boundaries of the material since the test piece is of finite size; consequently, the maximum possible time for the thermal conductivity measurement depends on the test-piece geometry and thermal diffusivity (Anter Co., 2008).

The temperature variations T (t) are measured with a pure platinum wire, which also works as the line heat source (Anter Co., 2008). The rate of temperature increase of the platinum wire is precisely determined by measuring its increase in resistance $R\ (T)$ in the same way a platinum resistance thermometer is used (Anter Co., 2008).

The thermal conductivity is finally expressed as (Anter Co., 2008):

$$k = \frac{VI/L}{4\pi} \times \frac{R_0(\beta+2\gamma T)}{d_{R(T)}/d_{\ln(T)}}$$ Equation 16

Where T is the temperature of the sample, L is the distance between the wire taps, I is the current flowing through the platinum wire, V is the voltage drop between the wire taps, R_0 is the resistance of the platinum wire at $0°C$, β= 0.00397414 $\Omega \cdot K^{-1}$ and γ= -5.78694·10^{-1} $\Omega \cdot K^{-2}$, $d_{R(T)}/d_{\ln(T)}$ is the slope of the linear part of the plot of the resistance of the platinum wire vs. the logarithm of the time.

Jaeger and Sass (1964) developed a line source method to determine thermal conductivity and diffusivity of cylindrical specimens which involved heating the specimen by a wire placed in a shallow longitudinal saw cut. Somerton and Mossahebi (1967) presented a ring heat source probe for rapid determination (2-3min) of thermal conductivity of rocks which is similar to line heat source except in shape. Fernandez (1986) designed a heat line source instrument to measure the relative values of thermal conductivity of consolidated rocks which needed calibration to obtain absolute values. He used the parameters of T_{Max} and slopes from $T - t$ graph to determine the thermal conductivity while the test duration lasted about $170s$ and has the reproducibility error of less than %2.5. Bristow (2001) developed a probe which measured soil thermal properties, water content and electrical conductivity simultaneously that is particularly suitable for near surface soils.

Hammerschmidt (2003) introduce a pulse hot strip method very similar to probe method which measured the thermal conductivity and thermal diffusivity together. It is based on monitoring the temperature response of a sample to a very short heat pulse from a strip heat source. The instruments uncertainty is estimated to be less then %3.

At last it should be noted that there are other various methods for measuring the thermal conductivity of soils and rocks. But the principle of each method is on the basis of either steady state technique or unsteady state technique with a little difference in structure and procedure. Also there are indirect methods for measuring thermal conductivity from other thermal properties, like laser flash method (Blumm 2002) or optical scanning technique which allows thermal conductivity estimation from thermal diffusivity.

Chapter 4: Properties of Primary Materials

4.1. Introduction

Mine backfill materials are classified in three major components including inert material (the major part of backfill), binder and water (Hassani and Archibald, 1998). The properties of these materials are the most important factors in determining the chemical and physical properties of backfill (Fall, 2005). The inert materials commonly used are mineral processing tailings, sand or gravel, waste rock and coarse slag. Binding agents, such as normal Portland cement, ground slag, or fly ash, are applied in backfill technology to improve the mechanical properties of the fill and sometimes chemical additives such as flocculants, accelerators, and retarders are added to improve the fill permeability, flowability of the slurry and the consolidation properties of the fill (Hassani and Archibald, 1998).

4.2. Mineral processing tailing

Tailing materials can be used either as received or prepared 'full plant tailings' or deslimed by using hydro cyclones to reach the desired size requirements. Their size distribution largely depends on ore processing and desliming technology. The fraction of 10 mm particles in classified tailings is usually less than 20% of total mass by weight (Hassani and Archibald, 1998).

In this research, mineral processing tailings of the Creighton mine which is an underground nickel mine from Vale Inco Corporation, is employed. Composition tests showed that tailing consists of mainly quartz, Albite, small amount of Calcite, Muscovite, Actinolite, Anorthite, Chalcopyrite, Biotite, Pyrrhotite, Epidote and Chlorite. The particle size distribution using the combination of sieving and laser diffraction methods (ASTM C136-96; 1996) is shown in the Figure 27.

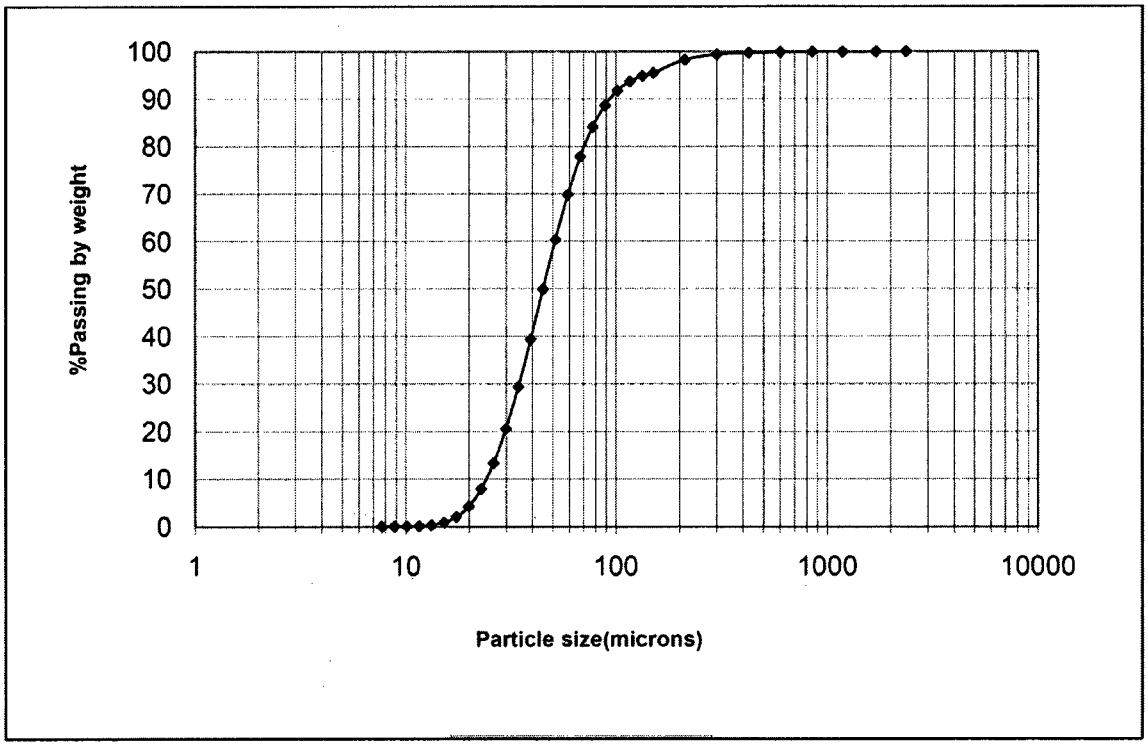

Figure 27- Particle size distribution of mineral processing tailing

4.3. Silica sand

Sand from surface alluvial basins is widely used in mine backfill, and its particle size is generally less than 2 mm. The Silica sand used in this research is obtained from Opta Minerals Incorporation. Figure 28 shows the texture and shape of the sand and

Table 5 shows its physical properties. The sand's chemical composition is shown in Table 6. As it can be seen from Table 6 more than 99% of this sand consists of quartz. Since the particle size distribution largely influences the physical properties of backfill (Benzaazoua et al., 2006), particle size analysis has been done on the silica sand sample using the same method for the mineral processing tailing. The sieve analysis has been used for materials retained on the number 100 sieve (75μm), and for fine materials (finer than 75μm) Laser Diffraction analysis has been used.

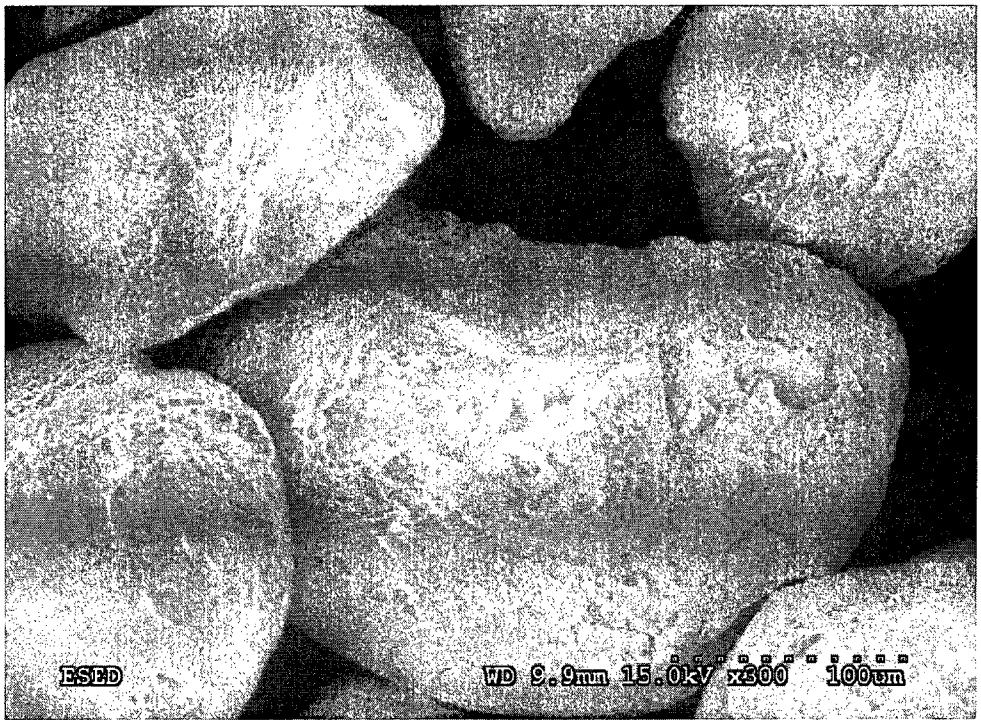

Figure 28- SE image of silica sand (Kermani, 2008)

Table 5- The physical properties of sand

Material	**Color**	**Mineral**	**Specific Gravity** gr/cm^3	**Grain Shape**	**Bulk Density** Kg/m^3	**Hardness** (Mohs)
Sand	White	Quartz	2.65	Rounded	1586	7

Table 6- The chemical composition of sand

Material	SiO_2	Al_2O_3	Fe_2O_3	CaO	TiO_2
%wt	99.50	0.05	0.03	0.01	0.03

According to the Massachusetts Institute of Technology (M.I.T) the original sand sample were classified which the results are shown in Table 7.

Table 7- The particle sizes of the silica sand based on the M.I.T. classification System

Material	Gravel	Sand	Silt & Clay	Category
%wt	0	26.4	75.4	Silt-Sand

The coefficient of uniformity and coefficient of gradation have been calculated. The coefficient of uniformity (C_u) is defined as :

$$\boldsymbol{C_u = \frac{D_{60}}{D_{10}}} \qquad \text{Equation 17}$$

Where:

D_{60} is the diameter of the particle of which 60% of the particles are smaller and D_{10} is the diameter of the particle of which 10% of the particles are smaller.

C_u shows the slope of the particle size distribution curve. The higher difference from unity shows the wider range of particle sizes in a sample. The coefficient of curvature(C_c), also called the coefficient of gradation (C_g), describes the shape of the particle size distribution curve between D_{60} and D_{10} which is defined as :

$$\boldsymbol{C_c = \frac{{D_{30}}^2}{D_{10} \times D_{60}}} \qquad \text{Equation 18}$$

Where, D_{30} is the diameter of the particle of which, 60% of the particles are smaller. According to the Unified Soil Classification System (Bowles, 1988), well-graded sand has a C_u value greater than 6 and a C_g value between 1 and 3. Since the coefficient of curvature and the coefficient of uniformity of this silica sand used is 0.84 and 2.48 respectively, the sand is classified as poorly graded sand.

Also, to see the particle size effect on thermal conductivity of backfill, silica sands were crushed and ground to have different particle size distributions of the same material. For this purpose, a laboratory scale Denver grinding rod mill has been employed. The grinding rods weigh approximately about 17 kg, which were made up of four different diameters. Both the mill and the grinding rods are made of mild steel.

4.4. Blast furnace slag

A combination of 10% of Type GU cement (PCX) and 90% of Blast Furnace Slag (BFS) was used as the binder component in this research. Both of these materials were obtained from Lafarge Canada Inc. Company (Pointe-Claire, Montreal, Quebec). The particle size distribution of the binder has an influential effect on hydration of binders (Neville, 1996).

Blast furnace slag (BFS) is described as a non-metallic by-product of manufacturing iron and steel in a blast furnace where the residual siliceous and aluminous materials remain after the separation of the metal from ore, which reacts with limestone and coke ash (Kermani, 2008). Blast furnace slag approximately comprises up to 20% (by mass) of the metal production. In this research, Lafarge blast furnace slag (NewCem® slag) has been used. Due to the very small particles of blast furnace slag and Portland cement, laser light

diffraction technique has been used to obtain particle size distribution which is shown in Figure 29 for blast furnace slag. D_{60} and D_{10} values of this slag have been obtained as 4.41 μm and 1.53 μm respectively. Using the MIT classification system, this slag can be classified as "silt-clay" category. Figure 30 is the SEM image of this slag, which shows the shape, size and texture of slag. To determine the chemical compositions of the slag, the XRF analysis was conducted, and the results are shown in Table 8.

Table 8- The chemical composition of blast furnace slag

Material	SiO_2	Al_2O_3	Fe_2O_3	CaO	MgO	K_2O	Na_2O	SO_3
%wt	36.42	10.21	0.58	38.12	9.42	0.44	0.52	3.01

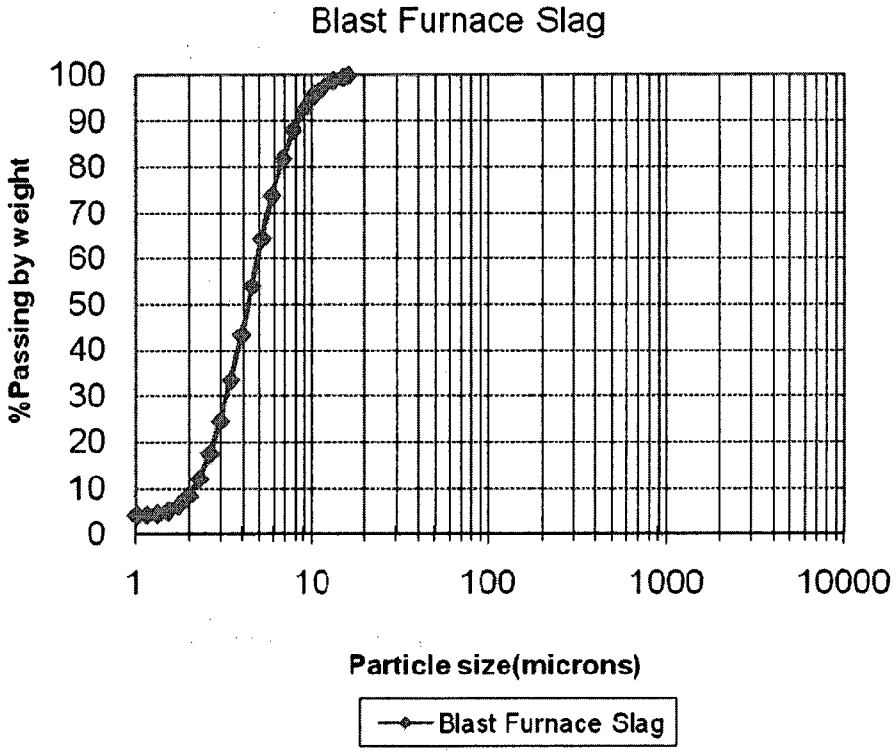

Figure 29- The particle size distribution of Lafarge blast furnace slag

Figure 30- SEM image of slag (Kermani, 2008)

4.5. Portland cement

Normal Portland cement is a crystalline material consisting of CaO, SiO_2, Al_2O_3, and Fe_2O_3. Four major components, alite (50-70%), belite (15-30%), aluminates, and ferrite (5-15%), make up cement. Portland cement has a very important contribution to binding and hydration action in backfill. Type GU Portland cement from Lafarge has been used in this research. As with the slag, the laser light diffraction technique has been used in order to determine the particle size distribution of Portland cement. The result is shown in Figure 31. D_{60} and D_{10} values of this Portland cement have been determined as 3.45 μm and 1.21 μm respectively. Considering the particle size distribution, Type GU

cement used in this research is classified in the "Silt-Clay" category according to the MIT classification system. In order to obtain the chemical compositions of this Portland cement, the XRF analysis has been applied and the results are shown in Table 9. Figure 32 is the SEM image of typical Portland cement, which shows the shape, size and texture.

Table 9- The chemical composition of Portland cement

Material	SiO_2	Al_2O_3	Fe_2O_3	CaO	MgO	K_2O	Na_2O	SO_3
%wt	19.39	4.61	2.27	61.13	2.01	0.71	2.01	3.30

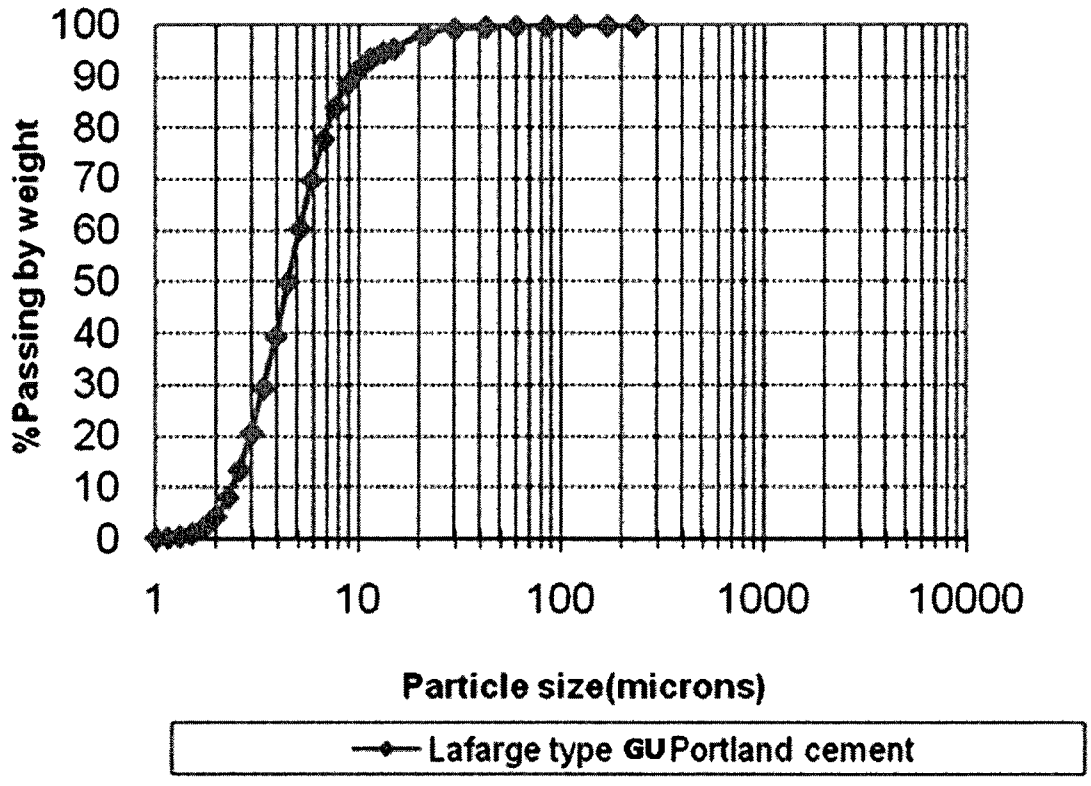

Figure 31- The particle size distribution of Lafarge type 10 Portland cement

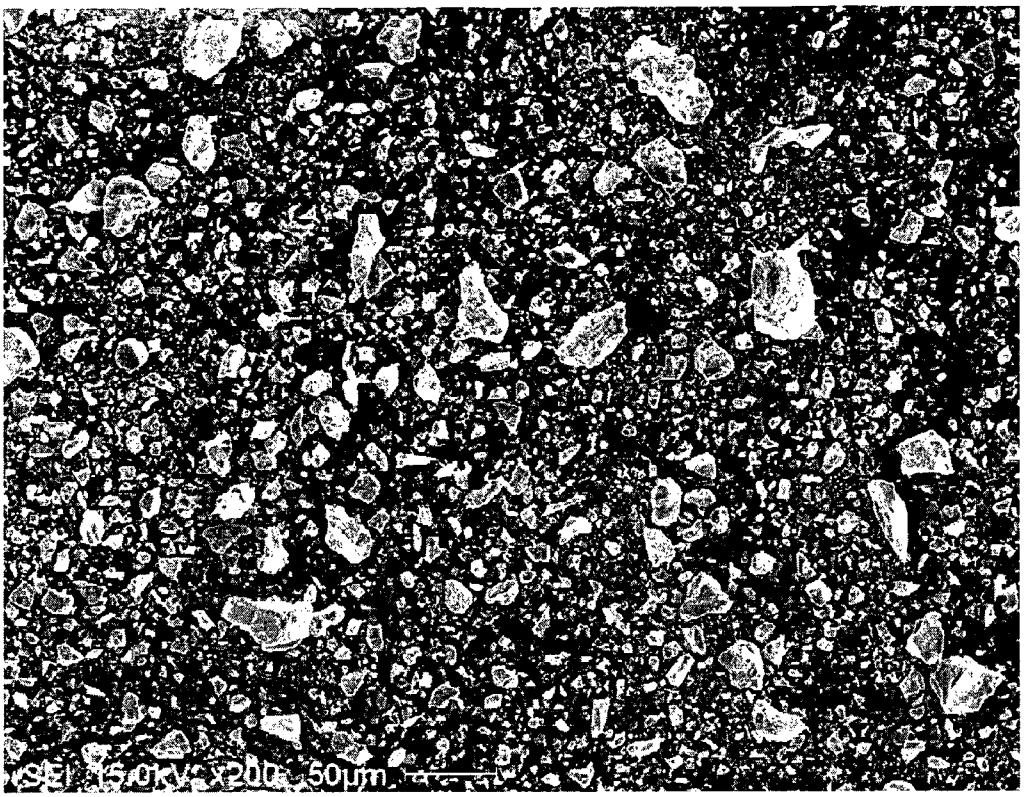

Figure 32- SEM image of Lafarge type 10 Portland cement (Kermani, 2008)

4.6. Sodium silicate

Known as water glass, sodium silicate is manufactured from varied proportions of $Na_2CO_3$and SiO_2 by smelting silica with sodium carbonate at 1100-1200 °C. The major applications of sodium silicate are in pulp and paper industries, detergent industries, and waste treatments and as a binder in construction industry. In civil engineering and mining industries, especially where concrete is used, sodium silicate has been used for different purposes including an alkali activator of slag and fly ash, a penetrating sealant and a hydration accelerator. Sodium silicate in backfill has been used as an accelerator for Portland cement, fly ash and slag (Kermani, 2008). Type N® sodium silicate was used in this investigation. This sodium silicate was produced by PQ National Silicate Company.

4.7. Water

Water which is used in backfill production is typically provided from industrial water from mining operation or water from underground water sources running into excavated stopes that should be pumped out or simply fresh water. Soluble chemical components of water have some effects on chemical and physical properties of backfill which has been investigated by many researchers. However, in this research, in order to standardize and eliminate the effect of water chemical compositions, tap water was used; therefore, the influence of soluble chemical components in water is almost negligible as compared to mine process water.

Chapter 5: Experimental Procedure and Setup

5.1. Objective of the research

In order to achieve cheaper energy for production in mines, one way is to take advantage of potential geothermal energy usage. To evaluate the rate of recoverable energy in underground mines, it is important to know about thermal properties of rocks and especially the kind of backfill used in that mine. In this work, the following objectives have been considered:

- A general view about thermal properties of backfill
- Evaluating the thermal conductivities of different backfills
- Determining the effective factors on thermal conductivity of backfill
- Investigating the effect of these factors on thermal conductivity of backfill

In order to conduct this investigation, many backfill specimens have been prepared and consequently many different tests have been carried out. In this chapter, the procedure for preparing the specimens is described. In addition, the thermal conductivity measurement devices and the experiment procedure also are explained. Besides, supportive tests which have been done to achieve the approaches to control the rate of effective factors on thermal conductivity of backfill will be described.

5.2. Mold preparation

Three sizes of cylindrical samples were used for this work. One series of samples were 10cm (4 inches) in diameter and a height of at least 5cm, the second series were 5cm (2 inches) in diameter and a height of at least 4cm and the third series were 2.5cm

(1 inch) in diameter and also 4cm in height. Here, it must be noted that the preparation procedure was exactly the same for all of these samples series. To make the samples, first appropriate molds were prepared. Molds have been made from Polyvinyl Chloride (PVC). These molds were perforated at the bottom to simulate the drainage condition in mines. Five centimeter diameter molds had 30 orderly distributed holes and 10cm-diameter molds had 50 orderly distributed holes. Also to prevent fine particle loss, woven Geotextile CC315 from Canada Culvert Company was used as a filter that has been placed at bottom of each mold before pouring backfill mixture in the molds. For providing fully saturated samples, in cases where needed, imperforated molds or perforated ones which had been sealed precisely in advance by Silicone glue without the filter were used. Two and a half centimeter molds were just used for providing fully saturated samples. The molds and filter shape could be seen in Figure 33 below.

Figure 33- Different kinds of molds and filter which used in sample preparation

Also to facilitate the extruding of samples from molds after curing, very small amount of vegetable oil was sprayed on the wall of the molds to reduce the friction of samples with the mold's wall. In some cases, in order to make sure of enough height a short additional piece of cylinder with the same diameter and characteristics was connected to the lower part with paper tape which could be seen in Figure 33.

5.3. Sample preparation

For making samples, appropriate recipes were prepared. Two important factors in providing the recipes are pulp density and binder content. Pulp density represents the amount of solids in the mixture which determines the viscosity of mixture. This factor is a very important factor in designing the backfill (Hassani and Archibald, 1998). Pulp density in the recipes which were prepared in this work defined as below:

$$Pulp\ Density = \frac{Inert\ materials\ (Tailings + Sand) + Binder\ (Slag + Portland\ Cement) + Gel\ (Sodium\ Silicate)}{Inert\ materials + Binder + Gel + Water}$$

Pulp density is a dimensionless number and presented in percentage and all other terms are in mass units.

Binder content also represents the amount of total binder in mixture in comparison to the total solid content. Binder content is determined as below:

$$Binder\ Content = \frac{Binder\ (Slag + Portland\ Cement)}{Iner\ materials + Binder}$$

Binder content is also a dimensionless number presented in percentage and all other terms are also in mass units. For the binder mass, considering the economic view as well as mechanical properties requirement, a composition of 10% Portland cement and 90% Slag of total binder mass was used.

Sodium Silicate (gel) content is determined as below:

$$Gel\ Content = \frac{Gel(Sodium\ Silicate)}{Inert\ materials + Binder + Gel}$$

Gel content is a dimensionless number in percentage and other terms are in mass units. Depending on the objective of each test, different recipes were prepared. To make the mixture of backfill, each material was weighed to the exact amount. Then the inert material (Tailing, Silica Sand, or the mixture of both) was poured into a 5-litre stainless steel bowl which was perforated at the bottom. A 1.5-cm diameter PVC pipe with stopcock to control the exit of mixture was connected to the bowl. To prevent the run off of fine material and water and also clogging a plastic cork was put into the hole at the bottom of bowl. The mixing action was done by a stainless steel wire whip blade which also ensured a homogenous product. The rotation speed of the blade was set according to the density of solid mixture and the tendency of the solid material to settle. The inert material was allowed to mix (150 rpm) in the bowl of a KitchenAid mixer (Commercial 5 Series, Model: KM25G0X) for 1-2 minutes for homogeneity purposes. For the other materials, first $^3/_4$ of total water was added in a period of 30-60 seconds, then the binder (the mixture of Slag and Portland cement) was added slowly enough to ensure that it was dispersed in the whole mixture, then the remaining water was added. At this time, the desired rotation speed was set (400-500 rpm) and the mixture was mixed for 5 minutes. For the samples that Sodium Silicate was used as an auxiliary binder, the procedure was a bit different. Since Sodium Silicate tends to dry, after weighing the desired amount of this material it was mixed with 20-30 ml of the remaining water and stirred, then it was added to the mixture immediately after adding the binder and before adding the remaining of

water while the mixer was stirring. Normally, considering the tendency of Silica Sand to settle down rapidly, the high rotation speed 500-550 rpm was applied in the mixing process.

After the mixing time was over, the mixture was poured into the molds slowly while the mixer still working to avoid settling and heterogeneity, then the molded specimens were placed into the humidity room for the curing process.

5.4. Curing process

After preparing the mixture and pouring it into the molds, samples were taken to the humidity room and left there to cure for the desired time. As most literature uses 28 days, the curing time was considered 28 days except for those tests that were carried out to see the time effect. In curing process, the binder is hydrated and binding process is done while excess water drainage occurs in the first days. After 28 days, it is assumed that no other significant process would happen in the backfill samples. As it has been mentioned, the curing process is being done in the humidity room to simulate underground mining stopes condition. To do this, two crucial factors should be controlled; moisture and temperature. The moisture is controlled by a laboratory humidifier from Carrier Company (Comfort Series) and the temperature is controlled by a Heating/Cooling air conditioner from UL Listed Company (92 UK) which can be seen in Figure 32. According to underground geological condition and the effect of humidity and temperature on hydration rate in backfill, the humidity was kept in the range of 90% $\pm$ 5% and the temperature was kept in the range of 25°C $\pm$ 2°C (Kermani 2008). When

fully saturated samples were desired, humidity of up to 99% was allowed. The samples in humidity room are shown in Figure 35.

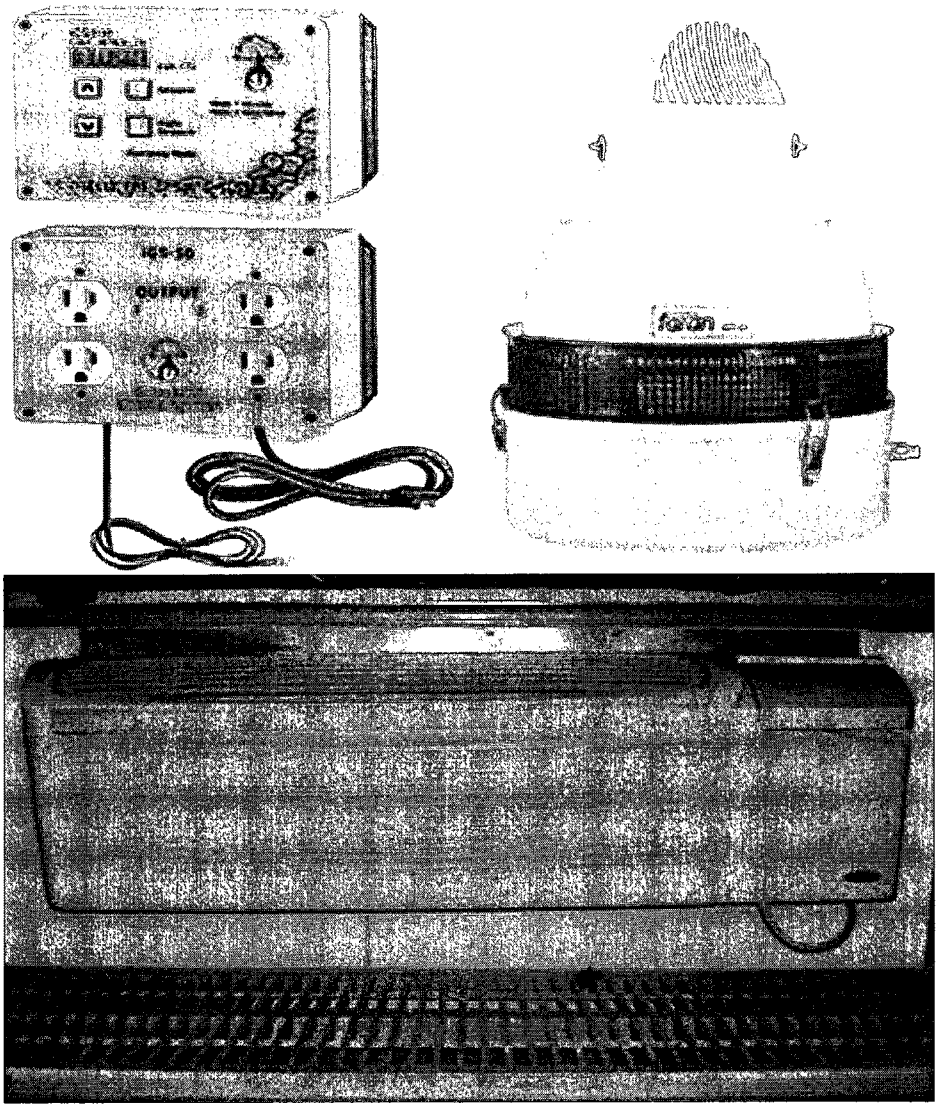

Figure 34- Humidity (up) and temperature (bottom) controllers

Figure 35- Samples in humidity room

5.5. Description of test plan

In order to carry out the tests, the framework of this study was defined. First of all, the effects of defining parameters in backfill from the mining view were considered. These parameters are pulp density and binder content. So recipes for different pulp densities and binder contents within acceptable ranges were provided to cover hydraulic backfill and paste fill. Also with the introduction of sodium silicate as an auxiliary binder, some tests to see the effect of this factor were designed.

Besides this, the concept of evaluating a backfill with different physical characteristics from different materials and the effect of them was investigated. In fact it would be

valuable to anticipate the thermal behavior and especially thermal conductivity as the main goal of this work considering the changes in the density, saturation, porosity.

5.5.1. Mining view tests

This series of tests was designed to see the effect of pulp density and binder content on thermal conductivity behavior. Also for some tests, sodium silicate was added to see if it would have any effect on thermal conductivity. A range of 65% to 80% for pulp density was considered and for the binder content, a range of3% to 9% selected. Also, for sodium silicate the range of 0.1% to 0.5% of gel content was chosen. Mineral processing tailing, blast-furnace slag, Portland cement, water and if needed, sodium silicate, were used to make each batch of samples. For comparing the results, the physical situation should be almost kept the same for all the samples, so material with particle size of a limited range was chosen through sieving to keep the porosity as similar as possible in the samples. Besides, to keep the moisture also constant, relative humidity of curing room was set to98% for some of the tests. Both perforated and sealed molds were used. The effect of curing time on thermal conductivity was assessed to see if, similar to compressive strength, curing time has any effect on thermal conductivity of backfill. As well, to see if the volume of samples, which represented by the sample diameter, has any effect on thermal behavior and to choose the optimum sample size, some tests were designed with different diameters from 1 *inch* to 4 *inches* while other properties kept almost constant.

5.5.2. Physical view

In backfill operation, different kinds of material are used and different physical conditions could be expected after placing backfill. Also backfill could be classified as a soft rock or more of a kind of cemented soil. From this view, many variables could be considered influential and should be assessed. Since different kinds of backfill are used in underground mines and different conditions exist in these environments, it would be extremely useful and valuable if their thermal behavior especially in terms of thermal conductivity could be predicted through a model. This subject has attracted attention toward designing another series of tests concentrating especially on determining the most influential physical factors on thermal conductivity of backfill. Referring to other research done previously, the most effective parameters were determined to be saturation (moisture content), porosity, density and the kind of inert material. In this part of work, physical properties of one kind of backfill were changed and the procedure was repeated for different kind of backfills. Making changes in one property while other properties were kept constant was problematic work which enforced some pre-tests to see and find out the possibility of doing such work to get desired results. The details describes below.

5.5.2.1 Saturation

Saturation, according to the previous similar work for soils, could be considered the most influential parameter in thermal conductivity behavior of any material. So in many experimental projects done in this project different saturations (water content) were considered. In order to do so, first of all saturation homogeneity should be assessed in the

samples first during the curing process, and second during the test in each degree of saturation. The moisture homogeneity test during curing process was done as below.

Moisture homogeneity test

Twenty four samples, half of them $50mm\,(2\,inches)$ in diameter and the others $100\,mm\,(4\,inches)$ in diameter, from tailing with pulp density of 70% and binder Content of 5% have been provided for this test. Moisture content tests were carried out every 7 days for 42 days, although after 28 days the backfill sample was assumed to be cured and no considerable further changes happened. Sample preparation and curing was the same as normal procedure but only sealed molds were used.

After 7 days two samples were recovered from curing room. To perform the homogeneity test for saturation, approximately $1.5\,cm$ from each end was cut and about $5\,cm$-height sample remained. One of two samples was cut in two 2.5 cm slices and each slice was cut into four quarters (see Figure 36, left). The other cylinder also cut into two half but this one was divided into 4 pieces parallel to the diameter with the spacing of half of the radius of the cylinder. These samples were put into the oven (according to ASTM D 2216-98). The mass loss of water was used to calculate the moisture content.

This procedure was repeated for $50\,mm\,(2-inch)$ and $100\,mm\,(4-inch)$ diameter samples. Every 7 days this experiment was repeated until 42 days to make sure about the moisture homogeneity in the samples. The geometry of pieces could be seen in Figure 36 below.

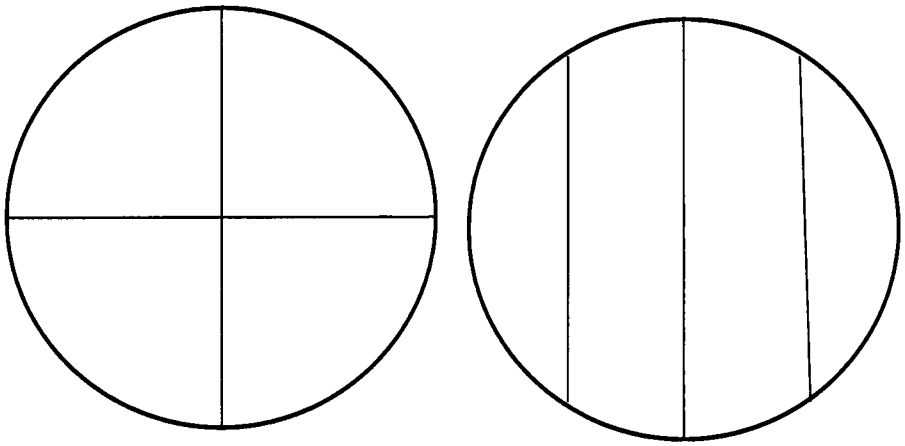

Figure 36- Geometry of saturation homogeneity test for each part of samples

Changing saturation

After curing, the most critical action was to change saturation homogeneously so that the effect of the degree of saturation could be observed. To achieve this goal, 3 kinds of drying processes were tried including room drying, oven drying, and microwave drying, which are described as follow.

- Out of curing room drying : This series of tests were done to evaluate the possibility of saturation control and its rate by exposing samples out of mold to the open air for different lengths of time. Eight samples of the same characteristics as above were prepared and after curing were taken out of molds and were weighed. Then each two of them were left out in the room for 3, 5, 7 and 10 days. After each period, each sample was weighed again to see the difference in moisture content. These tests stopped after 10 days due to very slow rate of moisture lost.
- Microwave drying: This test was done to see the effect of microwaving on degree of saturation and how saturation could be changed homogenously by

microwaving. To carry out this experiment, 19 samples were made. One sample was made to see the effect of microwaving on moisture loss, structure influence and for approximation of microwaving time to change the degree of saturation. Sample characteristics were defined as a mixture of tailing, water, slag and Portland cement as binder with the pulp density of 75% and the binder content of 5%. These samples were cured for 28 days and afterward were taken out of their molds. Then, they were microwaved with an 800W microwave with different power levels from 1 to 4 on the basis of 10 levels and in different times from 2-6 minutes to avoid structural damage. After theoretically achieving a desirable degree of saturation, all the samples were sealed precisely (by cling wrap and zip lock plastic bags). Afterward, half of the samples were left to cool to room temperature and half of them were put back into the humidity room to allow internal moisture distribution without any exchange of moisture with the environment for 7 days. Then the moisture content was performed similar to the above procedures.

- Oven drying: The sample preparation was exactly the same as the samples for the microwave drying test. The difference was in that the samples were left in oven at 110 °C for different lengths of time to achieve different saturation levels. The other difference was that no samples were put back in curing room again after oven drying. Then after cooling to room temperature, moisture contents tests were performed.

Due to homogeneity matter and time saving, a limited volume around the center of each sample was used for measurement after drying for unsteady state tests.

5.5.2.2. Porosity

The other parameter which can be considered influential on thermal conductivity to some extent is porosity. Porosity could be considered as the representative of bulk density as well, since porosity has a inverse relation with bulk density in that with increasing porosity, bulk density would decrease and vice versa. The point in this series of tests is that porosity in backfill and any granular material with limited particle size distribution cannot be changed in an extensive range due to physical confinements. So the porosity of samples was changed within as the widest range as possible. In order to achieve this, silica sands from 3 different categories were used. The coarsest one has the particle size distribution of more than mesh number 18 ($1000\mu m$), number 80($177\mu m$) for middle and less than number 200($75\mu m$) for the finest according to American standard sieve size classification. The pulp density and binder content, including Portland cement and slag, for all the samples were designed to be 75% and 5%, respectively. Six different batches were designed for this part and the difference was in the various portions of each size of sand in the inert material. Also some samples of each batch underwent saturation tests.

5.5.2.3. Solid particles thermal conductivity

The last case which was considered as an influential parameter in thermal conductivity of backfill is thermal conductivity of solid particles. This means that, what could be the effect of different solid particles with different thermal conductivities on thermal conductivity of a backfill with the same pulp density and binder content. As we

know the largest portion of each backfill is the inert material part, consequently, the determining factor in changing the solid part of backfill is in changing the thermal conductivity of inert materials. For this purpose, inert material designed as a composition with different portions of silica sand ($6.80 - 7.5\frac{W}{m°C}$) and tailing ($2.70 - 3.20\frac{W}{m°C}$) that have different thermal conductivities. But in order to keep the porosity constant so that the comparison would be possible, very similar range of particle size distribution should be provided. To meet this criterion, both sand and tailings were sieved and the portion of finer than mesh number 100 according to American standard sieve size classification was applied in making the samples. The pulp density and binder content, including Portland cement and slag, for all the samples were designed to be 70% and 5% respectively.

5.6. Measurement devices

In order to carry out the tests as accurately and reliably as possible, tests using both main measurement methods were done. First of all, measurements were done in the Steady-State condition using a divided-bar method. Then measurements were done in the Unsteady-State method using line source method (needle method).

5.6.1. Steady state method

In the first stage, a set up according to the divided-bar method was used, which is a method that follows the steady state condition. Figure 37 shows the experimental set up used in this stage. It comprises a thermal conductivity cell surrounded by an insulated and temperature controlled box inside a large cold room maintained at relatively constant temperature of 4°C below the average temperature used in the controlled box. Two copper

disks with diameter of 101.6*mm* had been designed which each of them has five thermistors embedded in them with arrangement shown in Figure 37. These copper disks were so thin than no temperature gradient would be created in them. The measurement unit included the sample and the copper disks. Two independent heat exchangers were used to create a constant vertical heat flow through both the sample and the copper disks, and to maintain the temperature boundary conditions constant at the top and the bottom of this three-layer system. Two brass plates of 1 cm high were used to diffuse the heat evenly from heat exchangers through the system of sample and copper disks. The Heat exchanger's temperature is changed by a heating and cooling system through cooling liquid. The ambient temperature of the insulated box is maintained equal to the mean value of temperatures applied at each of the heat exchangers. A load between 5-7 kg was applied to keep the good contact between heat exchangers, brass plates, copper disks and the sample. The sample, copper disks, brass plates and heat exchangers were tightly surrounded by a 50 mm thick polystyrene jacket and this whole thermal conductivity cell was covered by glass wool during the test to minimize radial heat losses and any kind of heat exchange with the external environment as much as possible. The heat flux in the thermal conductivity cell was measured through the copper disks. The temperatures at top and bottom of each sample were recorded every 15 minutes through a data acquisition system and plotted as a function of time. When temperature became constant with time, steady-state heat flow is established.

The thermal gradient in the sample is determined from the temperature average from each set of thermistors at the interfaces of sample and copper disks. The thermal conductivity of the tested sample is calculated as below (Côté and Konrad, 2005a):

$$k = \frac{q_{uf}+q_{lf}}{2}\frac{\Delta h}{\Delta T} = \left\{\left[k_{uf}\frac{\Delta T_{uf}}{\Delta h_{uf}} + k_{lf}\frac{\Delta T_{lf}}{\Delta h_{lf}}\right]\frac{\Delta h}{\Delta T}\right\}\Big/_{2} \qquad \text{Equation 19}$$

Where q is the heat flux$\left({}^{W}/_{m^2}\right)$; Δh is the distance between the copper disks which is equal to sample height (m); ΔT is the temperature difference between the upper and lower copper disks mean temperature (°C) and the subscripts uf and lf refer to the upper and lower heat fluxes, respectively.

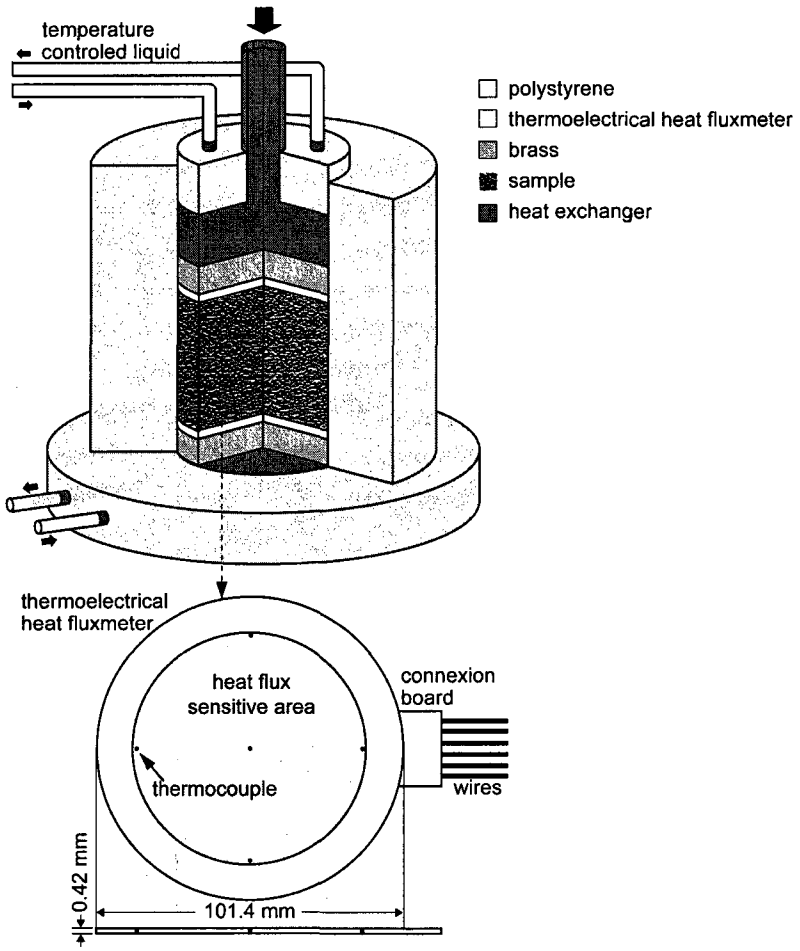

Figure 37- Steady-state experimental set up

The tests were carried out at a mean temperature of about 5 ± 1°C. Temperature gradients of 0.2–0.6 $°C/cm$ were obtained across the backfill samples. The effect of the thermal gradient is neglected in this study since it does not have considerable effect on measured values (Cote, 2005a). It is noted that the relative error on the thermal conductivity measurements due to the precision of the thermistors (±0.025°C) is less than ±5%. Another factor that can influence the thermal conductivity measurements is the thermal resistance that may occur at the contact between the heat flux meters and the sample. This effect has been discussed by Birch and Clark (1940), in which the reported contact resistance, expressed as an equivalent thickness of materials, was about 0.6 mm for limestone ($k = 2.9 {}^{W}/_{m°C}$) for sample thicknesses varying from 5 to 20 mm. Considering that the height of samples tested in the present study is 50 mm, contact resistances, expressed as an equivalent thickness, of 0.6 mm for the materials with the low conductivities will lead to an overestimation of the thermal conductivity of less than 1%. The contact resistance was thus neglected in this study. The thermal conductivity measurement system has also been tested with a reference material which consisted of two stacked Pyrex disks (1.015-1.090 ${}^{W}/_{m°C}$) (Côté and Konrad, 2005a). The measured thermal conductivities agreed with theoretical values within less than 5% of deviation, that was considered sufficiently accurate for the purpose of this study and which also confirms that the contact resistance can indeed be neglected.

5.6.2. Unsteady state method

The unsteady state measurement method used in this work was a needle method which the whole setting is called KD2 Pro from Decagon Devices Company. The KD2

Pro is a battery-operated, menu-driven device which can measure thermal conductivity and resistivity, volumetric heat capacity and thermal diffusivity. It is a portable device used to measure thermal properties. It consists of a handled controller and sensors (needles) that can be inserted into the material. It offers three sensors to choose from including the standard single-needle sensor, an extended-length single-needle sensor and a dual-needle sensor. The single-needle sensors can measure thermal conductivity and resistivity; while the dual needle sensor also measures volumetric heat capacity and thermal diffusivity. Data stored in KD2 Pro can be downloaded to any computer using the KD2 Pro Utility program. The specification of KD2 Pro could be seen in Figure 38 below.

Operating Environment:
Controller: 0 to 50 °C
Sensors: -50 to +150 °C
Power: 4 AA cells
Battery Life: Approx. 1800 readings in constant use or 3 years with no use (battery drain in sleep mode < 50 uA)
Case Size: 15.5 cm x 9.5 cm x 3.5 cm
Display: 3 cm x 6 cm, 128 x 64 pixel graphics LCD
Keypad: 6 key, sealed membrane
Data Storage: 4095 measurements in flash memory (both raw and processed data are stored for download)
Interface: 9-pin serial
Sensor cable length: 0.8 m
Read Modes: Manual and Auto Read
Sensors:
6 cm (small) single-needle (KS-1):
Size: 1.3 mm diameter x 60 mm long
Range: 0.02 to 2.00 W/m °K (thermal conductivity)
0.5 to 50 m °K/W (thermal resistivity)
Accuracy (Conductivity): ± 5% from 0.2 - 2 W/m °K
±0.01 W/m°K from 0.02 - 0.2 W/m °K

10 cm (large) single-needle (TR-1):
Size: 2.4 mm diameter x 100 mm long
Range: 0.10 to 2.00 W/m°K (conductivity)
0.5 to 10 m °K/W (resistivity)
Accuracy (Conductivity): ±10% from 0.2 - 2 W/m°K
±0.02 W/m°K from 0.1 - 0.2 W/m°K

30 mm dual-needle (SH-1):
Size: 1.3 mm diameter x 30 mm long, 6 mm spacing
Range: 0.02 to 2.00 W /m°K (conductivity)
0.5 to 50 m°K/W (resistivity)
0.1 to 1 mm^2/s (diffusivity)
0.5 to 4 $MJ/m^{-3}°K^{-1}$ (volumetric specific heat)
Accuracy: (Conductivity) ± 5% from 0.2 - 2 W/m°K
± 0.01 W m^{-1} $°K^{-1}$ from 0.02 - 0.2 W/m°K
(Diffusivity) ±5% at conductivities above 0.1 W/m°K
(Volumetric Specific Heat) ±7% at conductivities above 0.1 W/m°K

Figure 38- Specification of KD2 Pro device

The basis for calculating thermal properties of a material in KD2 Pro is line source theory. This device works by fitting time series temperature data during heating and cooling period after a heating pulse is produced. Thermal conductivity and thermal diffusivity are measured directly and volumetric specific heat determined from following relation:

$$C_p = \frac{K}{\rho D} \qquad \text{Equation 20}$$

Where k is the thermal conductivity; D is the thermal diffusivity, C_p is specific heat capacity and ρ is density. In each case, K and D are obtained by a non-linear least squares procedure. It should be pointed out that reliable measurements of D can be only obtained from the dual needle measurements. In case of dual needle, needles spacing is of high importance due to high sensitivity. For instance, 1% difference from $6mm$ assumed spacing, could result in at least 2% error in the measurements of C_p and D. In Figure 39, the KD2 Pro with its three different needles can be seen. In this work, the dual-needle probe was used for almost all the tests.

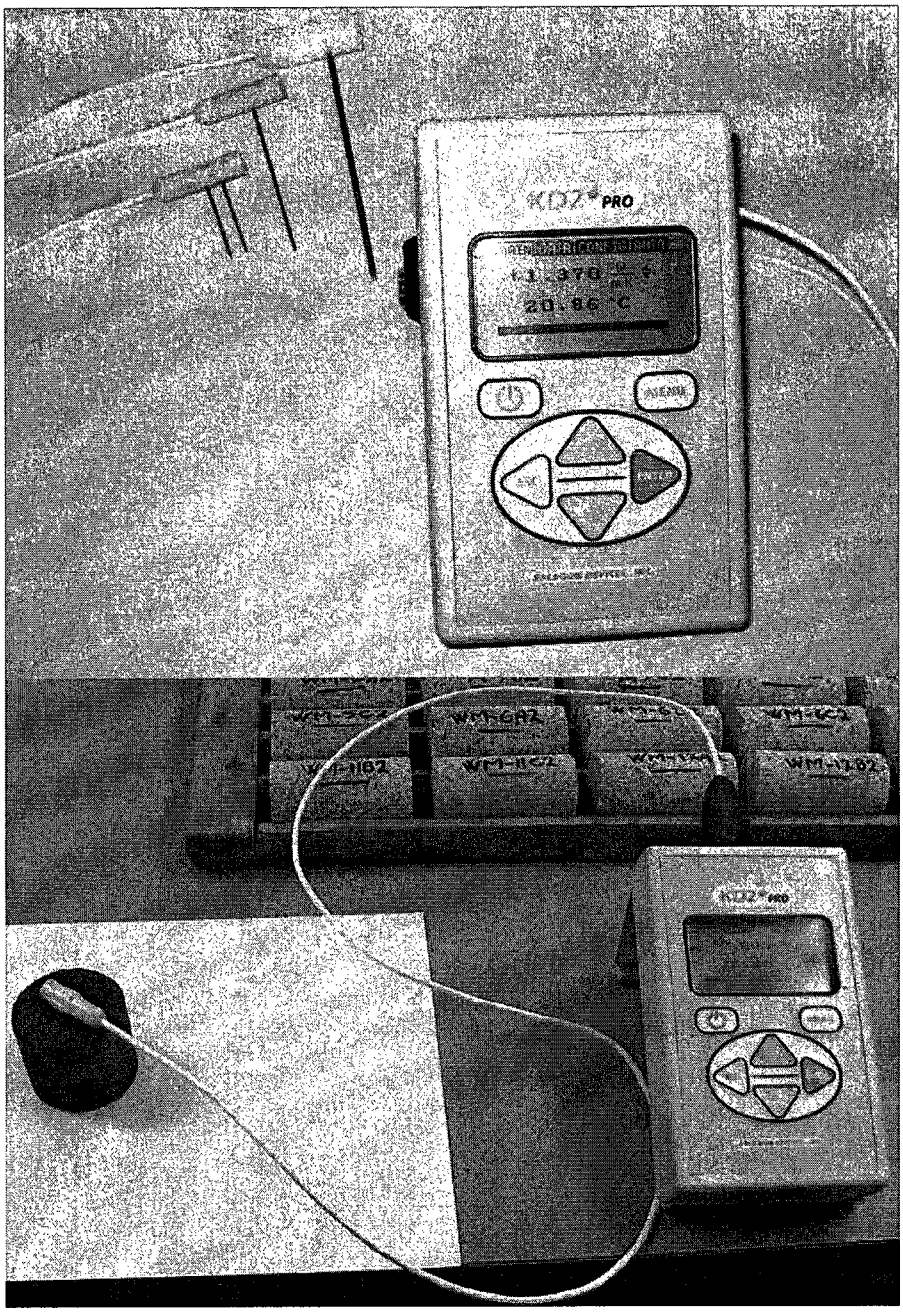

Figure 39- KD2 Pro and its measurement needles

Chapter 6: Results and Discussion

6.1. Introduction

In this chapter the results from experiments carried out, will be presented and discussed. The results have been achieved from more than 2000 samples were tested including those which have been done to lead the research in the right direction. Here the effect of different parameters and sometimes the mixed effect of parameters will be explained on samples which their provision, were discussed in previous chapters. Therefore, only the results are going to be presented and discussed. Different notations also are used that will be introduced below.

Due to availability (Steady State test location distance), most of the tests were done using the Unsteady State method. Also, in some cases, volumetric heat capacity and thermal diffusivity will be shown even though it is not within the focus range of this research and were done in order to give a clue about these parameters which are somehow influential in geothermal assessment. Results are presented in some graphs and for most of these graphs saturation is considered as a constant influential factor against the thermal conductivity. For all tests, at least 2 cm from each end of sample were removed. To facilitate the understanding and helping in estimation of thermal conductivity of backfill, a known relationship called Côté-Konrad model for soils, Figure 22, was also used and the results were compared to experimental results. Notations used in this chapter include $K(^{W}/_{m°C})$: Thermal conductivity, C($^{MJ}/_{m^3°C}$) : Volumetric heat capacity, D($^{mm^2}/_{s}$) : Thermal diffusivity, PD(%) : Pulp density, UCS(MPa) : Uniaxial compressive strength, BD($^{gr}/_{cm^3}$) : Bulk density, BC(%) : Binder content, GT(hr) : Grinding time, d(mm) :

Diameter of sample, S(%): Degree of saturation, n (%) : Porosity, CT(day) : Curing time, SS (%) : Sodium silicate content and $K_S(^{W}/_{m°C})$: Thermal conductivity of solid particles.

6.2. Sample size

Prior to investigating the other variables, the effect of sample volume was investigated to see if volume and consequently the diameter could have any effect on measurements. In fact, this test was designed to make the size optimization for the unsteady state tests, since very limited size constraints existed in this case (height and diameter). For this test, 3 different sample diameters were considered including 25mm (1-inch), 50 mm (2-inch) and 100mm (4-inch). Inert material for this test was tailings only. Pulp density of mixture chosen as 75% and the binder consumption was equal to 5%. For each diameter, 8 samples from 2 similar batches were provided. The tests were carried out in the saturated condition for each sample. Figures 40 and 41, show test results.

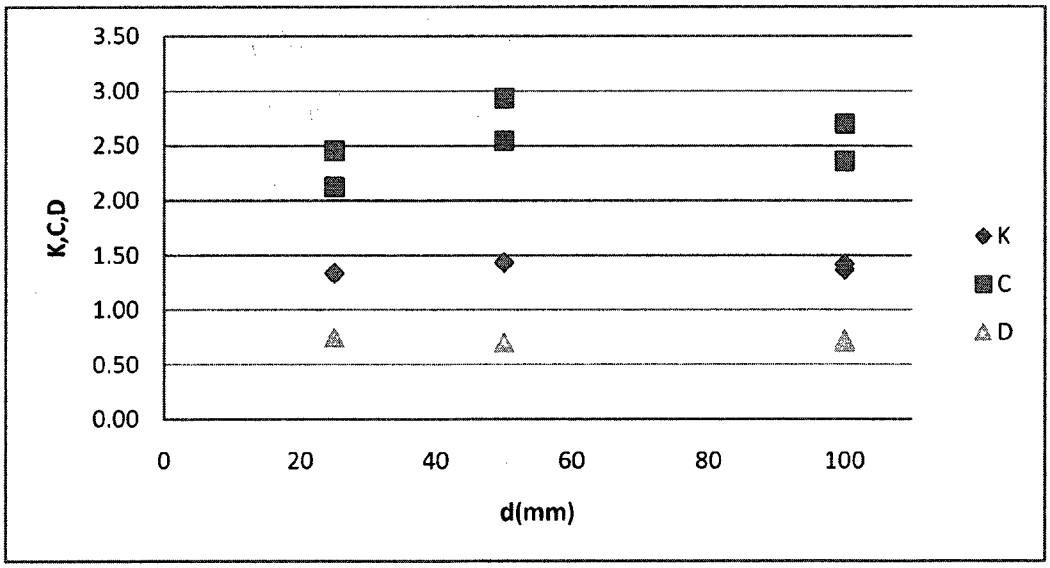

Figure 40 – The effect of sample diameter on thermal conductivity of backfill

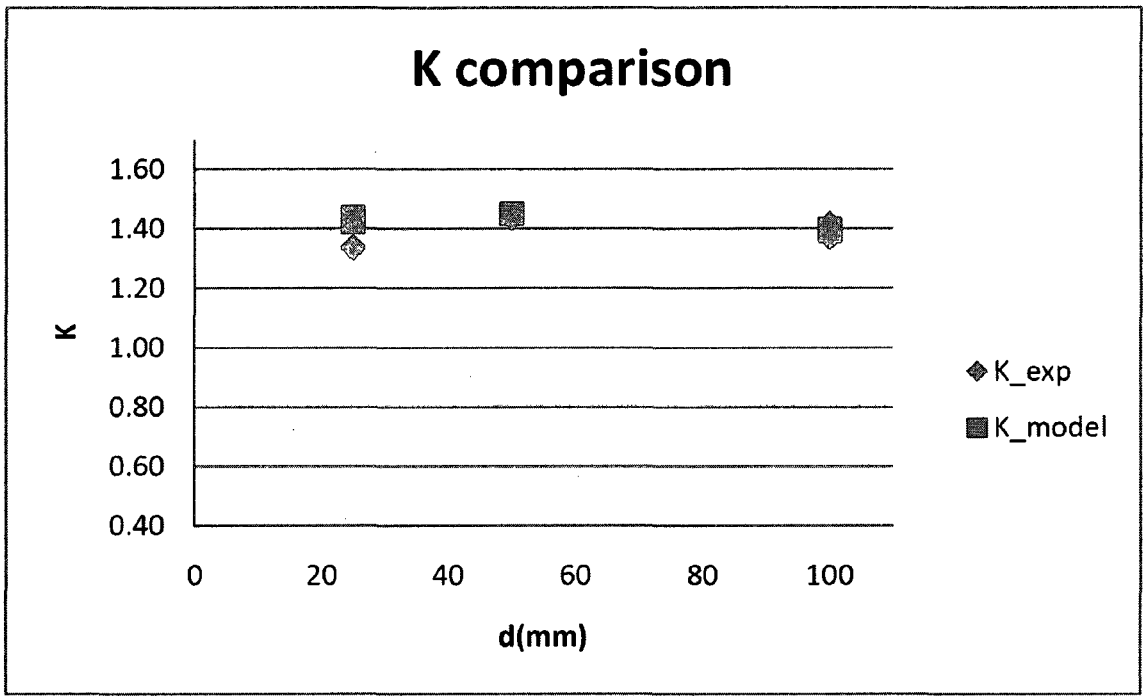

Figure 41 – Comparison of experimental results with Côté- Konrad model for size test

The first Figure shows that very little difference in thermal conductivity could be observed with the varying diameter. In Figure 41, the results were compared to the model and it is seen that for the 50mm (2-inch) samples the best correlation exists, although for other sizes specially the 100mm (4-inch) one, this good relation is also observable. So according to this experiment, 50mm (2-inch) samples for needle probe test would give the best results and was chosen for unsteady state tests.

6.3. Measurement location

The needle device measurement is done locally, in that the measurement is done in a very limited space around the probe. To make sure that if satisfying results would be achieved from unsteady state measurements, this test was designed. For this test two different series of samples were made. One of them was made from mineral processing tailing as inert material, and silica sand was used to make the other one. Pulp density was set to

70% and binder was set to 5% for both of these samples. Samples were cured 28 days and tested in the saturated condition. Measurements were carried out on 14 different locations including 4 different locations on both top and bottom (1 in center and 3 with $\frac{1}{3}$ distance from each other starting from center and at 120° from each other) of samples (8 locations total) and 6 locations on the periphery of each sample (with same distance from each other starting from top and 60° distance from each other). Samples were made using 100mm (4-inch) molds. The results are shown in the Figure 42.

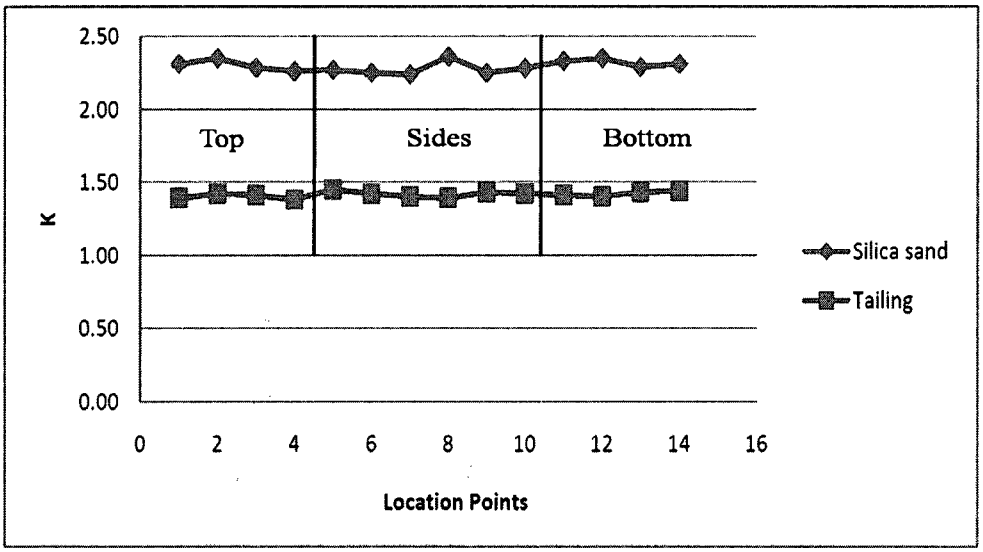

Figure 42 - Thermal conductivity measurement in different locations of sample

From the graph, it can be seen that very little changes were observed in different locations, all variations are within the error range of the device. So this means that the measurement could be carried out in any location of the sample.

6.4. Curing time

It is assumed that cemented backfills become cured in 28 days and no further considerable changes happen after that. In relation to thermal properties, there has been

no clue about the time effect on thermal properties. So in this experiment, samples of backfill were tested each 7 days for 42 days. Again for these experiments, backfill samples were made from mineral processing tailing. Pulp density and binder consumption were set to 75% and 5%, respectively. Unsteady state method was used for testing. All the samples cured in 50mm (2-inch) molds. The results of this experiment are presented in Figures 43 to 45.

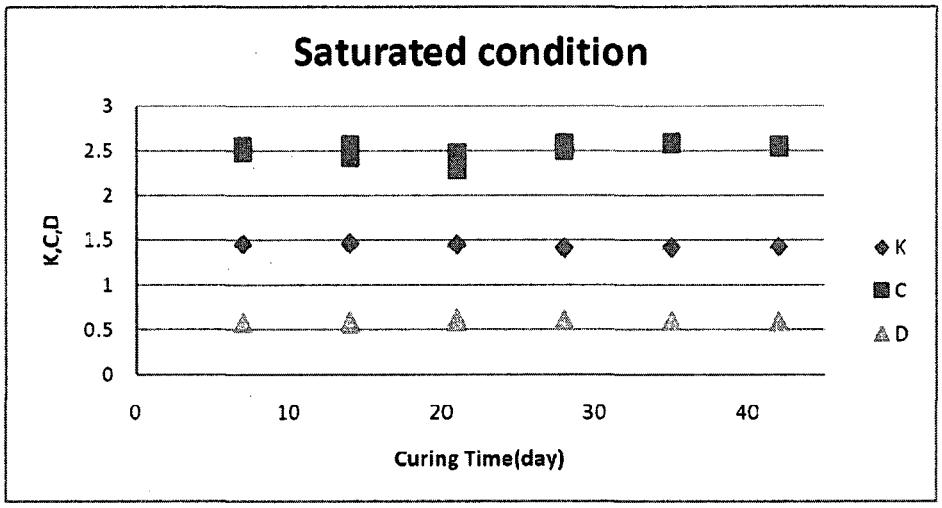

Figure 43 - The effect of curing time on thermal conductivity of saturated samples

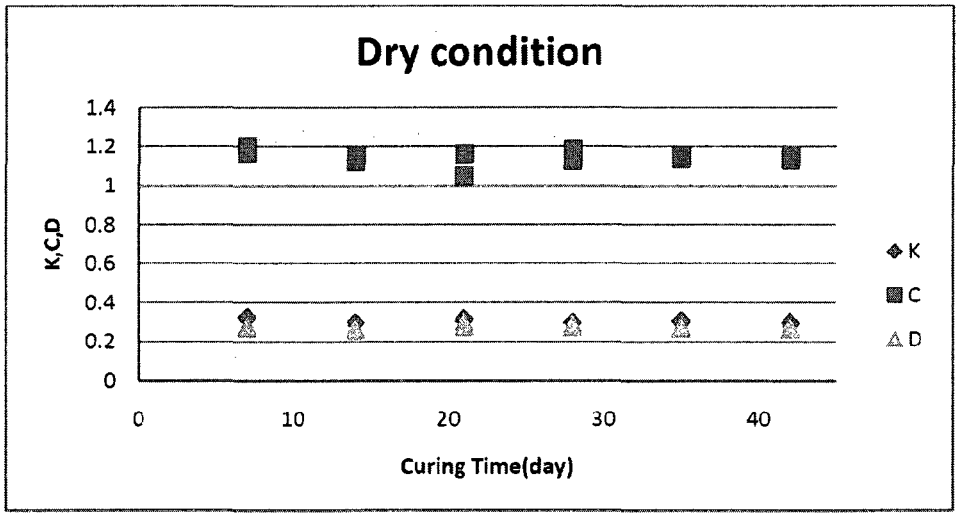

Figure 44 - The effect of curing time on thermal conductivity of dried samples

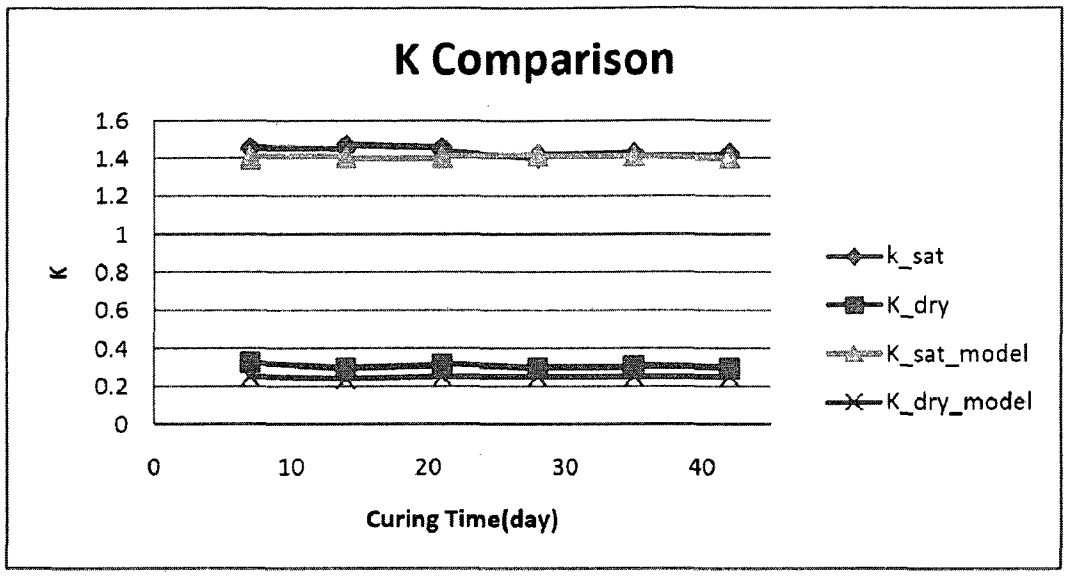

Figure 45 - Comparison of experimental results with Côté-Konrad model for curing time effect test

From the Figures 43 and 44 it is understood that thermal conductivity, thermal diffusivity and volumetric heat capacity are independent from curing time although very small changes could be observed before 21 days of curing. Also from Figure 45, a very good agreement between the Côté-Konrad model and the experimental results especially for the saturated samples can be seen. This agreement is strong after 28 days of curing. But again, slight difference in the dry condition exists between the model and the results.

6.5. Pulp density

In this part, several samples prepared with pulp densities as 68%,70%, 72%, 74%, 76%, 78% and 80%. The binder content was constant at 5%. Thermal conductivity of Tailing, slag and Portland cement were measured before the tests carried out. Samples of 100mm diameter (4-inch) were used for the steady state tests and 50mm (2-inch) samples were used for unsteady state tests. Figure 46 shows the results of Steady state method as well as uniaxial compressive strength (UCS) and bulk density results.

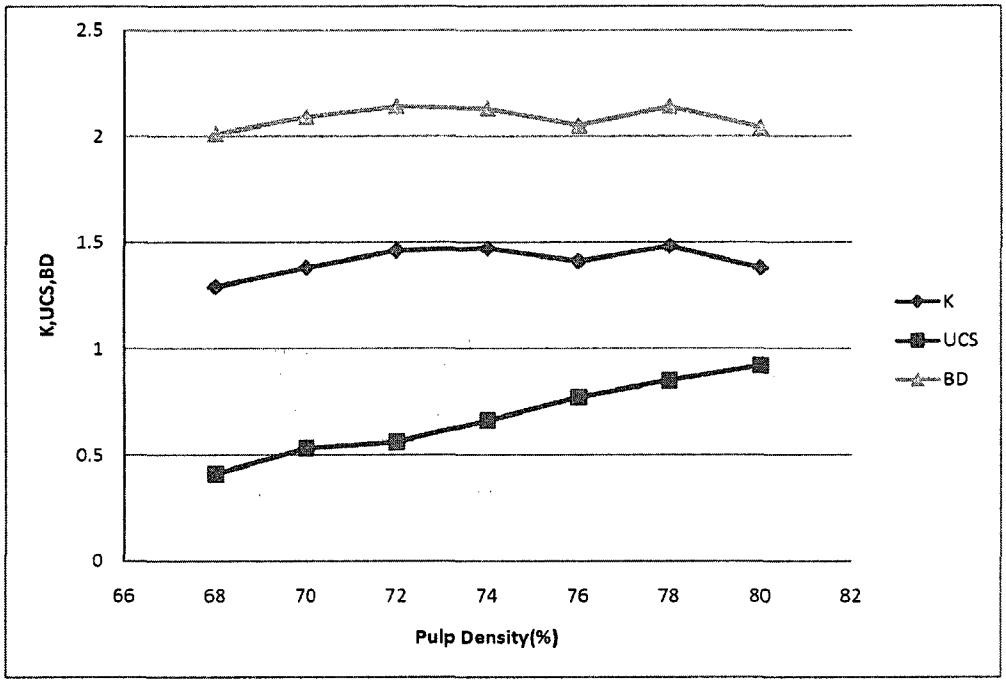

Figure 46 - The effect of pulp density on thermal conductivity (steady state), strength and bulk density

It can be observed that thermal conductivity has a slight increase with pulp density within the hydraulic backfill range (65%-75%) and toward paste fill (75%-80%), the trend becomes almost steady. A little difference in thermal conductivities was assumed to have occurred due to change in porosity which will be discussed more, later in this chapter. Also it can be seen even though uniaxial compressive strength increased with pulp density, but no similar increase is observed for thermal conductivity. From the graph, almost the same trend between pulp density and bulk density is considerable. In Figure 47 the comparison between Côté-Konrad model and the experimental results for saturated and dried samples are shown.

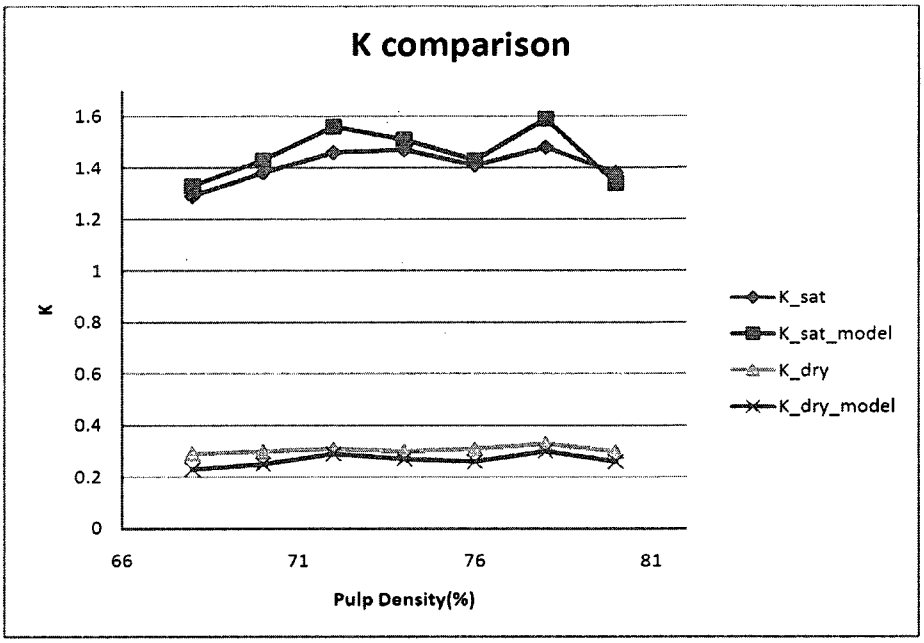

Figure 47 - Comparison of experimental results with Côté-Konrad model using steady state method (PD)

Some discrepancies here also are due to moisture loss during the test. Because steady state test takes about 6-12 hours, and even though a saturated environment was provided in the cold room, it couldn't prevent moisture loss during the test. This matter has been encountered before in pre-test stage and the results were forced to be omitted because of this matter. Because of moisture loss problem and as mentioned before, the availability problem, most of the experiments were done by unsteady-state method. From the graphs fairly good relation between the results and the model can be seen for the saturated condition and for the dry condition it gets better. In both cases, the model slightly under predicts the experimental data.

In Figures 48 and 49 the results of Unsteady State method can be seen. These tests were carried out on different recipes from the previous tests. Pulp densities of 65%, 68%, 70%, 72%, 75%, 77% and 80% with the same binder consumption as before were considered for these tests.

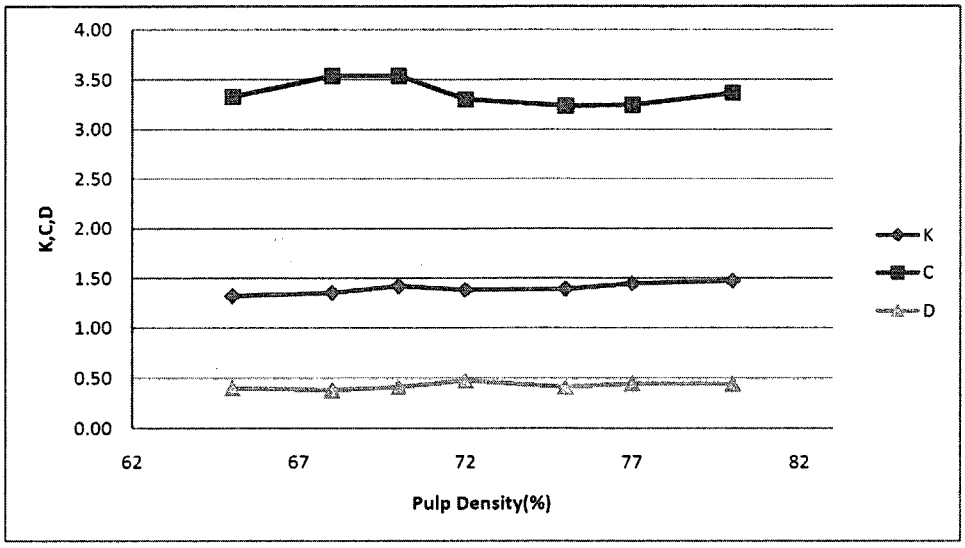

Figure 48 – The effect of pulp density on thermal conductivity using unsteady state method

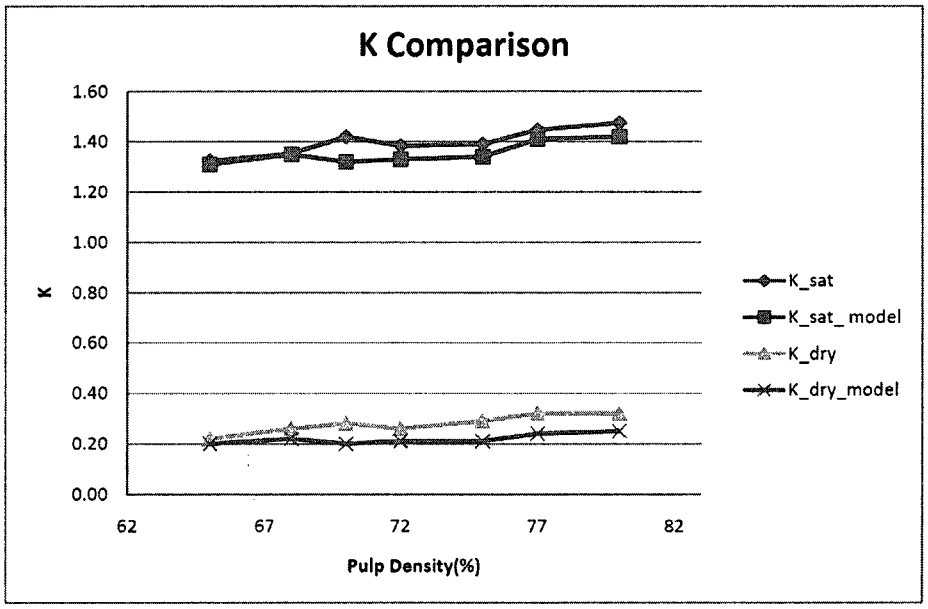

Figure 49 – Comparison of experimental results with Côté-Konrad model using unsteady state method (PD)

From the graphs it is understood that thermal conductivity increases slightly with pulp density especially for 77% and 80% and this would be resulted from decrease in porosity. Thermal diffusivity has the same trend as thermal conductivity but volumetric

heat capacity has somehow different trend than thermal conductivity. This could be due to higher error probability for the device in this case.

In Figure 49, good agreement between results and model can be observed especially for the saturated samples. Although dried samples agree less with the model, reasonable agreement was found.

6.6. Binder content (consumption)

For binder content experiments were carried out both using Steady State method and Unsteady State method. At first samples with 4 different binder contents tested. Binder consumption of 3%, 5%, 7% and 9% were chosen and the pulp density of each mixtures was designed as 70%. Samples with 100mm diameter (4-inch) were used for the steady state tests and 50 mm (2-inch) samples were used for unsteady state tests. The results are shown in Figures 50 and 51.

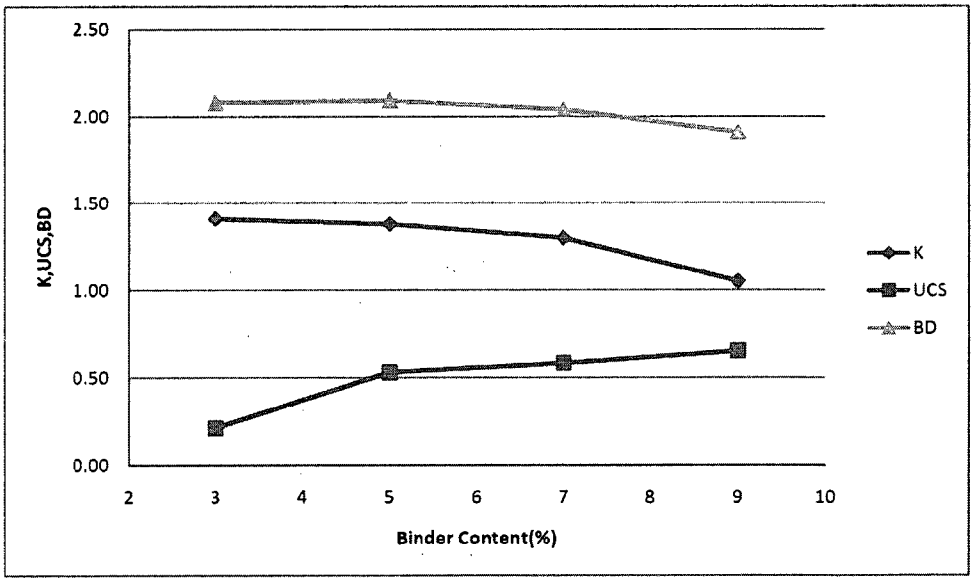

Figure 50 - The effect of binder content on thermal conductivity using steady state method

From the above Figure, it is conveyed that thermal conductivity decreases with binder consumption. But in fact due to porosity increase and degree of saturation decrease with binder content increase, one cannot be sure of reality of this trend caused by binder content change. Besides as mentioned before the moisture loss during the Steady state measurement is effective on the thermal conductivity amount.

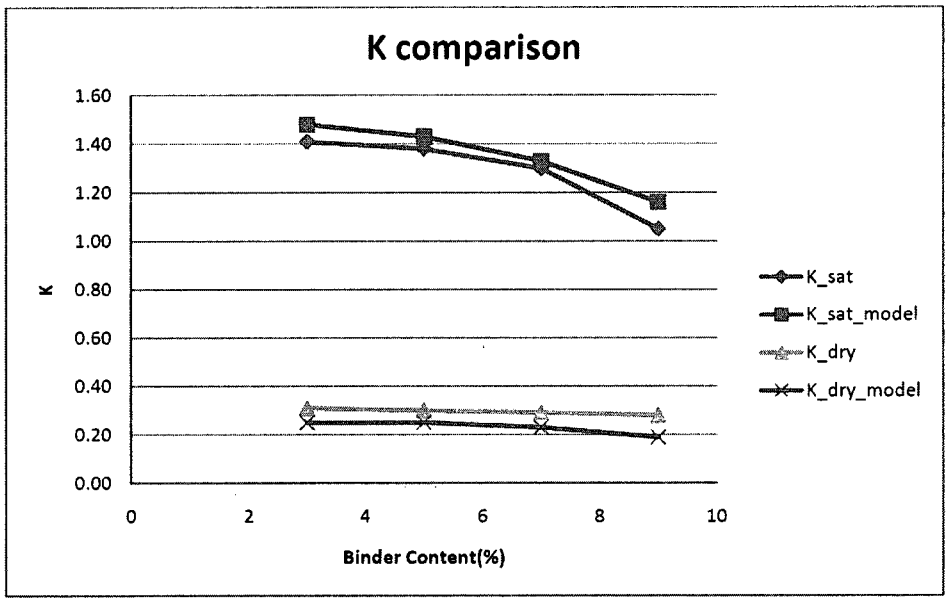

Figure 51 - Comparison of Experimental results with Côté-Konrad model using steady state method (BC)

Also like previous section a similar trend for thermal conductivity and bulk density exists but not with the uniaxial compressive strength that normally should increase with more binder content. Again in this case an acceptable agreement between results and model could be seen in Figure 51. Similar to pulp density, this test also was done for unsteady state method. In this part the same binder consumption include 3%, 5%, 7% and 9% but the pulp density equal to 75% were chosen. The results are shown in Figures 52 and 53.

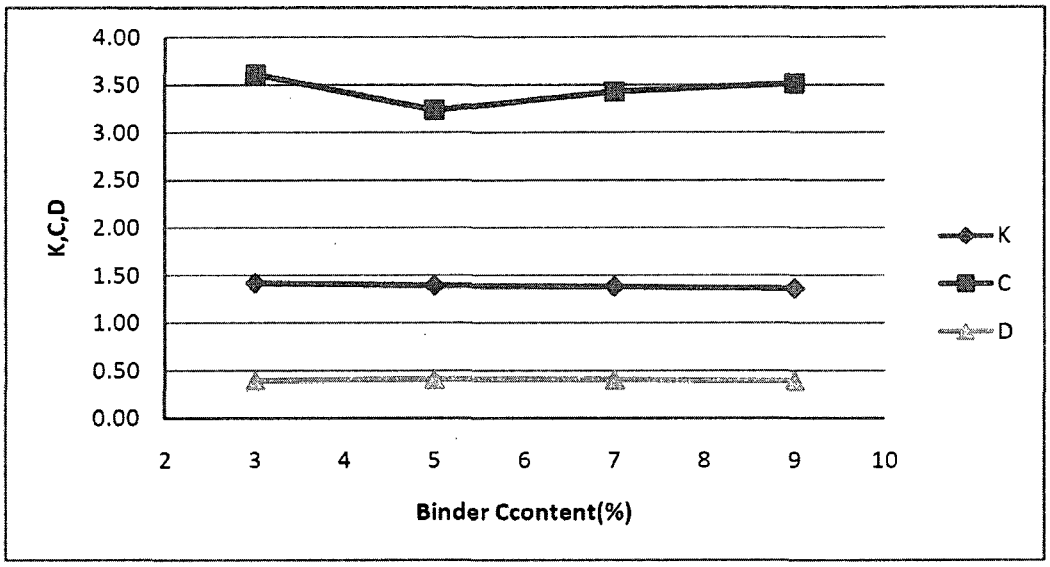

Figure 52 - The effect of binder content on thermal conductivity using unsteady state method

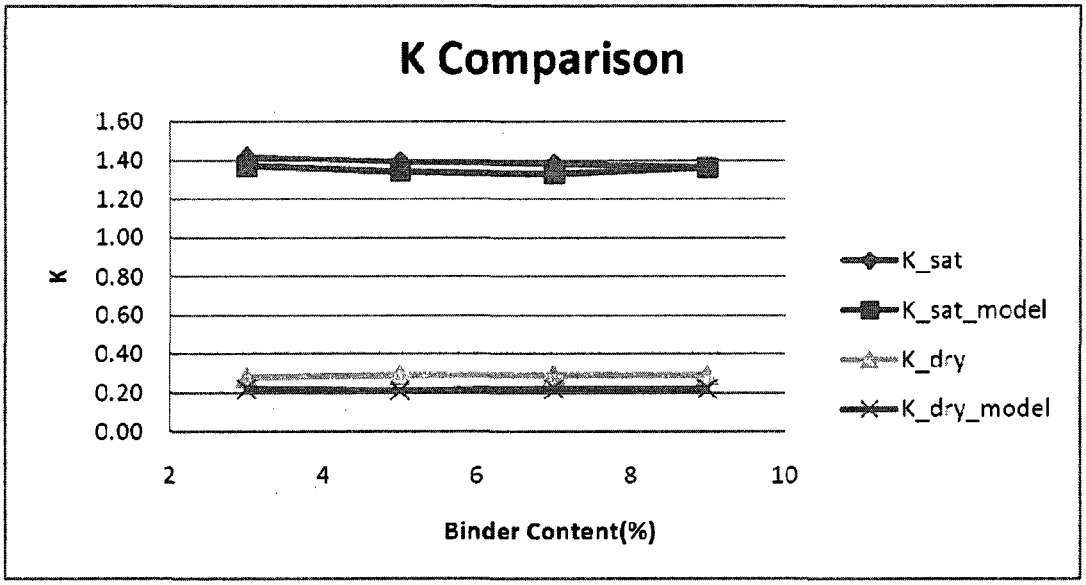

Figure 53 – Comparison of experimental results with Côté-Konrad model using unsteady state method (BC)

From Figure 52 it is observed that thermal conductivity remains almost constant against binder content increase, this behavior is similar for thermal diffusivity also, but not for volumetric heat capacity, because of device error range, it could be guessed that volumetric heat capacity remains constant as well. In Figure 53 a very good agreement between the model and results can be seen, although for dried condition a little more

difference exists. Figure 54 gives the normalized conductivity with saturation in this case was obtained and good conformity for these different binder consumptions is observed.

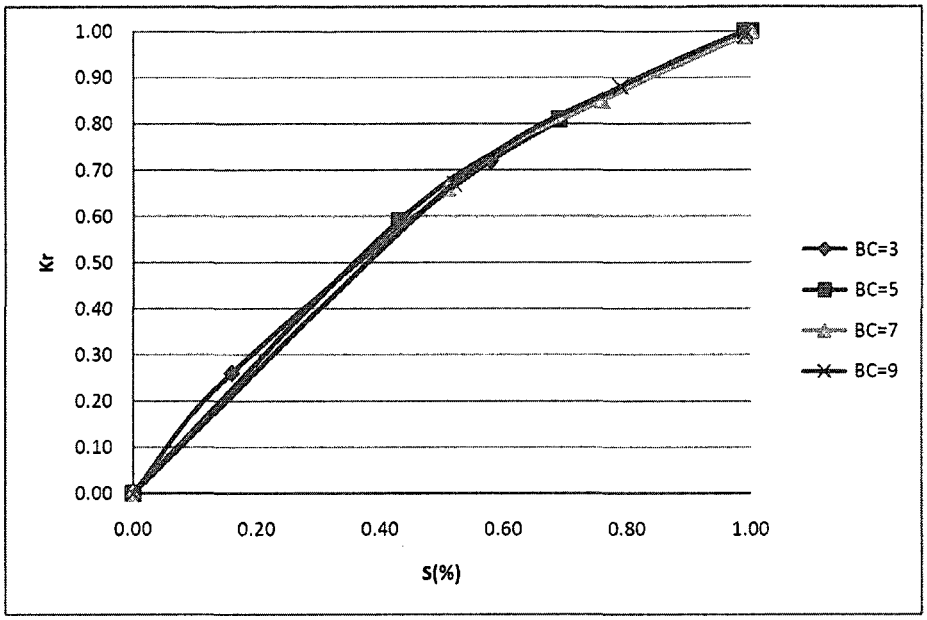

Figure 54 - Normalized thermal conductivity versus saturation comparison for different binder contents

6.7. Sodium silicate

By introduction of sodium silicate in the backfill system, it has been shown that sodium silicate has positive effect in increasing the strength of backfill as a binder additive (Kermani, 2008). This composition is sometimes named Gelfill in backfill classification. Therefore, here a series of tests was designed to investigate the effect of sodium silicate on thermal properties of backfill. The range for sodium silicate content was chosen according to previous works (Razavi, 2007, Kermani, 2008). Here again, mineral processing tailing chose as inert material. Pulp density of 75% and binder content of 5% were selected. According to Kermani (2008), a sodium silicate content of 0.3% would give the best results from the geomechanical aspect. So in this part, the

sodium silicate content amounts was chosen as SS=0.1%, SS=0.3% and SS=0.5%. Degree of saturation(S) also was changed. The needle probe was applied in this experiment. The resulted graphs from the experiments of this part are presented in the Figures 55 to 58.

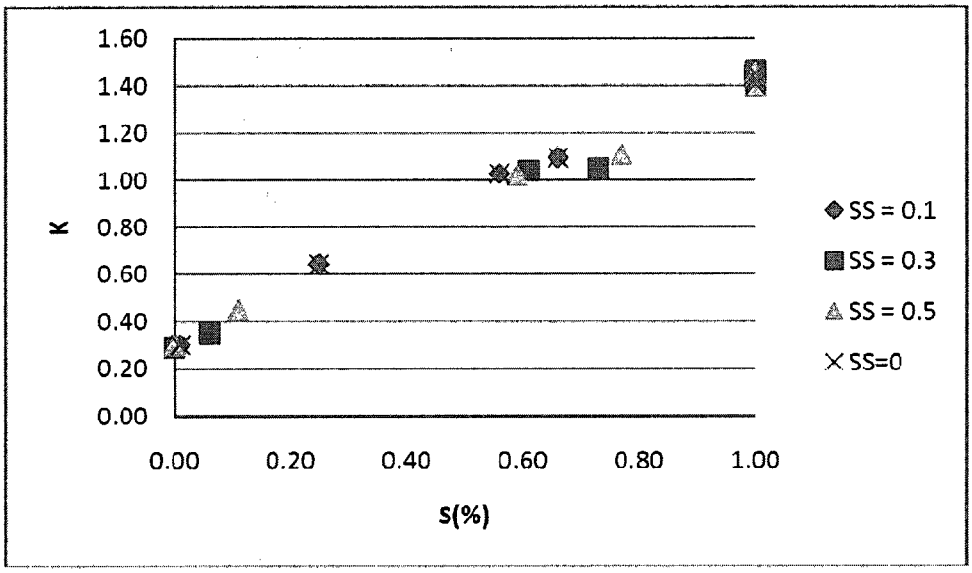

Figure 55 - The effect of Sodium silicate on thermal conductivity of backfill at different saturation

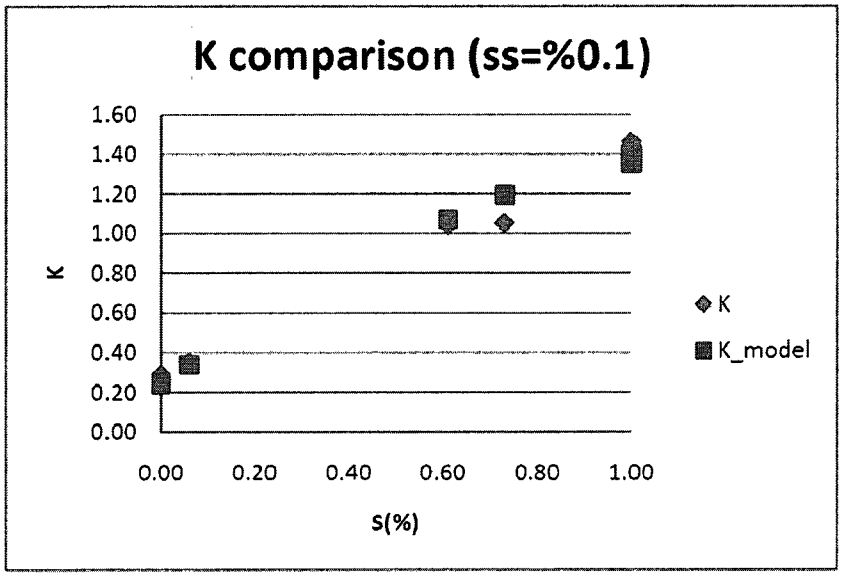

Figure 56 - Comparison of experimental results with Côté-Konrad model for sodium silicate content=0.1%

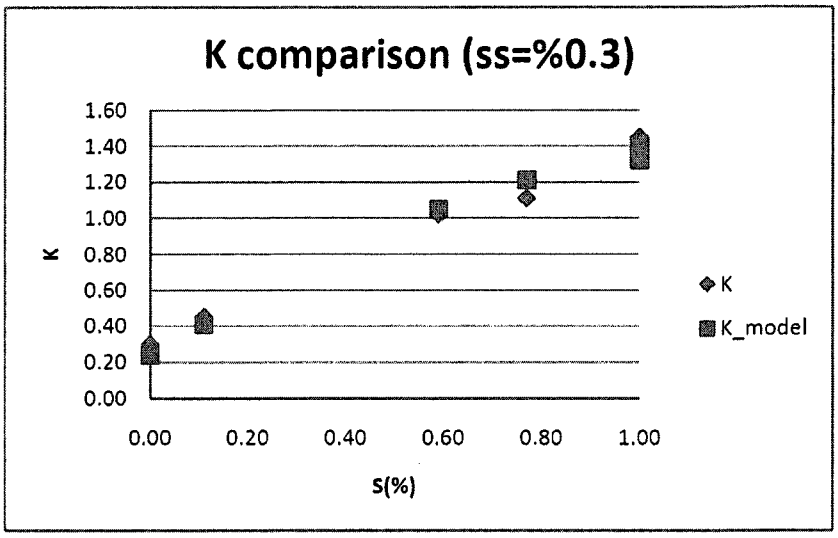

Figure 57 - Comparison of experimental results with Côté-Konrad model for sodium silicate content=0.3%

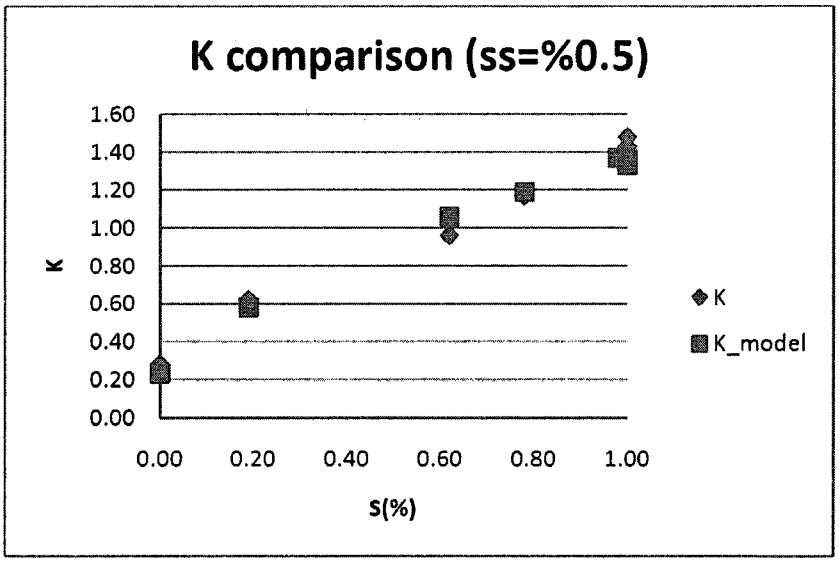

Figure 58 - Comparison of experimental results with Côté-Konrad model for sodium silicate content=0.5%

From Figure 55, it can be understood that sodium silicate, whatever the amount is, does not have any influence on thermal conductivity of backfill since all the diagrams almost coincide with each other. From Figures 56-58 it can be seen that there is good agreement between Côté-Konrad model and the results from the experiments for each sodium silicate content and it means that sodium silicate does not have any contribution to thermal conductivity behavior. In fact, the model results are the same in each case.

6.8. Saturation

Degree of saturation could be considered as the most important geophysical factor in thermal conductivity of soils and rocks. This matter has been addressed in many previous works before. Throughout this research, this point also was observed for backfill. This test was designed to see the detailed behavior of backfill with the degree of saturation. For this test, mineral processing tailings were used as inert material. Pulp density of backfill was designed at 75% and the binder content was set to 5%. Fifty millimeter (2-inch) molds were used to make backfill samples. This experiment was carried out by needle probe. Figures 59 and 60 show the behavior of thermal conductivity, thermal diffusivity and volumetric heat capacity with degree of saturation.

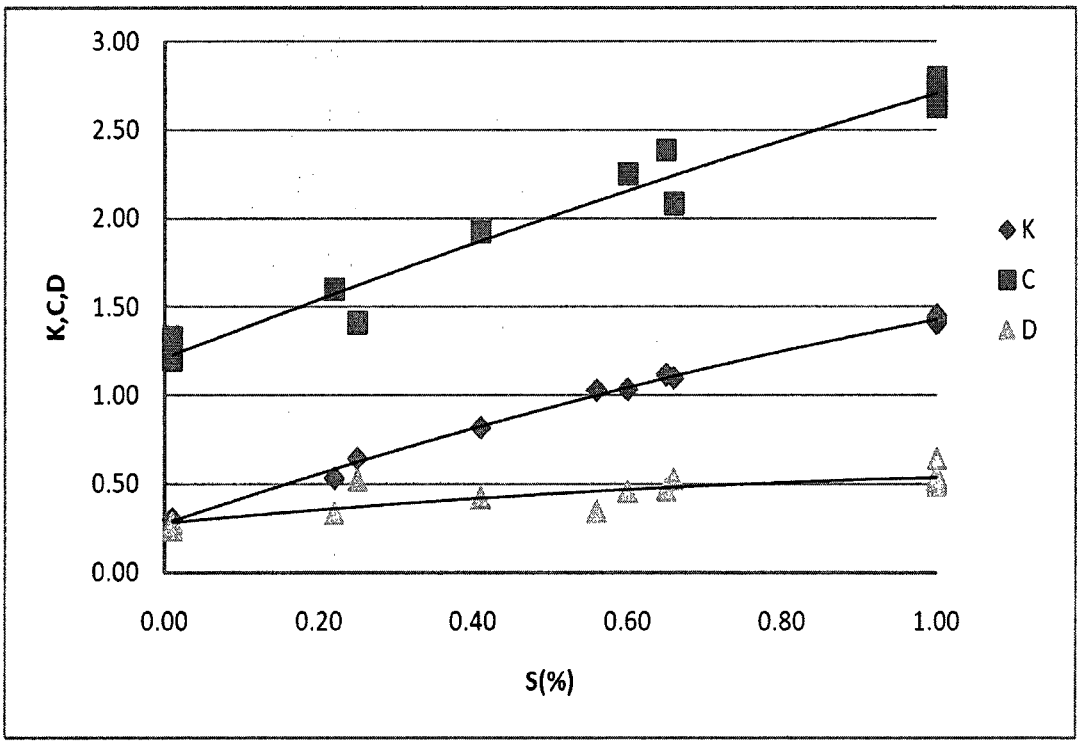

Figure 59 - The effect of saturation on thermal properties of backfill

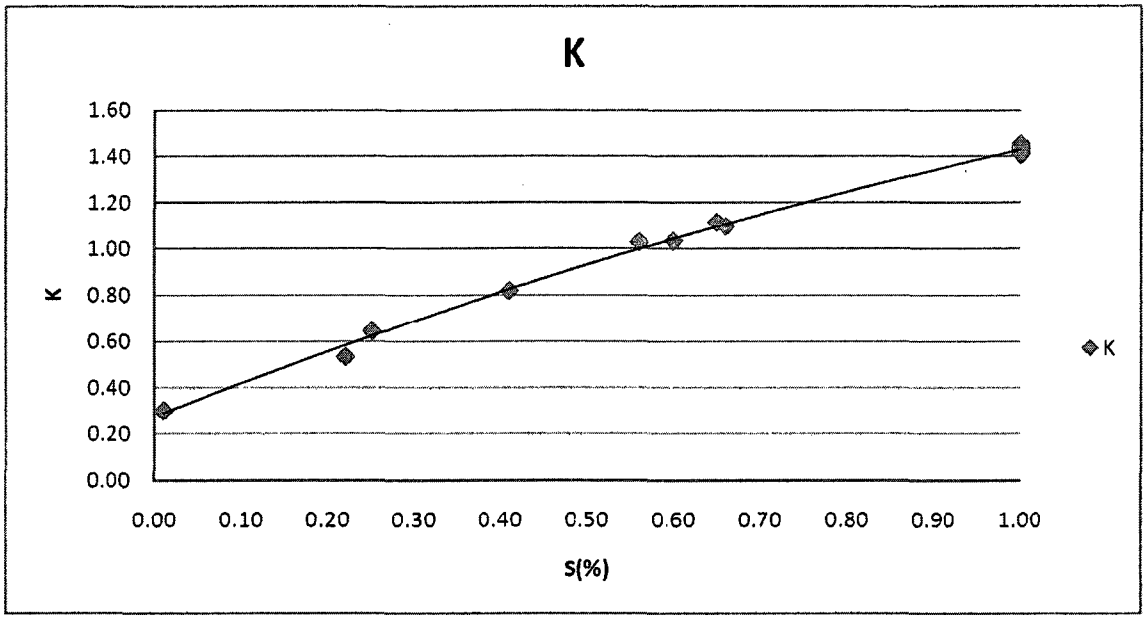

Figure 60 - The effect of saturation on thermal conductivity of backfill

In general, all the thermal properties increase with increasing saturation. From these figures it can be seen that accuracy decreases for thermal diffusivity and especially volumetric heat capacity which to some extent, is because of error range of device. Very good relation between thermal properties according to relation between thermal conductivity, volumetric heat capacity and thermal diffusivity ($K = D.\rho.C_p$) shows the accuracy of the experiment. Also a similar to linear increase could be observed in Figure 60 with saturation. This could be resulted from many small pores distributed consistently throughout the whole sample.

In Figures 61 and 62, the comparison between Côté-Konrad model and the experimental results along with the normalized thermal conductivity behavior with saturation are presented. The value of κ=1.9 was selected for the calculation of K_r due to particle size (silty, clayey) of material used in this test. From these figures, it can be seen that good agreement between results and the model exists.

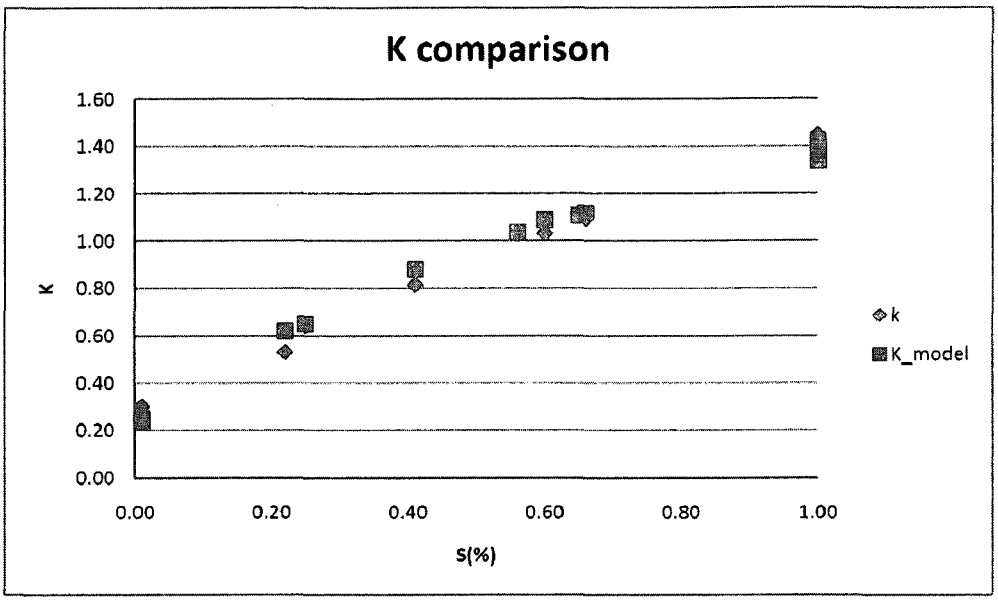

Figure 61 - Comparison of experimental results with Côté-Konrad model for saturation rate

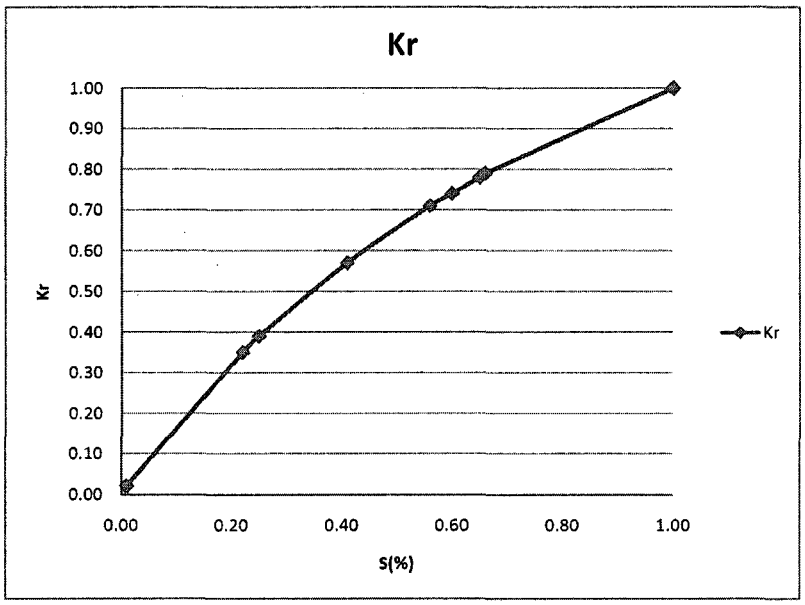

Figure 62 - Normalized thermal conductivity behavior with saturation rate

6.9. Grinding time

Even though this matter is a function of porosity, it was studied separately using the Steady state method. For this test silica sand as inert material was used. The pulp density and binder content were considered as 70% and 5%, respectively. The samples

were $100mm$ $(4inches)$ in diameter for this test. The results of this experiment are shown in Figure 63. In Figure 64 the comparison between the experiment results and the outputs of the Côté-Konrad model is shown.

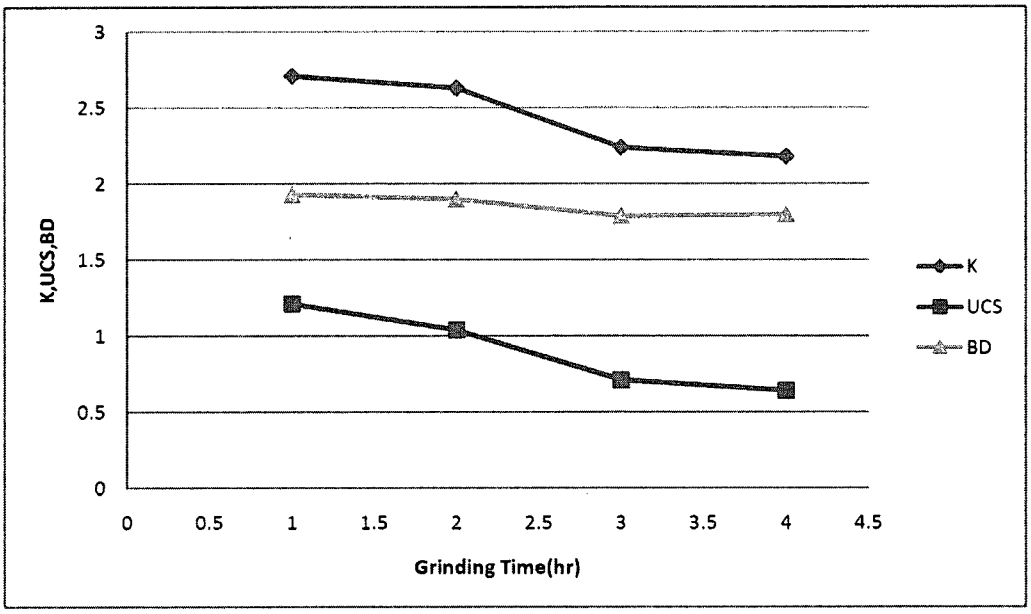

Figure 63 - The effect of grinding time on thermal conductivity using steady state method

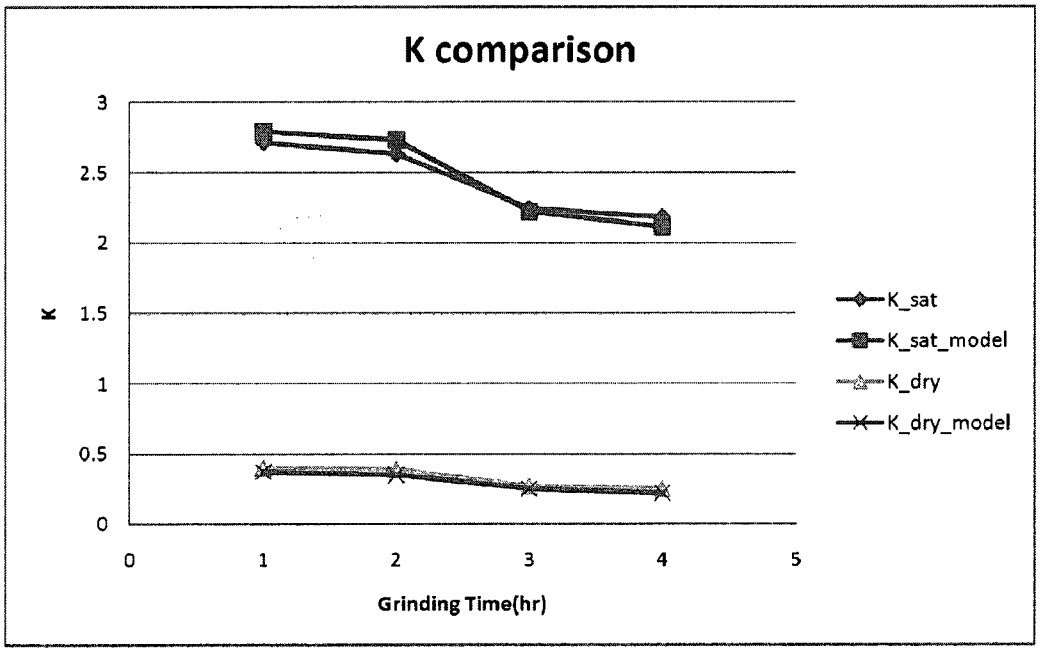

Figure 64 - Comparison of experimental results with Côté-Konrad model using steady State method (GT)

From these figures it could be understood that with increasing grinding time the thermal conductivity, bulk density and uniaxial compressive strength decrease. This of course could be resulted from increase in porosity. Also good agreement could be seen between the experimental results and the model, especially for the dried condition.

6.10. Porosity

Porosity is another important geophysical parameter in thermal conductivity. Generally, thermal conductivity has an inverse relation with porosity. To see the effect of this parameter on thermal conductivity of backfill, this test was designed. Silica sand of different particle sizes was chosen and a mixture of them was used as inert material. Pulp density of backfill was chosen as 75% and binder consumption was chose as 5% for this test. Backfill cured in 50mm (2-inch) molds and the measurements were done using the unsteady state method. The porosity was calculated using physical concepts : the volume of sample was determined by measuring sample heights at 3 points with $\frac{2\pi}{3}$ distance from each others, then saturated sample put in oven according to ASTM D2216-98 for moisture content test, having moisture loss, density and the volume of the sample, porosity can easily be calculated. In Figures 65 and 66 the results of this experiment are shown.

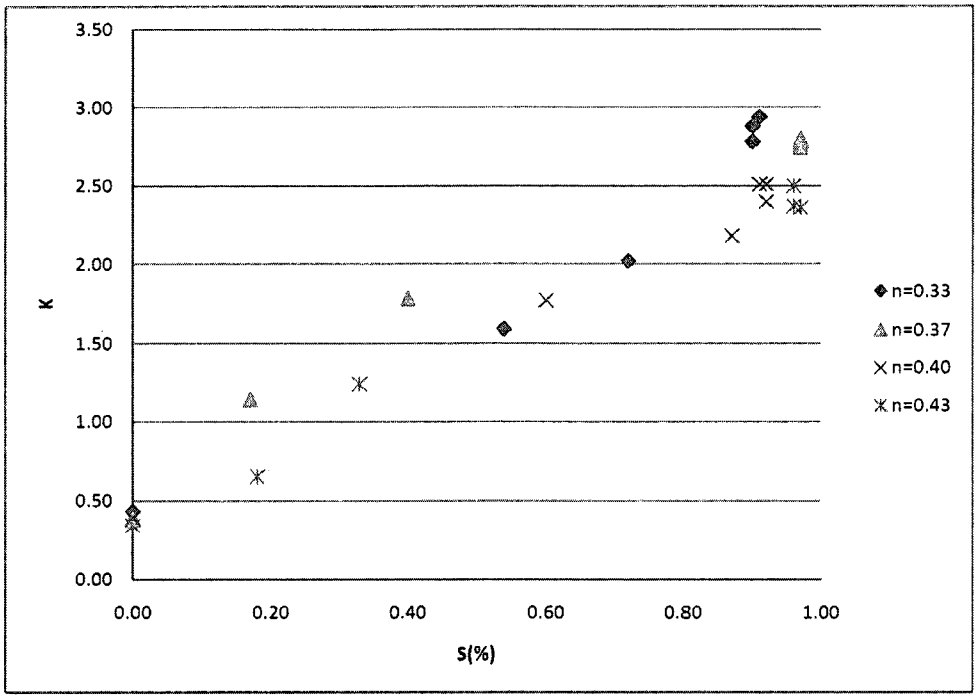

Figure 65 – Thermal conductivity Behavior with saturation at different porosities

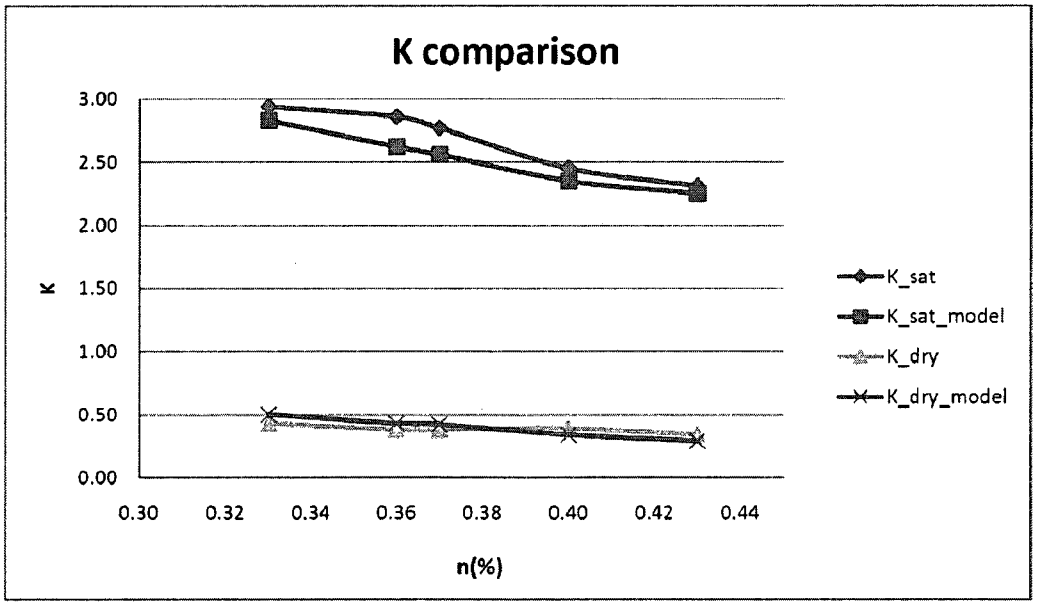

Figure 66 - Comparison of experimental results with Côté-Konrad model for different porosities

From this test, it was observed that porosity differences especially for hydraulic backfill (or Gelfill) and paste fill are not considerable. From the figures, it is obvious that thermal conductivity decreases with porosity generally in backfill; but some discrepancies could

be seen in the data points. This could have resulted from two matters: first, the accuracy of device falls for thermal conductivities more than $2\frac{W}{m°C}$, and second is that the porosity differences are very little in backfill which enforce more errors. In Figure 64, comparison between model and experimental results are given. It can be seen for saturated condition, that thermal conductivity of backfill, normally is higher than the device's reliable range. Therefore, there is more difference between model and results, although the trend is almost similar. But for the dry condition, in which the measured thermal conductivities are within the device range, the model and results agrees better.

6.11. Solid particles thermal conductivity

The last parameter which was investigated in this work is the thermal conductivity of solid particles. Normally with increasing thermal conductivity of solid particles the thermal conductivity of whole composition increases. For this experiment, a mixture of silica sand and tailing of same particle size was used as inert material and its thermal conductivity was calculated. Pulp density and binder consumption of backfill designed as 70% and 5%, respectively. Fifty millimeter (2-inch) molds were used to make the samples and the measurements were done through the unsteady state method. In Figures 67 and 68, the behavior of thermal conductivity with solid particles for fully saturated condition and thermal conductivity behavior with saturation are presented.

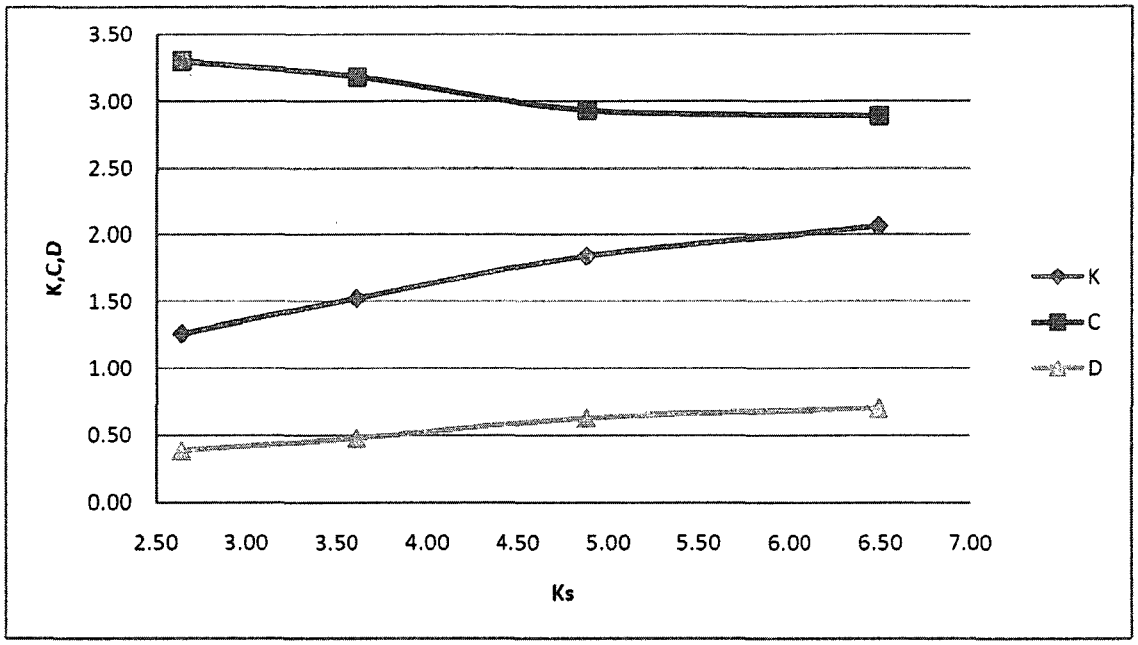

Figure 67 - The effect of solid particles thermal conductivity on thermal properties of backfill

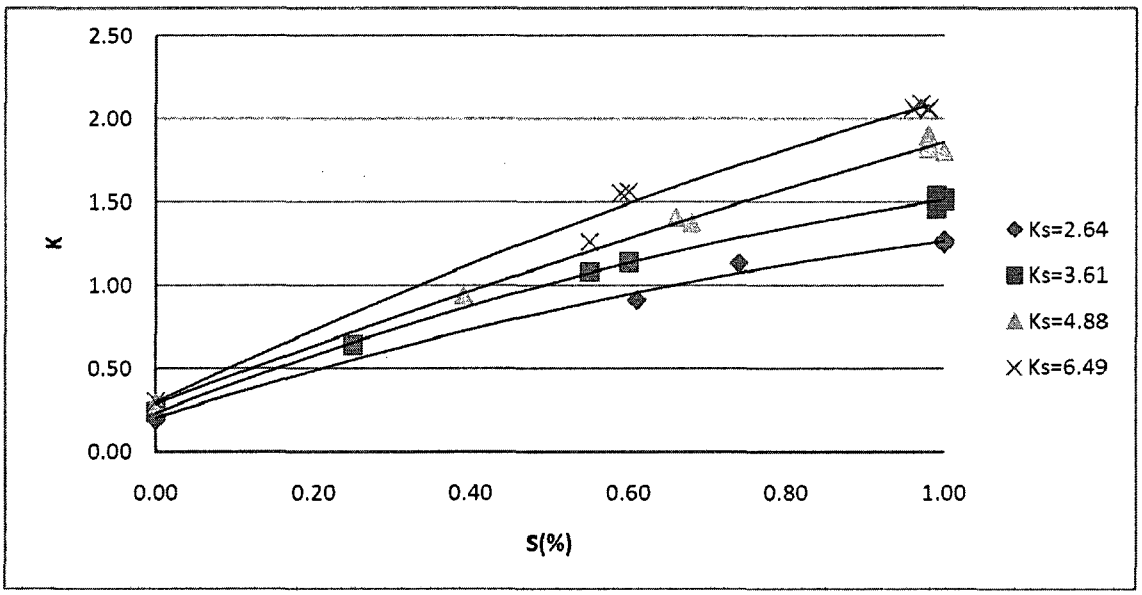

Figure 68 - Thermal conductivity behavior with saturation at different Solid particles thermal conductivities

In Figure 67, it is observed that thermal conductivity and thermal diffusivity increase with solid particles thermal conductivity but for volumetric heat capacity the behavior is vice versa since the ratio of the mixture is changed and denser and high heat capacity

tailing is replaced by less dense and lower heat capacity silica sand. From Figure 68, it could be understood that thermal conductivity in this case increases with solid particles thermal conductivity and this increase is milder at lower saturations since low conductivity air replaces higher thermal conductivity water (liquid).

In Figures 69 to 72, the experimental thermal conductivities are compared with the results produced from Côté-Konrad model. It can be seen that the results show good agreement with the model especially with lower solid particles thermal conductivity. Also the bigger difference between the model and results at higher solid thermal conductivity could be caused by the operational range limitation of the device for thermal conductivity, as one factor

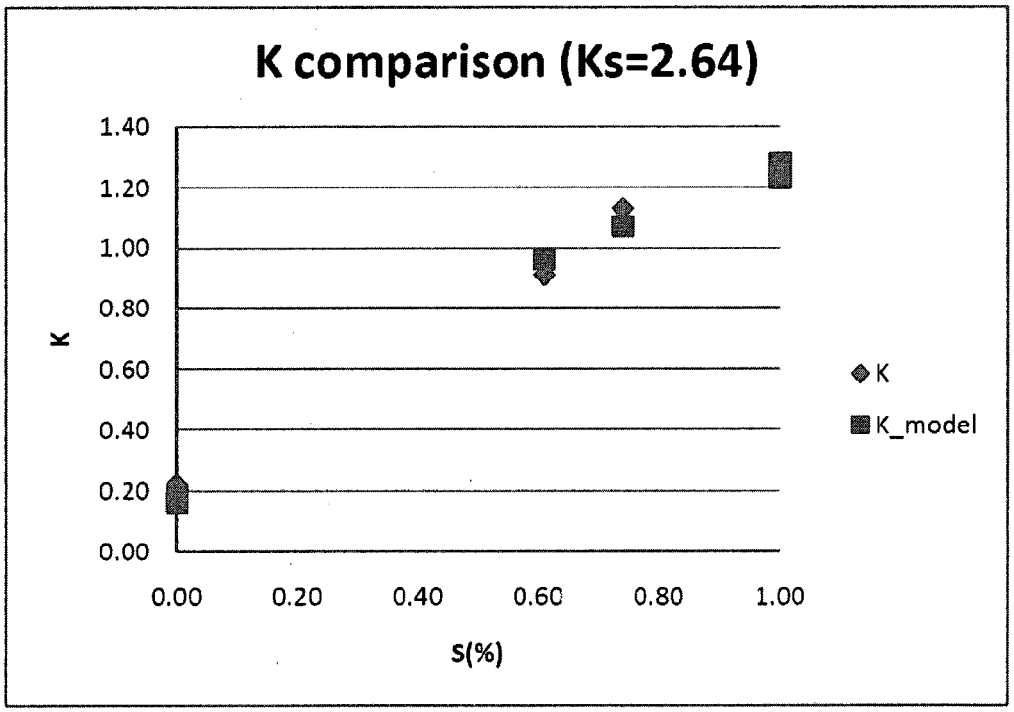

Figure 69 - Comparison of experimental results with Côté-Konrad model for $K_s = 2.64 \frac{W}{m°C}$

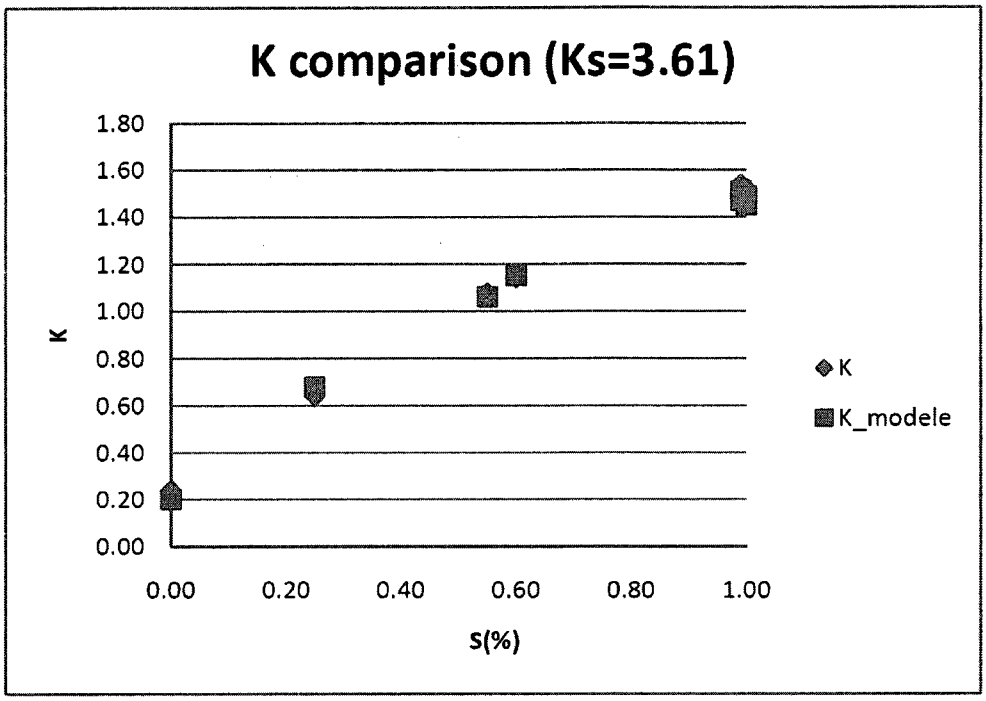

Figure 70 - Comparison of experimental results with Côté-Konrad model for $K_s = 3.61 \frac{W}{m°C}$

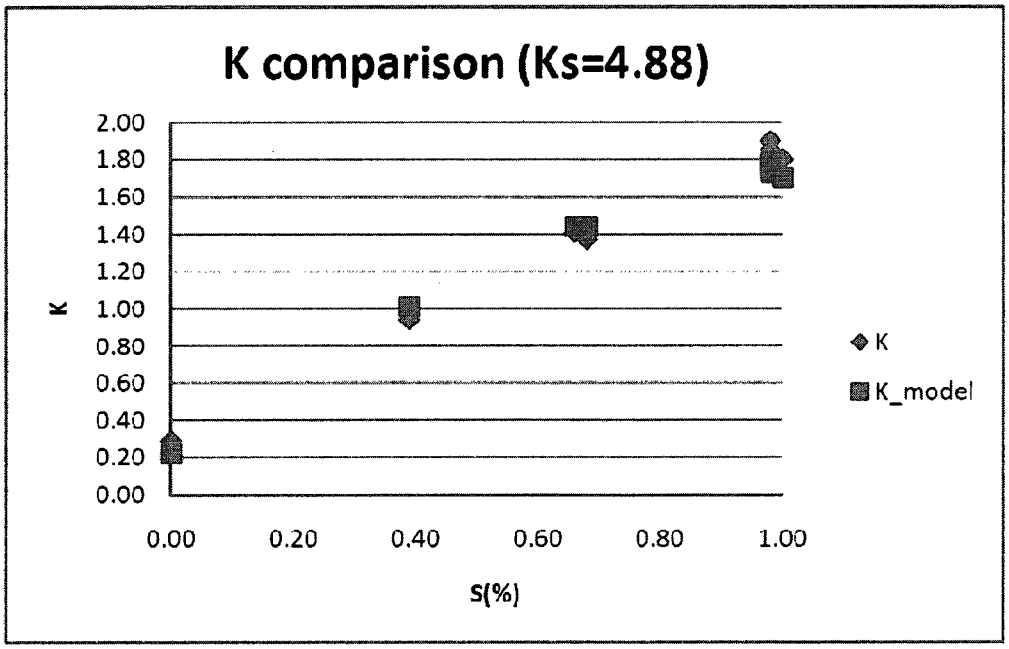

Figure 71 - Comparison of experimental results with Côté-Konrad model for $K_s = 4.88 \frac{W}{m°C}$

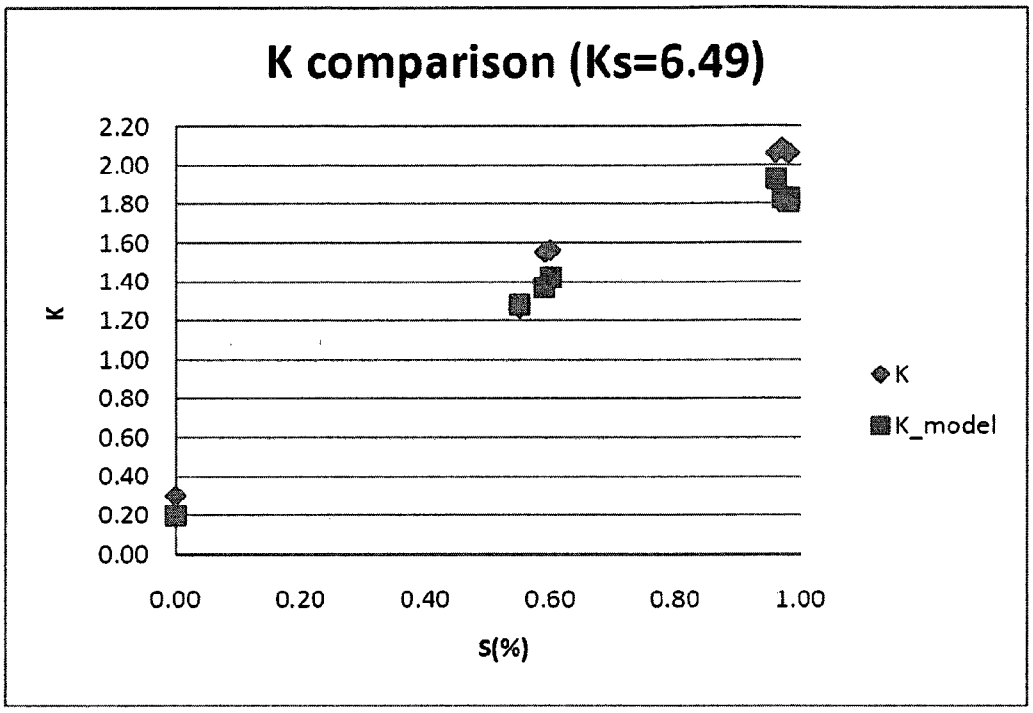

Figure 72 - Comparison of experimental results with Côté-Konrad model for $K_s = 6.49 \frac{W}{m°C}$

Chapter 7: Conclusions and Recommendations

7.1. Conclusions

* Sample size (if the diameter bigger than 40 mm) does not have considerable effect on thermal conductivity of backfill.
* Twenty-eight days of curing, which is accepted from geomechanical point of view, seems to be acceptable for thermal properties measurement also. But in case of emergency, fourteen days of curing could be considered reliable as well.
* Backfill could be considered a homogenous composition from thermal properties point of view if appropriate mixing process is done.
* Thermal conductivity of backfill decreases with increasing porosity.
* Thermal conductivity increases slightly with pulp density. This is because of porosity reduction to some extent. In fact, it could be supposed; considering the range of pulp density of backfills from the same category; pulp density has little or no effect on backfill thermal conductivity.
* Binder content, within the range used in backfill system, does not significantly affect the thermal conductivity of backfill. Therefore backfill thermal conductivity could be considered almost independent from binder content.
* Although adding sodium silicate to backfill has increasing effect on strength of backfill, but it does not have any considerable effect on thermal conductivity of backfill itself.
* Thermal conductivity of backfill increases with saturation.

* Thermal conductivity increasing trend in backfill is almost linear with saturation especially for lower degree of saturation.
* Moisture loss for backfill, when drying the samples in oven, is not consistent with time. Accordingly, drying the samples in oven is a trial and error procedure for each sample depending on sample size and porosity.
* Referring to the porosity range of hydraulic backfill and paste fill, no considerable big change in thermal conductivity could be expected in these kinds of backfill due to the porosity change.
* Smaller particle sizes from the same material could reduce the thermal conductivity. This matter could be attributed to the porosity increase due to particle size reduction.
* With increasing porosity it is expected that more amount of water is needed to reach the saturation state. On the other hand, it is observed that more water is also needed to make water bridges. This may translate in very small pores dispersed throughout the sample.
* Thermal conductivity of backfill increases with increasing solid particles thermal conductivity.
* Backfill thermal conductivity increase becomes less as solid particles thermal conductivity increases.
* For a special category of backfill, it can be said that thermal conductivity of backfill strongly depends on the inert materials and the degree of saturation.

* The semi empirical Côté-Konrad model to predict thermal conductivity of soils could also give good estimation for backfill thermal conductivity especially when lower thermal conductivity material is used.
* The humid environment in underground mines increases the potential ability toward higher recovery rate of geothermal energy in such mines. This is due to the fact that, the humid underground situation leads to a more saturated backfill, resulting in a more conductive backfill media.

7.2. Recommendations

- ❖ Resulted thermal conductivity from interaction of different parameters together should be investigated.
- ❖ Insitu measurement of thermal conductivity of backfills in different mines should be conducted and the results should be compared with the laboratory measurements.
- ❖ Moisture movement along with heat transfer due to moisture movement should be studied. This is needed for clarifying rate of moisture movement in heat transfer of backfill.
- ❖ Backfills structure, pore size and pores distribution in relation to heat transfer aspects due to degree of saturation and moisture movement should be studied. This work would be helpful in justifying the thermal conductivity behavior with saturation.

- Developing a model for predicting the thermal conductivity for any kind of backfill precisely will help to accurately design underground geothermal systems in mines.
- Investigating the possibility of designing an optimized backfill from the heat transfer point of view is an important issue in design of geothermal heat harvest from mines.
- Studying the possibility of including thermal conductivity of backfill as a parameter in mine designing and planning stage to achieve a better level of energy and environmental aspects optimization.
- Modeling the heat transfer in backfill as a porous media in order to reach better understanding of geothermal application in underground mines and the influence of backfills with different thermal conductivities.

References

- Abdulagatov I.M., Emirov S.N., Abdulagatov Z.Z.,Askerov S.Y., Effect of pressure and temperature on thermal conductivity of rocks, J. Chem. Eng. Data, 51, pp.22-33, 2006
- Anand J., Thermal conductivity of fluid saturated rocks at elevated pressures and temperatures, M.S. Thesis, University of California, Berkeley, 1971
- Anderson D.M., Tice A.R, The unfrozen interfacial phase in frozen soil water systems, in ecological studies, analysis and synthesis, vol. 4, pp.107-124, 1973
- Anter Corporation Catalogue, Thermal conductivity measurement by the line heat source method, Technical note # 74, 2008
- Beck A.E., An improved method of computing the thermal conductivity of fluid-filled sedimentary rocks, Geophysics, 41, pp.133-144, 1976
- Benzaazoua M., Fiset J.F., Bussière B., Villeneuve M., PlantSludge B., Sludge recycling within cemented paste backfill: Study of the mechanical and leachability properties, Minerals Engineering, Vol.19, Is.5, pp.420-432, 2006
- Birch F. Clark H., The thermal conductivity of rocks and its dependence upon temperature and composition. American Journal of Science, 238(8), pp. 529–558, 1940
- Birch F., Thermal conductivity, climatic variation and heat flow near calumet Michigan, Am. J. Sci., 252(1), pp.1-25, 1954
- Blumm J., Lemarchand S., Influence of test conditions on the accuracy of laser flash measurements, High Temp.-High Pressures, 34, pp.523-528, 2002
- Blumm J., Opfermann J., Improvement of the mathematical modeling of flash measurements, High Temp.-High Pressures, 34, pp.515-521, 2002

- Bowles J.E., Foundation analysis and design, 4th ed., New York: McGraw-Hill, 1988
- Bristow K.L., Kluitenberg G.J., Goding C.J., Fitzgerald T.S., A small multi-needle probe for measuring soil thermal properties, water content and electrical conductivity, Comput. Electron. Agric. 31, pp.265–280, 2001
- Buckman, H. O., and Brady, N. C., The Nature and properties of Soils, Mac Millan, London, 1975
- Campbell G.S., Callissendorff C.,Williams J.H., Probe for measuring soil specific heat using a heat pulse method, Soil Sci. Soc. Am. J. 55, pp.291–293, 1991
- Campbell G.S., Jungbauer Jr. J.D. , Bidlake W.R. , Hungerford R.D. , Predicting the effect of temperature on soil thermal conductivity, Soil Sci., 158, pp.307–313, 1994
- Carslaw H. S., Jeager J.C., Conduction of Heat in solids, 2nd Edition, Oxford, London, 1959
- Cermak V., Rybach L., Thermal conductivity and specific heat of minerals and rocks, In Landolt and Bornstein V/1: Physical properties of rocks, Angenheiser, G. Ed., Springer, Berlin, Vol. 1, pp.305-343, 1982
- Clark S.P.Jr., Thermal conductivity, in Handbook of physical constants, Edited by S.P. Clark Jr., Geol. Soc. Of America, Memoir 97, New York, pp.482-459, 1966
- Clauser C., Huenges E., Thermal conductivity of rocks and minerals, Washington, USA: American Geophysical Union,pp. 26-105, 1995
- Clauser C., The concept of radiative thermal conductivity, In Handbook of Terrestrial Heat Flow Density Determination, pp.143-164, 1988
- Clean energy ideas, History Of Geothermal Energy, http://www.clean-energy-ideas.com/articles/history_of_geothermal_energy.html

- Côté J., Konrad J.M., A generalized thermal conductivity model for soils and construction materials, Can. Geotech. J., no.42, pp.443–458, 2005b
- Côté J., Konrad J.M., Assessment of structure effects on the thermal conductivity of two-phase porous geomaterials, Int. J. Heat and Mass Transfer, 2008
- Côté J., Konrad J.M., Indirect methods to assess the thermal conductivity of Quebec marine clay solid particles, Can. Geotech. J., 44, pp.1117–1127, 2007
- Côté J., Konrad J.M., Thermal conductivity of base-course materials, Can. Geotech. J., no.42, pp.61–78, 2005a
- Das B.M., Principles of geotechnical engineering, Fifth edition, California State University, Sacramento, Brooks/Cole Thomson learning, 2002
- De Vries D.A., Thermal properties of soil, in: W.R. van Wijk (Ed.), Physics of Plant Environment, North-Holland, Amsterdam, pp 210–235, 1963
- Deminet W.H., Pratt H.R., Thermal conductivity of some rock forming minerals: a tabulation, U.S.G.S open file report 88-690, U.S. Geological survey, Denver Co., pp.15-26, 1988
- Demirci A., Gorgulu K., Duruturk Y.S., Thermal conductivity of rocks and its variation with uniaxial and triaxial stress, International journal of rock mechanics & mining sciences, 41, pp.1133-1138, 2004
- Dreyer W. Properties of anisotropic solid-state materials: Thermal and electric properties, 295, Springer, Wien, pp. 295-314, 1974
- Economy Watch, Geothermal Energy (Geothermal Electricity), http:// www. economywatch.com/renewable-energy/history-and-future-ofgeothermal-energy. html
- Encyclopedia of nations, Canada-Mining, http://www.nationsencyclopedia.com/ Americas/Canada-MINING.html

- Fall M., Benzaazoua M., Modeling the effect of sulphate on strength development of paste backfill and binder mixture optimization. Cement and Concrete Research, 35 (2), pp.301-314, 2005

- Farouki O.T., Physical properties of granular materials with reference to thermal resistivity, Highway research record, no.128, pp.25-44, 1966

- Farouki O.T., Thermal Properties of Soils, Series on Rock and Soil Mechanics, vol. 11, Trans Tech Publications, Switzerland, 1986

- Fernandez M., Banda E., Rojas E., Heat pulse line-source method to determine thermal conductivity of consolidated rocks, Rev. Sci. Instrum., 57(11), American Institute of Physics, pp.2832-2836, 1986

- Flynn D.R., Watson T.W., Measurements of the thermal conductivity of soils to high temperatures, Final report prepared for Sandia laboratories, Albuquerque, 1969

- Fricke H., A mathematical treatment of the electric conductivity and capacity of disperse systems I: the electric conductivity of a suspension of homogeneous spheroids, Phys. Rev., 24, pp.575–587, 1924

- Gemant A., The thermal conductivity of soils, J. App. Phy., Vol 21, aug., pp.750-752, 1950

- Goodman R.E., Introduction to rock mechanics, University of California at Berkeley, Second Edition, John Wiley & sons, 1989

- Gori F., Corasaniti S., Theoretical prediction of the soil thermal conductivity at moderately high temperatures, Journal of heat transfer, Vol. 124, pp.1001-1008, 2002

- Grice T., Underground mining with backfill, The second annual summit-Mine Tailings disposal Systems, Brisbane, pp.1-14, 24-25 November, 1998

- Hammerschmidt U., A new pulse hot strip sensor for measuring thermal conductivity and thermal diffusivity of solids, International journal of Thermo physics, vol.24, no.3, pp.675-682, 2003

- Hashin Z., Shtrikman S., A variational approach to the theory of the effective magnetic permeability of multiphase materials, J. Appl. Phys., 33, pp.3125–3131, 1962

- Hassan A., Optimizing insulation thickness for building using life cost, Applied Energy, 63, pp.115-124, 1999

- Hassani F.P., Archibald J., Mine Backfill, Canadian Institute of Mining, Metallurgy and Petroleum, 1998

- Hassani F.P., Bois, Economic and technical feasibility for backfill design in Quebec underground mines. Final report 1/2, Canada-Quebec Mineral Development Agreement, Research & Development in Quebec Mines. Contract no. EADM 1989-1992, File no. 71226002., 1992

- Hassani F.P., Proposal for Low temperature geothermal energy application in Underground Mines, Private Report, 2005

- Hofer M., Schilling F.R., Heat transfer in quartz, orthoclase, and sanidine at elevated temperatures, Phys. Chem. Miner., 29, pp.571-584, 2002

- Holman J.P., Heat transfer, Library of Congress Cataloging-in Publication Data, 1963

- Horai K., Simmons G., Thermal conductivity of rock-forming minerals, Earth and Planet Science Lett., 6, pp.359-368, 1969

- Horai K., Susaki J., The effect of pressure on the thermal conductivity of silicate rocks up to 12 kBar, Phys. Earth Planet. Int., 55, pp.292-305, 1989

- Horai K., Thermal conductivity of rock-forming Minerals, J. Geophysics Res.,76, pp.1278-1308, 1971
- Huenges E., Burkhard, H.; Erbas, K. Thermal conductivity profile of the KTB pilot core hole, Sci. Drill., 1, pp.224-230,1990
- Jackson R.D., Taylor S.A., Heat transfer, in: C.A. Black et al. (Eds.), Methods of soil analysis: Part 1, Agron monograph, 9, ASA, Madison, WI, pp. 349–356, 1965
- Jaeger J.C., Sass J.H., A line source method for measuring the thermal conductivity and diffusivity of cylindrical specimens of rock and other poor conductors, : British Journal of Applied Physics, vol.15, no.10, pp.1187-1194,1964
- Johansen O., Thermal conductivity of soils, Ph.D. Thesis, Norwegian Univ. of Science and Technol., Trondheim (CRREL draft transl. 637, 1977), 1975
- Kaviany M., Principles of heat transfer in porous media, second ed., Springer, New York, pp. 119–132, 1995
- KD2 Pro operator's manual, KD2 Pro Theory, pp.47-50, 2006
- Kermani M.F.An investigation into a new binder for hydraulic backfill, M.Eng. thesis, McGill University, Montreal, Canada, 2008
- Kersten M.S., Laboratory research for the determination of the thermal properties of soils, ACFEL Tech. Rep., 23. Univ. of Minnesota, Minneapolis, 1949
- Kersten M.S., Thermal properties of frozen ground, Proceedings of first Int. Con. On Permafrost, Lafayette, Indiana, Building research advisory board, National academy of sciences-National research council, pp.301-305, 1963
- Kudryavstev V.A., Fundamentals of frost forecasting in geological engineering investigations, CRREL draft translation 606, ADA 039677, 1974

- Lange G.R., McKim H.L., saturation, phase composition and freezing point depression in a rigid soil model, Proceedings, first international conference on permafrost, Lafayette, Indiana, Building research advisory board, National academy of science, pp.187-191, 1963

- Lu S., Ren T., Gong Y., Horton R, An improved model for predicting soil thermal conductivity from water content at room temperature, Soil science society of America journal, Soil Sci Soc America, pp.8-14, 2007

- Maxwell J.C., A treatise of electricity and magnetism, Clarendon Press: Oxford, Vol. 1, pp.435, 1904

- McGaw R., Thermal conductivity of compacted sand/ice moistures, Highway research record, no.125, pp.35-47, 1968

- Neville A.M., Properties of concrete, Longman Scientific and Technical-Longman, Singapore, 1996

- Nortest Supplier Data Catalogue(NSD), Thermal conductivity - determination of thermal conductivity using axial Flow, guarded hot plate and hot wire methods, 2004

- Ostridge R., Geothermal Energy, Written for Physics 261, University of Prince Edward Island, March 10, 1998

- Ozkahraman H.T., Selver R., Isik E.C., Determination of the thermal conductivity of rock from P-wave velocity, International journal of rock mechanics & mining sciences, 41, pp.703-708, 2004

- Rafferty K., Design aspects of commercial open-loop heat pump systems, Geo-Heat Center, Bulletin, pp.16-24, March 2001

- Ratclife E.H., Thermal conductivity of fused and crystalline quartz, Brit. J. Appl. Phys., 10, pp.22-35, 1959

- Razavi S. M., An investigation into the influence of sodium silicate on the physical and mechanical properties of mine fill, PhD thesis, McGill University, Montreal, Canada, 2007

- Reibelt M., Study of the influence of surface structure and fluid-saturation of rocks on the determination Thermal conductivity using a half-space line source, PhD Thesis, Berlin University of Technology,pp.111-132, 1991

- Robertson E.C., Thermal properties rocks, U.S.G.S. open file report, 88-441, U.S. Geological survey, Reston, Va., 1988

- Scharli U., Rybach L., On the thermal conductivity of low-porosity crystalline rocks, Tectonophysics, 103, pp.307-313,1984

- Schatz J.F., Simmons G., Thermal conductivity of earth materials at high temperatures, J. Geophys. Res., 77, pp.6966-6983, 1972

- Seipold U., Investigation of the thermal transport properties of amphibolites, I. Pressure dependence, High Temp.-High Pressures, 34, pp.299-306, 2002

- Seipold U., Measurements of thermal conductivity and thermal diffusivity of serpentinities at high pressures up to 500 MPa., HighTemp.-High Pressures, 27/28, pp.147-155. 1996

- Seipold U., Mueller H.J., Tuisku P., Principle differences in the pressure dependence of thermal and elastic properties of crystalline rocks, Phys. Chem. Earth , 23, pp.357-360, 1998

- Seipold U., Pressure and temperature dependence of thermal transport properties for granites, High Temp.-High Pressures, 22, pp.541-548, 1990

- Seipold U., Temperature dependence of thermal transport properties of crystalline rocks-a general law, Tectonophysics, 291, pp.161-171, 1998

- Seipold U., The variation of thermal transport properties in the earth's crust. J. Geodyn., 20, pp.145-154, 1995
- Singh T.N., Sinha S., Singh V.K., Prediction of thermal conductivity rock through pysico-mechanical properties, Building and Environment, 42, pp.146-155, 2007
- Smith W.O., The thermal conductivity of dry soils, Soil Science, Vol. 53, pp.435-459, 1942
- Somerton W.H., Mossahebi M., Ring heat source probe for rapid determination of thermal conductivity of rocks, Rev. Sci. Instrum., vol. 38, Issue 10, pp.1368-1371, 1967
- Staicu D.M., Jeulin D., Beauvy M., Laurent M., Berlanga C., Effective thermal conductivity of heterogeneous materials: Calculation methods and application to different microstructures, High Temp.-High Pressures, 23, pp.293-301, 2001
- Tarnawski V.R., Leong W.H., Bristow K.L., Developing a temperature dependent Kersten function for soil thermal conductivity, Int. J. Eng. Res., 24, pp.1335–1350, 2000
- US Department of Energy, A History of Geothermal Energy in the United States, http://www1.eere.energy.gov/geothermal/history.html
- Van Rooyen M.,Winterkorn H.F., Theoretical and practical aspects of the thermal conductivity of soils and similar granular systems, Highway research board Bulletin, pp.143-205, 1957
- Walsh J.B., Decker E.R., Effect of pressure and saturating fluid on the thermal conductivity of compact rock, J. Geophys. Res., 71, pp.3053-3061, 1966
- Wilson J.C., Fill technology in underground metalliferous mines. Foreword. (Ontario: International Academic Services Ltd.), 1979

- Winterkorn H.F., In discussion on water and its conduction in soils, Highway research board bulletin, 287, pp.81-82, 1961
- Woodside W., Cliffe J.B., Heat and moisture transfer in closed systems of two granular materials, Soil Science, Vol. 87, pp.75-82, 1959
- Woodside W., Messmer J.M., Thermal conductivity of porous media II. Consolidated Rocks, J. Appl. Phys., 32 (9), pp.1688–1706, 1961
- Xu Y.S., Shankland T.J., Linhardt S., Rubie D.C., Langenhorst F., Klasinski K., Thermal diffusivity and conductivity of olivine, wadsleyite and ringwoodite to 20 GPa and 1373 K, Phys. Earth Planet. Int., 143, pp.321-336, 2004
- Zimmerman R., Thermal conductivity of fluid saturated rocks, J. Pet. Sci. Eng., 3, pp.219-227, 1989